

**MOLECULAR METHODS FOR ASSESSING THE RESPONSE OF
ARABIDOPSIS THALIANA PLANTS TO POLYCHLORINATED BIPHENYLS
AND HYDROXYLATED POLYCHLORINATED BIPHENYLS**

In Partial Fulfillment
of the Requirements for the Degree
DOCTOR OF PHILOSOPHY
IN ENVIRONMENTAL ENGINEERING

by

Srishty Subramanian

December 2018

Examining Committee Members:

Benoit Van Aken, Ph.D., Advisory Committee Chair, Chemistry & Biochemistry,
George Mason University
Rouzbeh Tehrani, Ph.D., Civil and Environmental Engineering, Temple University
Nancy Pleshko, Ph.D., Bioengineering, Temple University
Iyad Obeid, Ph.D., Electrical and Computer Engineering, Temple University

ABSTRACT

Polychlorinated biphenyls (PCBs) are a class of persistent organic contaminants that are ubiquitous and persistent in the environment. In the environment, PCBs have been shown to undergo various degradation processes and generate hydroxylated metabolites known as hydroxylated polychlorinated biphenyls (OH-PCBs). There is a growing scientific interest in studying OH-PCBs as they are being increasingly detected in biotic and abiotic samples.

Due to their widespread presence in the air, water, and soil, as well as their ability to bioaccumulate in living organisms, they pose a high danger to human beings and thus need to be remediated. Though phytoremediation has been proposed as a useful technology for the environmental management of PCBs, there is a lack of information about potential phytoremediation of OH-PCBs

The hypothesis underlying this study is that hydroxylation of PCBs to OH-PCBs results in different toxicity and physiological effects on plants. In order to test this hypothesis, we conducted experiments aimed at understanding the toxicity and metabolism of PCBs and OH-PCBs by *A. thaliana* plants at physiological and transcriptomic levels. The applicability of FTIR to analyze lignin and cellulose content in the cell wall was tested for the purpose of biofuel production.

More precisely, the specific aims of this study are as follows:

1. To determine the toxicity of selected PCBs and their hydroxylated metabolites (OH-PCBs) toward the model plant *A. thaliana*.

2. To understand the regulation of the response to and metabolism of PCBs and OH-PCBs in exposed *A. thaliana* at the transcriptomic level.
3. To determine the change in the biomass composition of *A. thaliana* upon exposure to different PCBs and OH-PCBs.

Toxicity results indicated no observable toxicity of the parent PCBs toward the plants. However, lower chlorinated OH-PCBs resulted in a significant reduction in the growth and germination rate of the plants. Genome wide expression microarrays were used to investigate the transcriptional response of *A. thaliana* plants to 2,5-DCB and three of its OH-metabolites. Exposure to 2,5-DCB caused up-regulation of genes that are involved in toxic stress response and detoxification functions, and induction of multiple xenobiotic response genes.

FTIR analysis was used to determine the effects of different PCBs and their hydroxylated metabolites on the composition of the plant biomass. Significant changes in the lignin and cellulose content were observed between different treatments, which indicated an overall effect on the cell wall components upon exposure to PCBs and its OH metabolites.

ACKNOWLEDGEMENTS

I would like to take this opportunity to thank my advisor Dr. Benoit Van Aken for accepting me in his research group and constantly guiding me through my Ph.D. journey. His support and words of wisdom have always motivated me to strive for the better.

I also would like to thank Dr. Nancy Pleshko and the entire TISL lab for providing me all the help and equipment for the spectroscopy. They were always ready to help me out and provide valuable suggestions.

I would also like to acknowledge Dr. Rouzbeh Tehrani for being a mentor and friend at the same time and his ever helping attitude towards graduate students. I would also like to thank Dr. Iyad Obeid for his time and acceptance as my dissertation committee chair.

I would also like to acknowledge the department chair, Dr. Rominder Suri, for his continuous support and encouragements.

Special thanks to my dear friend Ramya Ailavajhala for her support and encouragement through these years.

The research presented in this thesis has been funded by the Iowa Superfund Basic Research Program, National Institute of Environmental Health Sciences (NIEHS) and the PA Sea Grant Program.

Finally, I would like to thank the Department of Civil and Environmental Engineering and the Graduate School of Temple University for their financial assistance and TA support to complete my Ph.D. work.

Lastly, I would like to dedicate my thesis to my dear family and friends for their faith in me.

TABLE OF CONTENTS

ABSTRACT	II
ACKNOWLEDGEMENTS	IV
LIST OF FIGURES	VIII
LIST OF TABLES	XI
LIST OF ABBREVIATIONS	XIII
CHAPTER 1 INTRODUCTION	1
1.1 Problem Statement	1
Environmental Contamination	1
PCBs and OH-PCBs.....	1
Phytoremediation	2
Molecular Mechanisms	3
Use of FTIR to Enhance Bioethanol Production	4
1.2 Overall Objective and Hypothesis	5
1.3 Specific Objectives	5
1.4 Significance of this Study	7
CHAPTER 2 LITERATURE REVIEW	9
2.1 Model Plant Used in this Study	9
2.2 Polychlorinated Biphenyls (PCBs) Used in this Study.....	10
2.3 Hydroxylated Polychlorinated Biphenyls (OH-PCBs).....	12
2.4 Phytoremediation and the Effects of PCBs and OH-PCBs on Plants.....	13
2.5 Use of Molecular Approaches in plant science.....	17
2.6 FTIR and its application in plant science.....	19
CHAPTER 3 EFFECTS OF POLYCHLORINATED BIPHENYLS (PCBS) AND THEIR HYDROXYLATED METABOLITES (OH-PCBS) ON ARABIDOPSIS THALIANA	22
3.1.....	23
Abstract	23
3.2 Introduction.....	23

3.3 Methods.....	25
Chemicals.....	25
Germination and growth tests	26
Gene expression analysis using microarrays	27
Reverse-transcription real-time PCR	28
3.4 MIAME compliance	30
3.5 Results and discussion	30
Toxicity testing	30
Gene expression microarrays	40
Functional categories of differentially expressed genes	43
3.6 Acknowledgements.....	54
CHAPTER 4 TRANSCRIPTOMIC RESPONSE OF <i>ARABIDOPSIS THALIANA</i> EXPOSED TO HYDROXYLATED POLYCHLORINATED BIPHENYLS (OH- PCBS).....	55
4.1 Abstract.....	56
4.2 Introduction.....	56
4.3 Materials & Methods	58
Toxicity tests.....	58
Gene expression analysis using microarrays	59
Reverse-transcription real-time PCR	60
MIAME compliance	61
4.4 Results and discussion	62
Toxicity testing	62
Gene expression microarrays	64
Functional categories of differentially expressed genes	67
Comparison between 2'-OH-, 3'-OH-, 4'-OH-2,5-DCB, and 2,5-DCB	71
Comparison of expression profile of 2,5-DCB and OH-2,5-DCBs with other chemicals.....	75
4.5 Acknowledgements.....	82

CHAPTER 5 <i>ARABIDOPSIS THALIANA</i> BIOMASS ASSESSMENT FOR BIOFUEL GENERATION USING FTIR-ATR	83
5.1 Introduction.....	83
5.2 Materials and Methods.....	87
FTIR ATR data collection and processing.....	88
Statistical Analysis	89
5.3 Results.....	91
Pure component spectral data:	91
Spectral data of non-exposed controls and exposed samples:	92
5.4 Discussion.....	101
5.5 Conclusion	103
CHAPTER 6 CONCLUSION	106
REFERENCES.....	112
 APPENDIX - DEVELOPMENT OF A REAL-TIME PCR METHOD FOR THE EARLY DETECTION OF AQUATIC INVASIVE SPECIES IN PENNSYLVANIA WATERSHEDS.....	 128

LIST OF FIGURES

Figure 2.1 Structure of PCBs (Faroon and Ruiz, 2015).....	10
Figure 2.2 Structure of hydroxy polychlorinated biphenyls	12
Figure 2.3 Different processes of phytoremediation of organic pollutants.	14
Figure 2.4 The Green liver model (Van Aken 2008).....	15
Figure 3.1 Dose-response curves of <i>A. thaliana</i> exposed to PCBs (panels A, C) and OH-PCBs (panels B, D) as determined through germination tests (panels A, B) and growth tests (panels C, D). Solid lines for significantly toxic compounds (4-CB, 4'-OH-4-CB, 4'-OH-2,5- DCB, and 4'-OH-2,4,6-TCB) were obtained by fitting to a 3-parameter sigmoidal inhibition model (Prism 5.04, Graphpad). Solid lines for other, non-toxic compounds were obtained by 2nd-order smoothing of experimental data (Prism 5.04, Graphpad). The error bars represent standard deviations between biological replicates.	31
Figure 3.2 Dose-response curves of <i>A. thaliana</i> exposed to OH-PCBs.....	34
Figure 3.3 Dose-response curves of <i>A. thaliana</i> exposed to OH-PCBs (panel A: mono-chlorinated congeners, panel B: di-chlorinated congeners, panel C: tri-chlorinated congeners, and panel D: tetra-chlorinated congeners) as determined through biomass growth tests. The inhibitory effect of PCBs and OH-PCBs is presented as a percentage of the biomass in non-exposed controls. Solid lines for significantly toxic compounds were obtained by fitting to a 3-parameter sigmoidal inhibition model (Prism 5.04, Graphpad). Solid lines for other, non-toxic compounds (4'-OH-3,3',4-TCB and all tetra-chlorinated congeners, except 4'-OH-2,2',5,5'-TeCB) were obtained by 2nd-order smoothing of experimental data (Prism 5.04, Graphpad). The error bars represent the standard deviation between biological replicates.....	36
Figure 3.4 Hierarchical clustering of gene expression profiles of <i>A. thaliana</i>	42
Figure 3.5 Comparison of relative gene expression levels in <i>A. thalianae</i> exposed to 2,5-DCB (left) and 4'-OH-2,5-DCB (right) using reverse-transcription real-time PCR (RT-	

qPCR) and microarrays (Arabidopsis Gene 1.0 ST Arrays, Affymetrix). Error bars represent the standard deviations of three biological replicates.	43
Figure 3.6 Comparison between gene expression profiles of <i>A. thaliana</i> exposed to 2,5-DCB and other chemicals.	49
Figure 3.7 Chemical structure of fenclorim, 4-chloro-6-methyl-2 phenylpyrimidine (CMP), and sulfomethuron methyl.	50
Figure 4.1 Dose-response curves of <i>A. thaliana</i> exposed to OH-PCBs.....	62
Figure 4.2 Hierarchical clustering of gene expression profiles of <i>A. thaliana</i> (Arabidopsis Gene 1.0 ST Arrays, Affymetrix) exposed to 2,5-DCB (blue – 4), 2'-OH-2,5-DCB (orange – 1), 3'-OH-2,5-DCB (green – 2), 4'-OH-2,5-DCB (yellow – 3), and non-exposed controls (orange – 5). The analysis was performed on three biological replicates using the Affymetrix Expression Console™.....	66
Figure 4.3 Expression levels obtained by microarrays plotted against expression levels obtained by RT-qPCR.....	67
Figure 4.4 Structure of Brassinazole, Propiconazole, Uniconazole and Paclobutrazole .	76
Figure 5.1 Second derivative inverted average (n=3) spectra of lignin and cellulose standards obtained in the MIR region using FTIR.....	91
Figure 5.2 Second derivative average (n=3) spectra of samples exposed to 4-CB and 4-OH-4'-CB compared to control.....	92
Figure A.1 <i>Hydrilla verticillata</i>	133
Figure A.2 <i>Myriophyllum spicatum</i>	134
Figure A.3 <i>Trapa natans</i>	135
Figure A.4 <i>Didymosphenia geminata</i>	136
Figure A.5 Relative real-time PCR amplification signals of <i>T. natans</i>	147
Figure A.6 Relative real-time PCR amplification signals of <i>H. verticillata</i>	147

Figure A.7 Standard curves of SYBR Green assays for <i>T. natans</i> , <i>D. geminata</i> , and prokaryotes (using <i>E. Coli</i> DNA).	150
Figure A.8 Standard curves of fluorescent assays for <i>T. natans</i> , <i>M. spicatum</i> , and <i>H. verticillata</i>	151
Figure A.9 Amplification levels of <i>T. natans</i> biomarkers	153
Figure A.10 Map of sampling points along Little Neshaminy Creek.....	154
Figure A.11 Amplification levels of <i>H. verticillata</i> and <i>M. spicatum</i> biomarkers	155
Figure A.12 Map of sampling points on Lake Nockamixon	155
Figure A.13 Amplification levels of <i>D. geminata</i> biomarker	156
Figure A.14 Map of sampling points along the Big Gunpowder Falls.....	157

LIST OF TABLES

Table 3.1 List of primers used for the reverse-transcription real-time PCR of selected genes	29
Table 3.2 Toxicity of PCBs and OH-PCBs for <i>A. thaliana</i> as determined through germination and growth tests. IC50 were computed from the dose-response curves using a three-parameter sigmoidal model. IC50, 95%-confidence interval (CI 95%), coefficients of determination R^2), and octanol-water partition coefficients (K_{ow}) are presented.....	32
Table 3.3 Enrichment analysis of genes up- and downregulated upon exposure to 2,5-DCB and 4'-OH-2,5-DCB based on Biological Processes and Molecular Functions.	46
Table 3.4 Expression levels of potential xenobiotic response genes (XRGs) in <i>Arabidopsis</i> plants exposed to 2,5-DCB versus non-exposed controls (upper part) and 4'-OH-2,5-DCB versus non-exposed controls (lower part)	51
Table 4.1 List of primers used for the reverse-transcription real-time PCR (RT-qPCR) of selected genes.....	61
Table 4.2 Enrichment analysis of genes up- and down regulated upon exposure to 2,5-DCB and 4'-OH-2,5-DCB based on Biological Processes and Molecular Functions. Only gene ontology (GO) terms of special interest are shown.....	70
Table 4.3 Enrichment analysis of genes up- and down regulated upon exposure to 2,5-DCB, 2'-OH-, 3'-OH-, and 4'-OH-2,5-DCB based on Biological Processes. Only the most specific gene ontology (GO) terms (lowest hierarchical level) are shown.	74
Table 4.5 Genes involved in brassinosteroid and iron response differentially expressed in response to 2'-OH-, 3'-OH-, 4'-OH-2,5-DCB, and 2,5-DCB.	78
Table 4.6 Chemicals resulting in expression profiles most similar to 2'-OH-, 3'-OH-, 4'-OH-2,5-DCB, and 2,5-DCB.....	81
Table 5.1 PCB compounds and hydroxylated PCBs tested on <i>A. thaliana</i> plants	88

Table A.1 List of the target invasive species, <i>M. spicatum</i> , <i>T. natans</i> , <i>H. verticillata</i> and <i>D. geminata</i> and a suite of related specimen obtained from different sources.	139
Table A.2 List of primer and probe sequence specific to the three target plant species, <i>M. spicatum</i> , <i>T. natans</i> , and <i>H. verticillata</i> , and the diatom, <i>D. geminata</i>	146
Table A.3 Assay characterization for the six biomarkers for <i>T. natans</i> , <i>H. verticillata</i> , <i>M. spicatum</i> , <i>D. geminata</i> , and prokaryotes: the standard curve characteristics (number of points, R ² , equation), the estimated detection limit of the assay, and the amplification efficiency are presented	152

LIST OF ABBREVIATIONS

ANOVA: Analysis of Variance

DCB: Di-Chlorobiphenyl

DNA: Deoxyribonucleic Acid

FTIR-ATR: Fourier Transform Infrared- Attenuated Total Reflectance

IC50: Inhibitory Concentration 50% (half-maximum inhibitory concentration)

K_{ow} : Octanol-Water Partition Coefficient

mRNA: Messenger RNA

MIR: Mid-Infrared

OH-PCB: Hydroxylated Polychlorinated Biphenyl

PCB: Polychlorinated Biphenyl

PCR: Polymerase Chain Reactions

RNA: Ribonucleic Acid

ROS: Reactive Oxygen Species

RT-qPCR: Reverse Transcription-quantitative PCR

TCB: Tri-Chlorobiphenyl

TNT: Tri-Nitro Toluene

CHAPTER 1 INTRODUCTION

1.1 Problem Statement

Environmental Contamination

Many toxic chemicals have entered the environment due to increased anthropogenic activities. Humans are exposed to these contaminants by ingestion of contaminated food or water. These toxic chemicals are known to have detrimental effects on soil ecosystems, environment and human health (Khan, 2006). Human exposure to these toxic chemicals can lead to their bioaccumulation and serious health issues.

PCBs and OH-PCBs

Polychlorinated biphenyls (PCBs) and hydroxylated polychlorinated biphenyls (OH-PCBs) are a class of persistent organic pollutants that are carcinogenic in their nature and are widespread in the environment. Between the 1930s and 1970s, they were used industrially as coolants and lubricants in transformers and other uses primarily due to their stable chemical nature (Faroon and Ruiz, 2015). Though they were banned by the late 70s, there is widespread contamination to this day, due to their ability to persist and bioaccumulate (Ribas-Fitó et. al, 2001). According to Hansen and Robertson (2001), approximately 1.5 million metric tons of PCBs have been produced worldwide, out of which 30% has been released into the environment. About a decade ago, hydroxylated PCBs have been found in the fishes in the Great Lakes (Campbell et al., 2003). Humans and wildlife have been shown to metabolize PCBs into hydroxylated PCBs by cytochrome P450 pathway or the direct hydroxylation of the parent PCB (Letcher, 2005; Letcher, 2000; H. Li, 2003). OH-PCBs have been shown to have estrogenic and

antiestrogenic effects on wildlife (Wiegel, 1999; Bergeron, 1994; Connor, 1997; Delzell, 1994). They could potentially be more toxic than the parent PCB, as they tend to remain in the body for a longer time and their bioaccumulation in the liver and adipose tissues due to their high hydrophobicity (Tampal et al., 2002; Tehrani and Van Aken, 2014). Tehrani and Van Aken (2014) have suggested that OH-PCBs could be more toxic than their parent compounds showing certain toxic effects not exerted by the parent PCB compounds. This hypothesis has been tested in this thesis specifically in Aims 1 and 2, by exposing *A. thaliana* plants to a suite of PCBs and corresponding OH-PCBs. The plants were then examined for differences in germination, growth and transcriptomic responses.

Phytoremediation

Though there are methods that have been developed for the remediation of PCBs, however, these methods are hard to use due to their high costs, inability to be used on large contaminated areas and the destruction they cause to the native environment (Chekor et al., 2004). This has led to exploration of more environmental friendly and considerably cheaper options for the remediation of PCBs (Schnoor et al., 1995).

The increase of toxic contaminants in the environment has led to exploring self-cleansing capacities of natural systems. Physical, chemical and biological processes determine the fate and transport of these contaminants through the environment (Macek et al., 2004). The use of plants to remove contaminants is termed as phytoremediation. It was discovered few decades ago that plants are capable of taking up and even degrading toxic contaminants from their rhizosphere (Van Aken, 2009). However, there are certain limitations associated with phytoremediation (Chaudhry et al., 2002). Firstly, plant

growth rate may be limited by a number of environmental factors, such as water and nutrient availability, pH of the soil and other climatic factors (Ali et al., 2013). Secondly, there is a high probability of the contaminants entering the food chain via animal consumption of contaminated plants (Singh et al., 2003). Therefore, it is of utmost importance that this uptake and transformation of toxic contaminants be studied.

Molecular Mechanisms

However, the uptake and translocation of environmental contaminants by plants is not very well understood since the catabolic pathways involved may vary based on the contaminant and the plant species used for remediation. Plants possess various mechanisms of xenobiotic sensing, and it is difficult to distinguish between responses directly induced by the toxic compounds and indirectly induced by their deleterious effects (Ramel 2012). The understanding of the pathways affected by contaminant exposure in the plants, and the metabolism of plant response to these changes, can help improve the efficiency of phytoremediation. Prior studies focusing on transcription factors in *A. thaliana* showed overlap of genes expressed in response to different types of stresses (Singh 2002). Toxic compounds have been reported to induce genes involved in response to oxidative stress and pathogens, which frequently produce toxins inside the host cells. Since plant response to various biotic and abiotic stresses occur by the transcriptional control of stress-responsive genes, it is important to identify the transcription factors involved in these responses. Plant defense responses can be well understood by the use of quantitative methods for expression profile analysis such as cDNA microarrays.

The response of living organisms, including plants, to xenobiotic pollutants is known to be primarily regulated at the transcriptional level. Little information is available regarding the effect and metabolism of toxic contaminants -- including PCBs and OH-PCBs -- on/by plants. Examination of the transcriptomic response of plants to PCBs will inform us on the toxicity of PCBs for plants, the plant response to PCBs, and the detoxification mechanisms.

Use of FTIR to Enhance Bioethanol Production

Fossil fuels are non-renewable, that is, they draw on finite resources that will eventually dwindle, becoming too expensive or too environmentally damaging to retrieve. Lignocellulosic bioethanol research has recently been on the rise, with the goal of producing environmentally safer fuels. In addition, certain plants, such as switchgrass (*Panicum virgatum*), can be used for cleaning up the environment through the process of phytoremediation, which can increase the competitiveness of 'second generation' bioethanol. In addition to their potential for phytoremediation, plants can be used to produce ethanol through the conversion of the cell wall component, cellulose. However, the cell wall also contains variable amounts of lignin, which constitutes the major technical obstacle to lignocellulosic biomass digestibility and conversion into bioethanol. The plant lignin content is susceptible to change when exposed to toxic chemicals, which would affect the biomass digestibility. Digestion of lignocellulosic biomass currently proceeds through the enzymatic breakdown of lignin, cellulose, and hemicellulose followed by the fermentation of resulting single sugars to produce ethanol, which can be substituted for fossil fuels. Therefore, the quantity of lignin and cellulose determines the

amount of ethanol that can be produced by plants. Fourier transform infrared (FTIR) spectroscopy coupled with fiber optics is a technique capable of capturing molecular vibrations that has been used to evaluate the composition of organic materials and tissues, including plants. In FTIR attenuated total reflectance (ATR) mode, compositional data can be collected within seconds without destruction of the plant. Aim 3 focuses on the use of FTIR spectroscopy for evaluation of the composition of *A. thaliana* in response to exposure to PCBs and OH-PCBs as compared to control plants, by characterizing changes in lignin and cellulose in the cell wall of *A. thaliana*. These results will be discussed in chapter 5 of this thesis.

1.2 Overall Objective and Hypothesis

The overall objective of this research was to characterize the molecular mechanisms underlying the uptake of PCBs and OH-PCBs by the model plant *A. thaliana* and to compare the toxicity of various PCBs and their OH-metabolites. The central hypothesis driving this study is that PCBs and OH-PCBs induce distinct toxicities in plants observable at transcriptomic and physiological levels. OH-PCB metabolites are more toxic compared to their parent PCBs and in turn could affect the gene expression pathways differently in *A. thaliana* plants. This overall objective was pursued by carrying out the three specific aims of this study, as described below.

1.3 Specific Objectives

- a) To determine the toxicity of selected PCBs and their hydroxylated metabolites (OH-PCBs) toward the model plant *A. thaliana*.**

In this experimental section of the thesis, physiological responses of *A. thaliana* to a suite of PCBs and their OH-PCB metabolites were investigated. The effect of the selected

contaminants on plant growth and biomass accumulation were determined by the means of germination and growth inhibition tests. Seeds were exposed to increasing doses of contaminants and several toxicity endpoints were recorded. Dose-response curves and tolerances indexes were computed.

The OH-PCBs with one to three chlorine atoms exhibited higher toxicity as compared to their parent PCBs. *A. thaliana* was also exposed to 2, 5-DCB and its OH-derivatives. The OH-derivatives were significantly more toxic than the parent PCBs.

b) To understand the regulation of the response to and metabolism of PCBs and OH-PCBs in exposed *A. thaliana* at the transcriptomic level.

In order to understand further the mechanisms of toxicity of PCBs and their OH-derivatives, we investigated the molecular bases of the regulation of the plant response to the toxicants. Transcriptomic analyses were conducted using expression microarrays. *A. thaliana* plantlets were exposed to the selected contaminants, RNA was extracted, and the transcriptome was screened to identify differentially-expressed genes using whole-genome expression microarrays. Expression level of gene of interest was further investigated using RT-qPCR

c) To determine the change in the biomass composition of *A. thaliana* upon exposure to different PCBs and OH-PCBs.

As toxic stress has been shown to affect the lignin content of exposed plants, and therefore potentially impact biomass conversion to biofuel. In this section on the analysis of the biomass of exposed plants. The effect of the PCBs and OH-PCBs on the biomass composition was determined by the analysis of lignin and cellulose content using FTIR spectroscopy.

FTIR spectroscopy helped identify peaks specific to lignin and cellulose. These peaks were compared for the exposed plants and non-exposed control plants. Changes in lignin and cellulose were studied. PCBs and OH-PCBs resulted in different changes in lignin and cellulose content.

Results from this research are expected to contribute towards understanding the molecular mechanisms that arise in *A. thaliana* plants upon exposure to PCBs and OH-PCBs. Whole genome microarrays have been used to characterize the effects of different OH-PCBs on the plants. The use of FTIR to study changes in lignin and cellulose offers insight into using non-invasive techniques for the characterization of cell wall components and their use in bioethanol production.

This thesis also includes a section on the application of qPCR for detecting aquatic plant invasive species. This research was conducted in parallel to the research on plant exposure to PCBs. There has been extensive contamination of natural water resources, by aquatic invasive species, that results in negative impact on the environment and proper usage of water. It is important to early identify these invasive species as they may create an environment not suitable to the indigenous species. Therefore, it becomes important to develop techniques that allows for the timely identification of these invasive species. Primers and specific probes were designed using genomic databases and sequence alignment tools. These primers and probes were shown capable of detecting even small amount of invasive species signature DNA in natural waters using qPCR.

1.4 Significance of this Study

Current technologies available for remediation of PCBs and OH-PCBs are expensive and thus phytoremediation can be a more feasible option. However, the

environmental fate and toxicology of these contaminants, in plants, has received little attention and is not well documented. Understanding the regulation of the plant response to toxic stress is therefore expected to help assess the risk that contaminants may impose on the environment and human health. Understanding the transcriptional response of *A. thaliana* plants to PCBs and OH-PCBs may help design transgenic plants capable of more efficient phytoremediation.

Also, the proposed research is innovative because it provides an incentive for using the plants exposed to contaminants, for biofuel production. Combining both the technologies can prove effective for a more environment friendly alternative to cleaning up contaminants and solving the problems of diminishing fuel resources.

CHAPTER 2 LITERATURE REVIEW

2.1 Model Plant Used in this Study

A. thaliana (Thale cress) is a small flowering plant of the mustard family (Brassicaceae) (TAIR). It was first used in experimental biology in 1907 by Friedrich Laibach (Meyerowitz, 1985). The *A. thaliana* functional genomics project was launched in 2001 with the aim of completion by 2010. The plant is found naturally in abundance in Europe, Asia and North America. Although many ecotypes have been identified for experimental analysis, the Columbia and Landsberg ecotypes are more commonly used in genetic and molecular studies (Page and Grossniklauss, 2002).

According to Hoffman (2002), *A. thaliana* has wide climatic amplitude but prefers moderate temperature zones of the world (Somerville and Koornneef, 2002). *A. thaliana* is a very small plant with seedlings growing into plants ranging from 2 cm to 10 cm in diameter. It is the first plant to have its entire genome fully sequenced (Bevan and Walsh, 2005). The entire life cycle of the *A. thaliana* plant is about 6 weeks which makes it a very good candidate for experimental studies. This includes seed germination until flowering and first seed maturation (The Arabidopsis Genome Initiative, 2000). *A. thaliana* has increased in popularity in recent times owing to its close relation to many other plant species. The small size and short life cycle make it very easy to grow in laboratory conditions. It is also a self-flowering plant capable of producing several seeds in turn producing an abundant progeny (Blanco and Koornneef, 2000). Another important factor is that it has one of the smallest known genome for flowering plants which is about 135 Mb. It is the most thoroughly studied plant amongst all flowering plants (Koornneef

and Meinke, 2010). There are numerous community resources available for *A. thaliana* genome analysis, such as the TAIR, ABRC stock center (Meinke et al., 1998).

2.2 Polychlorinated Biphenyls (PCBs) Used in this Study

PCBs are a class of colorless and odorless chemical compounds. They exist as 209 congeners based on the number and position of the chlorine atoms. Their state of existence varies between an oil to a waxy solid (EPA- <https://www.epa.gov/pcbs/learn-about-polychlorinated-biphenyls-pcbs>).

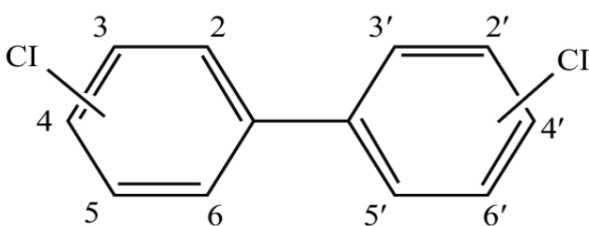


Figure 2.1 Structure of PCBs (Faroon and Ruiz, 2015)

They were discovered in 1865 and were produced commercially until 1970ies when they were banned in most countries because of their high toxicity and persistence in the environment (Jensen, 1972). PCBs are produced by chlorination of biphenyls at different positions. Clophen and Aroclor were the most popular commercially available mixtures (Schulz et al., 1989). An estimate amount of 1.5 million tons have been produced worldwide (IARC, 2013). In early 1936, acute toxic health effects were identified due to Aroclor exposure (Hens, 2017). They are known to cause deleterious carcinogenic, neurotoxic and developmental effects in humans and animals (ATSDR, 2000; Hansen, 1998; Winneke et al., 2002; Safe, 1989,; Brouwer et al., 1999; Kimbrough, 1995)

They were used industrially as coolants and lubricants in transformers, dielectric fluids in capacitors, glue wax, plasticizers, flame retardants, and for various other uses.

According to Holoubek (2000) around 31% of the PCBs produced were released into the environment; 65% of produced PCBs were still in use or in landfills and only 4% had been effectively destroyed. They were released into the environment as a result of leaking, evaporation, improper disposal, incineration, and accidental releases (Hansen and Robertson, 2015).

PCBs were detected in environmental samples and identified as toxic for humans and wildlife in 1966 by Tanabe et al. (1988). Since then, it has been shown that PCBs exist in human tissues as well as in the environment (USEPA, 2009). PCBs are highly volatile and stable in the environment, which makes them widespread. Based on their octanol-water partition coefficient (K_{ow}), lower chlorinated congeners tend to exist in gaseous phase which can then be transported to longer distances (Cicilio, 2013). Higher chlorinated congeners with a K_{ow} of more than 6, tend to partition into soils and sediments (Safe, 1994). Also being highly hydrophobic, PCBs bio-accumulate in living organisms causing a phenomenon called biomagnification (Norström, 2010). Due to this biomagnification, animals and humans are bound to accumulate a high concentration of PCBs (Kimbrough, 1995; Hooper et al., 1999).

Although persistent in nature, PCBs have been shown to undergo slow and limited aerobic as well as anaerobic microbial degradation. Anaerobically, PCB congeners with four and more chlorine atoms undergo reductive dechlorination. In this process, chlorine atoms are removed from the meta and para positions on the biphenyl (Pal et al., 1980). Aerobic microbial degradation is more common with lower chlorinated congeners. These congeners may well be the reduction products of anaerobic degradation.

2.3 Hydroxylated Polychlorinated Biphenyls (OH-PCBs)

Hydroxylated PCBs are formed in the environment by abiotic reaction with hydroxyl radical or biological transformation (e.g., oxidation by the cytochrome P-450 system) (Totten et al., 2002; Tehrani et al., 2013).

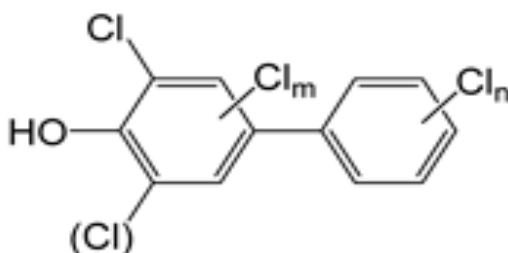


Figure 2.2 Structure of hydroxy polychlorinated biphenyls

Though the OH-PCBs have lower K_{ow} than their parent PCB compounds, they are still able to bioaccumulate due to their relatively hydrophobicity (Tehrani et al, 2014). They also have a high binding capacity to the transport protein, transthyretin (TTR), due to their structural similarity with T4 (Zheng et al., 2017). Bloom et al. (2009) have found that OH-PCBs compete with T4 for binding to TTR, thus, disrupting the transfer of thyroxine and retinol (Olsson et al., 2000). Meerts et al. (2001) have found evidence on the endocrine disrupting activities of certain OH-PCBs.

Metabolites of PCBs can be retained by humans and wildlife in concentrations only slightly less than the parent compound (Fängstöröm et al., 2002). It has been reported that OH-PCBs concentration may exceed 10% of the total PCB concentration in humans and other wildlife. As many as 38 OH-PCBs have been identified in the human plasma (Fängstöröm et al., 2002). Inside the body, PCBs follow the same pathway of degradation to OH-PCBs using the P-450 mediated oxidation process (Tehrani et al., 2014). Some of

the OH-PCBs may be more hydrophilic compared to their parent PCBs, and therefore may be excreted from the body more easily (Dreiem et al., 2009).

Another pathway by which parent PCBs convert to OH-PCBs may be very interesting to learn about. Many times PCBs, existing in gas phase may react with hydroxyl radicals to form OH-PCBs in the atmosphere (Totten et al., 2002).

Coonor et al. (1997) showed that OH-PCBs with chlorine at different positions exhibited different toxic effects. Therefore it becomes important to assess each PCB and its metabolites in a unique way.

There is not much known about the degradation of OH-PCBs in the environment. However, there have been few studies to understand bacterial metabolism of OH-PCBs (Tehrani et al., 2014).

Oxidative transformation and reductive dehalogenation have been identified as the two pathways of OH-PCB degradation by anaerobic bacteria (Grimm et al., 2015). Bhalla et al. (2016) used the Microtox bioluminescent assay to test the toxicity of 23 monohydroxylated derivatives of PCBs and 12 parent PCBs. The hydroxylated PCBs showed much higher toxicities compared to the parent PCBs.

2.4 Phytoremediation and the Effects of PCBs and OH-PCBs on Plants

Phytoremediation is the use of plants in situ for treating contaminated soil. Higher plants are capable to taking up contaminants from the soil, sediments, surface water and groundwater. Once these contaminants enter plant tissues, they undergo processes like biodegradation, immobilization, volatilization and photolysis (Van Aken et al., 2010). Phytoremediation involves different processes (Figure 2.3) as listed below:

1. Phytoextraction is the process by which pollutants are taken up inside by plant tissues.
2. Rhizofiltration is the process by which pollutants absorb to the roots of the plant.
3. Phytotransformation is the transformation of pollutants inside plant tissues facilitated by plant tissues.
4. Phytovolatalization is the process by which pollutants in plant issues volatilize into the environment.
5. Rhizosphere bioremediation is the degradation of pollutants in the root zone facilitated by the microbes present in the soil Microbes in the soil degrade the pollutants in the root zone.
6. Phytostabilization is the process by which pollutants present in the root zone are incorporated in soil materials.

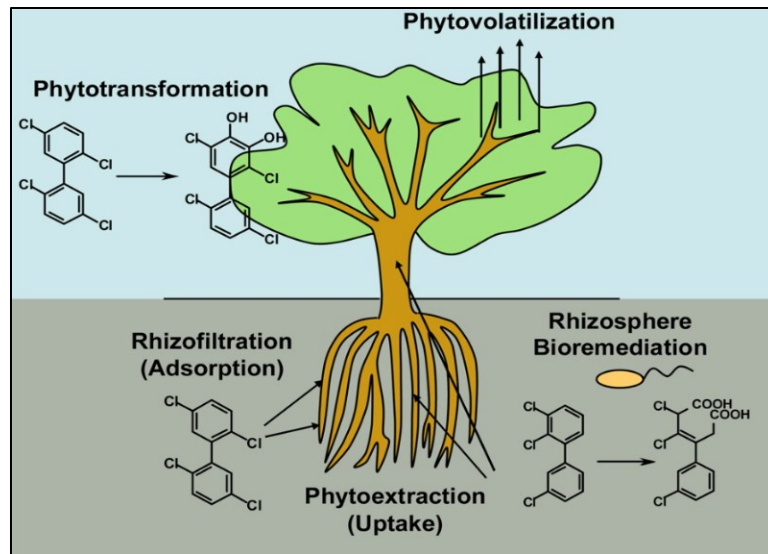


Figure 2.3 Different processes of phytoremediation of organic pollutants.

(Van Aken, 2008)

The transformation of contaminants inside the plant tissues can be explained by the green liver model (Figure 2.4) (Van Aken, 2008).

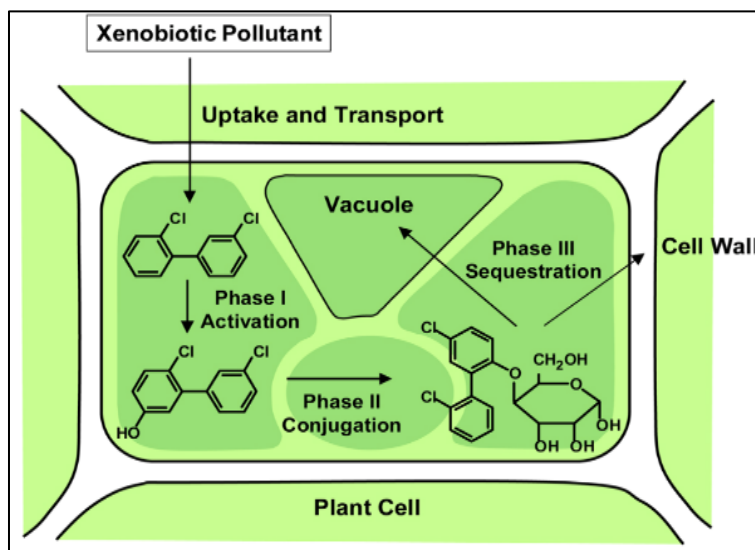


Figure 2.4 The Green liver model (Van Aken 2008)

The green liver model consists of 3 phases: Phase 1 is the initial activation which consists in oxidation, reduction or hydrolysis of the compound. The compound is then transformed into a more reactive metabolite. Phase 2 involves the conjugation between the activated product and a plant origin molecule. In phase 3, the conjugate product from phase 2 undergoes sequestration and is then stored in plant organelles such as vacuole, or incorporated into biopolymers such as lignin (Van Aken, 2008).

The first evidence of phytoremediation of PCBs came in around 1977. PCBs have been shown to undergo rhizoremediation, phytoextraction and phytotransformation in the plant. Evidence of uptake of PCBs by poplar plants was shown by Liu et al (2008). They developed a relationship between the $\log K_{ow}$ and translocation of PCBs in the plants. They predicted that only moderately hydrophobic PCBs could be efficiently taken up by the plant tissues.

Aslund et al., (2008) observed increasing PCB concentration in the stem and leaves of pumpkin plants exposed to PCB contaminated field.

PCBs with higher hydrophobicity ($\log K_{ow} > 3.5$) have initially been predicted not to be taken up within plants (Aslund et al., 2008). Despite this prediction, a number of recent studies on zucchini and pumpkin plants (*Cucurbita pepo*) have shown that hydrophobic PCBs are capable of uptake, accumulation, translocation and sequestration by plants.

Liu et al. (2008) conducted experiments with poplar plants exposed to lesser chlorinated PCBs in hydroponic solutions. They observed that up to 51.3% of the PCBs could be removed just by volatilization. The next observation was that up to 91% of the PCBs were removed by the whole poplar plants. After 20 days of exposure, a large proportion of the PCBs was found inside the root tissues. A few PCB congeners were also found in the shoot and leaves of exposed poplar plants.

Zhai et al. (2014) also confirmed the uptake of hydroxylated PCBs by plants by exposing whole poplar plants to the OH metabolites of 4-monochlorobiphenyl. They observed that the wood and the bark had higher concentration of the metabolites compared to the roots and the leaves. Also the concentration of the metabolites was higher in the plants as opposed to the solution. This indicates that the poplar plant is the main source of conversion of the parent PCB to its hydroxylated metabolites.

Nicotina tabacum (tobacco) has been studied by Rezek et al. (2008) for uptake and translocation of PCBs. Tobacco plants were exposed to dichlorinated PCB congeners for a time period of 14 days. Hydroxylated metabolites of the PCB were found to accumulate

in the plant. They also observed conversion of PCBs to methoxy PCBs and hydroxy-methoxy metabolites of PCBs.

2.5 Use of Molecular Approaches in plant science

Higher plants have been shown to be capable of metabolizing environmental contaminants and generating stress responses via various mechanisms (Skirycz, 2010). Plants continuously adapt to different stress conditions (Versulues et al., 2006) and most of these changes are regulated at transcriptional levels. For instance numerous studies have been performed on the toxicity response of plants to heavy metals (Hall, 2002). Van Assche and Clijsters (1990) showed that metals are capable of binding to sulphhydryl groups in proteins, which in turn can lead to the inhibition of activity. Dietz et al. (1999) reported the formation of free radicals and reactive oxygen species in plants, upon exposure to heavy metals, in turn causing oxidative stress.

Extensive research has also been conducted on the molecular response of plants to environmental stresses. Tsang et al. (1991) reported an abundant increase in the enzyme superoxide dismutase under different stress conditions such as photoinhibitory conditions and xenobiotic stresses upon exposure to the herbicide paraquat. Oxidative stress has frequently been associated with high temperature, salinity and drought conditions (Smirnoff, 1998). It is also known to cause denaturation of functional and structural proteins. Environmental stresses have been noted to cause activation of similar cell signaling pathways (Knight and Knight, 2001; Zhu, 2002).

Plants are known to modify their tolerance to stress by manipulating the genes involved in the functioning and maintaining of cellular components (Wang et al., 2003). Response to stress is activated by multiple signaling pathways that in turn activate gene

transcription and further mechanisms that occur subsequently (Wang et al., 2003). Chinnumswamy et al. (2004) provided a detailed study on several abiotic stress signaling pathways and molecules involved in stress responses.

Among the techniques used for studying these genetic and molecular changes is RT-qPCR, RNA sequencing, and microarrays. RNA sequencing would be the most preferred method due to its high-speed, high-sensitivity, and high-throughput (Han et al., 2015). However, it still harbors various challenges as it is still in the early stages of development. Some of the challenges involved are that protocols have not been fully optimized yet and it incurs high cost and high times consumption owing to complex computational analysis (Martin et al., 2016). RT-qPCR and microarrays combined can provide results that are as reliable and far more cost-effective. cDNA and microarrays have been widely used for gene expression analysis, since their discovery in the mid-90s (Wullschleger and Difazio, 2003). Microarrays enable the analysis of various molecular mechanisms involved in the regulation of plant defense mechanisms and stress responses (Aharoni and Vorst, 2002). This allows the possibility of linking gene expression to changes in physiology (Schena et al., 2000). Microarray gene expression profiling consists of mRNA isolation, labeling of the mRNA with a fluorophore, followed by hybridization to the microarray chips (Galbraith and Edwards, 2010). The results are often compared with RT-qPCR results for confirmation. The use of Minimal Information About Microarray Experiments (MIAME) guidelines also makes it possible for uniformity during reporting of results, as these guidelines have been adopted by a majority of plant expression databases (Rensink and Buell, 2005). As an example, Margini et al. (2009), conducted experiments to study the effects of soil metal

contamination on *A. thaliana* gene expression using microarrays. They were able to identify several up-regulated and down-regulated genes related to copper and lead contamination. Sudo et al. (2008) were successful in identifying genes involved in response of rice leaves to copper stress using microarrays and RT-qPCR.

2.6 FTIR and its application in plant science

With an increasing world population, it is estimated that we will need alternate sources of energy rather than tapping into more fossil fuels. This has led to a significant growth in studies related to bioethanol production from lignocellulosic plant materials (Kristensen et al., 2008). However, efficient bioethanol production highly depends on the lignification of the plant cell wall (Kang et al., 2014). The plant cell walls comprises a certain amount of lignin, which is a cross-linked heteropolymer. It is lignin that provides rigidity and chemical stability to the plant cell wall (Albersheim et al, 2010). Delignification of the cell wall is a major step in bioethanol production, which can results in high costs of the entire process. Thus the lignin removal plays a major role in enhancing the feasibility of bioethanol production (Polle and Douglas, 2010). It has been demonstrated by Chen et al. (2006) that high ethanol yield can be achieved by genetic engineering of the lignin content.

Wet chemical methods used to determine lignin content involve intense labor and are time consuming. Therefore, there is an increased demand for high-throughput, non-invasive techniques for lignin content determination (Zhou et al., 2011).

Spectroscopy is the study of the dispersion of light through an object into various colors that correspond to different energies. Based on the energies of the dispersed light, the composition of the object can be determined (Gok et al., 2015). For any light wave,

the energy and the wavelengths are inversely proportional. There are a range of spectroscopic techniques including IR, UV/Vis and NMR. Of all these, we will be studying our samples using IR spectroscopy. FTIR stands for Fourier Transform Infrared, and is the preferred method for IR spectroscopy. The basic principle underlying this method is that when a sample is exposed to IR radiation, based on the structure and composition of the sample, some of the radiation gets absorbed and some is transmitted (Baker et al., 2014). A fingerprint of the sample is generated by the resulting signal in the form of a spectrum based on interferometric modulation.

IR is an excellent tool to use because it allows for the analysis of the sample in a non-destructive manner. Baker et al. (2014) have described procedures for the sample preparation and analysis for different kind of biological samples. FTIR spectroscopy allows for the direct characterization of molecular components by measuring the absorbance of infrared light by the vibrational modes of the molecules (Brown et al., 2017). Alonso-Simon et al. (2011) have described the monitoring of plant cell wall composition with the use of FTIR spectroscopy. They were successful in analyzing the effect of cellulose biosynthesis inhibitors on the cell wall. Kacurakova et al. (2000) have studied in detail the plant cell walls using FTIR. They found that polysaccharides could be identified distinctively in the mid IR ($1200-800\text{ cm}^{-1}$) region. Studies have also been done on the chemical structure differences of soft and hardwood. They provided a summary of the IR bands observed which may help in our analysis.

FTIR has been known to be a non-invasive analytical technique, capable of providing unique molecular chemical composition information, based on the FTIR spectrum (McCann et al., 1992; Yu, 2004). Thumanu et al. (2015) investigated the

change in cellular components of cassava leaves using FTIR micro-spectroscopy. Using FTIR analysis, they were able to study changes associated with concentration changes in proteins, lipids, pectins and polysaccharides, in the epidermis and mesophyll tissues. There have been some studies conducted on the chemical composition of wood. For example, Chen et al. (2010) conducted FTIR spectroscopy along with multivariate analysis for the quantification of lignin, cellulose and hemi-cellulose content in the wood samples. Based on their analysis, they characterizes fingerprint wavelengths for the different components. For instance, the bending of different groups of lignin were assigned at 1595, 1510/1507, 1270 and 1230 cm^{-1} . In the same way, the wavelengths at 1739 and around 1321 -1317 were associated with the vibrations of the different groups of cellulose. The paper on the analysis of lignocellulosic biomass using infrared techniques by Xu et al. (2013), provides a summary on the progress and prospects for the applications of infrared techniques.

CHAPTER 3 EFFECTS OF POLYCHLORINATED BIPHENYLS (PCBS) AND THEIR HYDROXYLATED METABOLITES (OH-PCBS) ON ARABIDOPSIS THALIANA

The sections presented in this chapter have been published in Subramanian S., Schnoor J. and Van Aken B. "Effects of Polychlorinated Biphenyls (PCBs) and their Hydroxylated Metabolites (OH-PCBs) on Arabidopsis thaliana", Environ. Sci. Technol. 2017, 51, 12, 7263-7270.

This publication corresponds to Specific Aim 1 and in part with Specific Aim 2.

Specific aim 1 focuses on the physiological response of *A. thaliana* plants exposed to PCBs and OH-PCBs. In order to achieve this aim, *A. thaliana* plants were exposed to a suite of PCBs and their hydroxylated congeners. Germination and growth toxicity tests showed that most parent PCBs did not result in significant toxicity whereas the OH-PCB congeners of the mono-, di- and tri-chlorinated PCBs displayed a significant toxicity

This chapter also relates to **Specific aim 2**, which focuses on understanding the regulation of the metabolism of PCBs and OH-PCBs by *A. thaliana* at the transcriptomic level. In order to understand the toxic effects of PCBs and OH-PCBs on *A. thaliana*, the plants were exposed to subinhibitory concentration of 2,5-DCB and 4'-OH-2,5-DCB and expression microarrays were used to analyze differential gene expression. The analysis of gene expression patterns revealed that the genes up-regulated on exposure to 2,5-DCB were involved in response to toxic stress and detoxification mechanisms. Nevertheless, only 2,5-DCB resulted in the enrichment of up-regulated genes that are involved in the protection of plants against toxic compounds and thus, in the further detoxification mechanisms. This aim was further studied in detail in chapter 4.

3.1 Abstract

Plants metabolize polychlorinated biphenyls (PCBs) into hydroxylated derivatives (OH-PCBs), which are sometimes more toxic than the parent PCBs. The objective of this research was to compare the toxicity of a suite of PCBs and OH-PCBs toward the model plant, *Arabidopsis thaliana*. While parent PCBs and higher-chlorinated OH-PCBs exhibited a low or non-detectable toxicity, lower-chlorinated OH-PCBs significantly inhibited the germination rate and plant growth, with IC₅₀ ranging from 1.6 to 12.0 mg L⁻¹. The transcriptomic response of *A. thaliana* to 2,5-dichlorobiphenyl (2,5-DCB), and its OH-metabolite, 4'-OH-2,5-DCB, was then examined using whole-genome expression microarrays (Affymetrix). Exposure to 2,5-DCB and 4'-OH-2,5-DCB resulted in different expression patterns, with the former leading to enrichment of genes involved in response to toxic stress and detoxification functions. Exposure to 2,5-DCB induced multiple xenobiotic response genes, such as cytochrome P-450 and glutathione S-transferases, potentially involved in the PCB metabolism. On the contrary, exposure to both compounds resulted in downregulation of genes involved in stresses not directly related to toxicity. Unlike its OH-derivative, 2,5-DCB was shown to induce a transcriptomic profile similar to plant safeners, which are non-toxic chemicals stimulating detoxification pathways in plants. The differentiated induction of detoxification enzymes by 2,5-DCB may explain its lower phytotoxicity as compared with 4'-OH-2,5-DCB.

3.2 Introduction

Polychlorinated biphenyls (PCBs) are persistent and toxic pollutants which have been widely dispersed into the environment. Hydroxylated derivatives of PCBs (OH-PCBs)

are produced by biological and/or abiotic oxidation of PCBs (Tehrani & Van Aken, 2014). The first step of the metabolism of PCBs in higher organisms often involves the formation of OH-PCBs, which is catalyzed by oxidative enzymes, such as cytochrome P-450 monooxygenases (Buckman et al., 2006; Chroma et al., 2003; Grimm et al., 2015). It has also been suggested that OH-PCBs could be formed in the atmosphere through reaction with hydroxyl radicals and/or could originate from commercial formulations (Anderson and Hites, 1996; Marek et al., 2013). As transformation products of PCBs, OH-PCBs are widely dispersed in the environment and they have been detected in a variety of samples, including air, water, sediments, and animal tissues (Marek et al., 2013; Kawano et al., 2005; Awad et al., 2016). OH-PCBs have raised environmental concerns because of their reported toxicity for a variety of organisms – sometimes even higher than the toxicity of parent PCBs (Grimm et al., 2015; Montano et al., 2013; Bhalla et al., 2016).

Higher plants have been shown to take up, accumulate, and, to some extent, metabolize environmental pollutants, including PCBs (Sanderman, 1994; Schnoor et al., 1995; Van Aken et al., 2010). Several plant species were shown to uptake PCBs through the roots and, to some extent, translocate them to aerial parts (Zeeb et al., 2006; Liu & Schnoor, 2008; Aslund et al., 2008). Within plant tissues, PCBs are thought to be metabolized through a three-step process known as 'green liver model' (Sanderman, 1994), which is typically initiated by their oxidation into OH-derivatives (Van Aken et al., 2010; Lee and Fletcher, 1992; Kucerova et al., 2000). Phytotoxicity studies have shown that PCBs exert generally moderate effects, which are variable depending on the PCB congener and the plant species (Weber and Mrozek, 1979; Mahanty, 1986). For

instance, Weber and Mrozek (1979) reported that the PCB mixture, Aroclor 1254 (100 mg L⁻¹) resulted in 27% growth inhibition in soybean plants and 3% growth stimulation in fescue plants. On the other hand, no information is available about the toxicity of OH-PCBs for plants, even though the reported toxicity of PCBs may be, in part, due to OH-metabolites formed following the exposure.

Understanding the effect of PCBs and OH-PCBs on plants is important because plants are the basis of the terrestrial food web and can be used for soil remediation – a process known as phytoremediation. The objective of the present study is to determine and compare the toxicity of a suite of PCBs and their mono-OH congeners for the model plant, *Arabidopsis thaliana*. In order to further understand the effects of these compounds on plants, changes in gene expression were examined in *A. thaliana* exposed to the model PCB, 2,5-dichlorobiphenyl (2,5-DCB) and its major OH-derivative, 4'-OH-2,5-DCB, using whole-genome expression microarrays (Affymetrix). The hypothesis driving this research is that low-molecular weight OH-PCBs are more toxic than their parent compounds, which is reflected by distinct gene expression patterns.

3.3 Methods

Chemicals

Chlorobiphenyl (CB), dichlorobiphenyl (DCB), trichlorobiphenyl (TCB), tetrachlorobiphenyl (TeCB), and their OH-derivatives were purchased from Accustandard (New Haven, CT) in purity $\geq 99\%$ or custom-synthesized in purity $\geq 99\%$ by the Superfund Research Program Synthesis Core at the University of Iowa (Iowa City,

IA). Phytoagar was obtained from Plant Media (Dublin, OH). Murashige and Skoog (MS) salt base was obtained from Carolina (Burlington, NC).

Germination and growth tests

A. thaliana, ecotype Columbia (Col-0/Redei-L211497, Ohio State University, Columbus, OH) were grown as we described in Kaveh et al. (2013). Surface-sterilized seeds (95% ethanol for 5 min and 0.6% sodium hypochloride for 5 min) were placed in Petri dishes containing sterile semi-solid nutrient medium (0.5-strength MS nutrient solution with 0.3% sucrose and 0.7% phytoagar, pH 7.2) supplemented with increasing concentrations of the toxicants. Most PCBs and OH-PCBs were tested above their solubility limit and were added to the medium as an acetone stock solution (5,000-mg L⁻¹) to ensure proper dispersion of the toxicant, following the guidelines for testing aquatic toxicity of insoluble substances (OECD, 2006). Control seeds were grown in the nutrient medium supplemented with the solvent carrier only (acetone, ≤ 1% v/v). Seeds were incubated at 25°C under white (cool) fluorescent light (0.38 ± 0.02 W ft⁻²) with a 16-h light/8-h dark photoperiod. After 7 days, the germination rate was determined by visual observation (plantlets with two visible green leaves were counted as germinated) and expressed as the percentage of germinated seeds – (number of germinated seeds/initial number of seeds) × 100. After 21 days, surviving plantlets were removed from the medium, washed with water, dried by blotting, and weighed to determine the fresh biomass. The biomass growth was expressed as a percentage relative to the biomass of non-exposed controls – (biomass of exposed plants/biomass of non-exposed plants) × 100. Two or three replicate dishes containing at least 20 seeds/plantlets (from 20 to 32)

per dish were used for each treatment – representing a minimum of 40 seeds/plantlets per treatment. The phytotoxic effect of PCBs and OH-PCBs was expressed by the inhibition concentration 50% (IC50) obtained by plotting the experimental dose – response curve (percent inhibition vs. contaminant concentration) and computing a 3-parameter sigmoidal regression (Prism 6.0, GraphPad, La Jolla, CA).

Gene expression analysis using microarrays

A. thaliana was grown in 10*10-cm Magenta boxes as described above. Plantlets were exposed to sub-inhibitory concentrations of 2,5-DCB (50 mg L⁻¹) and 4'-OH-2,5-DCB (5 mg L⁻¹). Control plantlets were grown in the presence of the solvent carrier (acetone) only. Six boxes containing five plantlets each were used for each treatment. After 21 days of growth, plantlets were removed from the medium, immediately immersed in RNAlater™ (Ambion, Foster City, CA), and incubated at 4°C for 24 h. Plantlets were then washed, dried, and stored at -80°C until RNA extraction. The five plants from each box were combined, and RNA was extracted from the whole tissue using TRIzol® Plus RNA Purification kit with on-column PureLink® DNase treatment (ThermoFisher, Waltham, MA). Homogenization of plant tissue was performed using bead beating (1-mm glass beads, 4,200 rpm, 40 sec), after addition of TRIzol® reagent. Purified RNA was kept at -80°C. RNA was quantified by the OD₂₆₀ using a NanoDrop™ ND-2000 spectrophotometer (Vernon Hills, IL). The quality of RNA was assessed by the ratios OD₂₆₀/OD₂₈₀ and OD₂₆₀/OD₂₃₀ and using an Agilent 2100 Bioanalyzer (Santa Clara, CA). RNA used for microarray analysis had OD₂₆₀/OD₂₈₀ ratios of 2.0 – 2.2, OD₂₆₀/OD₂₃₀ ratios of 1.8 – 2.7, and RNA integrity numbers (RIN) of 6.9 – 8.0. RNA

samples were labeled and hybridized to the Arabidopsis Gene 1.0 ST Arrays according to the manufacturer's instructions (Affymetrix, Santa Clara, CA). Three biological replicates per treatment were utilized for microarray experiments. Scanned microarray images were analyzed using the Expression Console™ and Transcriptome Analysis Console version 3.0 (Affymetrix). Analysis of differential gene expression level was conducted using One-Way Between-Subject ANOVA (unpaired) with p -value < 0.01.

Reverse-transcription real-time PCR

Quantitative analysis of gene expression was performed for selected genes using reverse-transcription real-time PCR (RT-qPCR) as described in Kaveh et al.(2013). The internal standard was the 18S ribosomal DNA (rDNA) gene. RT-qPCRs were conducted using the same RNA as used for the microarray experiments. RNA was reverse-transcribed into cDNA using SuperScript® III First-Strand Synthesis system and oligo-dT primers (Invitrogen, Foster City, CA). Negative controls were generated by running the reactions without reverse-transcriptase. Gene sequences were retrieved from The Arabidopsis Information Resource (TAIR) database (www.arabidopsis.org/) and used to design gene-specific real-time primers using PrimerQuest (IDT, Coralville, IA). When possible (for 9 out of 12 genes), primers were designed with one primer spanning an exon-intron boundary (Table 3.1) Real-time PCR quantification of cDNA was performed on a StepOnePlus™ Real-Time PCR System using SYBR® Green PCR Master Mix (Applied Biosystems, Foster City, CA). CT (cycle threshold) values were computed by the StepOnePlus™ Software (version 2.1; Applied Biosystems).

Table 3.1 List of primers used for the reverse-transcription real-time PCR of selected genes

TAIR ID	Gene Description	Fold Change		Primer Sequences (5' → 3')	
		2,5-DCB	4'-OH-2,5-DCB		
AT1G6019 0	U-box domain-containing protein 19	-23.68	-36.64	Forward	GGATGTGGCGGAGAGTTTAG
				Reverse	CATCTCTTCTTCGTCTCCCTTG
AT1G2988 0	Plant intracellular ras group-related LRR 7	-7.98	-13.30	Forward	CCAAACTCCATTGGTTGTCCTTC
				Reverse	TCTTCGAGTGACCTGCAATTT
AT4G3441 0	Ethylene-responsive transcription factor ERF109	-11.43	-14.90	Forward	CCAGTGACAGCACAGTGATAAG
				Reverse	AGTTACAGCCGAGACATCCT
AT1G4949 0	Leucine-rich repeat family protein	-4.18	-4.97	Forward	GGTCTCATCACCAGAACAATCA
				Reverse	GATGTGTCAGTGGGAAGGAGAAG
AT3G4566 0	Probable nitrate excretion transporter 2	-3.08	-4.90	Forward	CATTTCTCTAGTGGGCGTAGTT
				Reverse	GGGCTTGACATAACTTTGATGC
AT2G4705 0	Plant invertase/pectin methylesterase inhibitor domain-containing protein	-3.95	-4.86	Forward	AAGAATGAGTGGTGAGTCTGTG
				Reverse	GAGCAACGTGTCGGTATCTT
AT5G3912 0	Germin-like protein subfamily 1 member 15	25.75	20.25	Forward	GTGCCACTGAGATCCTTGTT
				Reverse	GTTCAGCACTTTGGCGAATAAA
AT5G3911 0	Germin-like protein subfamily 1 member 14	7.47	8.32	Forward	ACCAAGCAGGAACCACTAATAA
				Reverse	GTCTATGCGGACCAAGGATATT
AT4G0877 0	Putative apoplastic peroxidase Prx37	4.00	6.76	Forward	ACCTTCCAGCTCCATTCTTTAC
				Reverse	AAGGTGTGACCACCAGAAAG
AT1G6417 0	Cytochrome P450 71A16 (CYP71A16)	3.48	4.78	Forward	GAGATCATTGGCGGGATTCTTC
				Reverse	TAGAGTGTGCGAGCACCGTTAG
AT3G1331 0	Chaperone DNAJ-domain containing protein	3.51	4.25	Forward	GTCGGAGAGTTTCTAGCCTCTA
				Reverse	CCGACGCATCTGGATGATATAC
AT3G0639 0	Hypothetical protein	4.57	3.81	Forward	ACTCGCCCGCTTTCATATAC
				Reverse	CAGGTTTCAAGAGTAGAGAGATGG
AT3G4176 8	18S ribosomal DNA (rDNA)			Forward	GGTGGTGCATGGCCGTTCTTAG
				Reverse	GGGCATCACAGACCTGTTAT

3.4 MIAME compliance

This article is written in compliance with the Minimum Information about a Microarray Experiment (MIAME) guidelines (<http://www.mged.org/miame>). Microarray data have been submitted to the Gene Expression Omnibus (<http://www.ncbi.nlm.nih.gov/geo>).

3.5 Results and discussion

Toxicity testing

The toxicity of 17 mono-OH PCBs and their 11 parent compounds (including mono-, di-, tri-, and tetra-chlorinated congeners) for *A. thaliana* was determined based on germination and growth tests conducted over 7 and 21 days, respectively (Figure 3.2, Table 3.2).

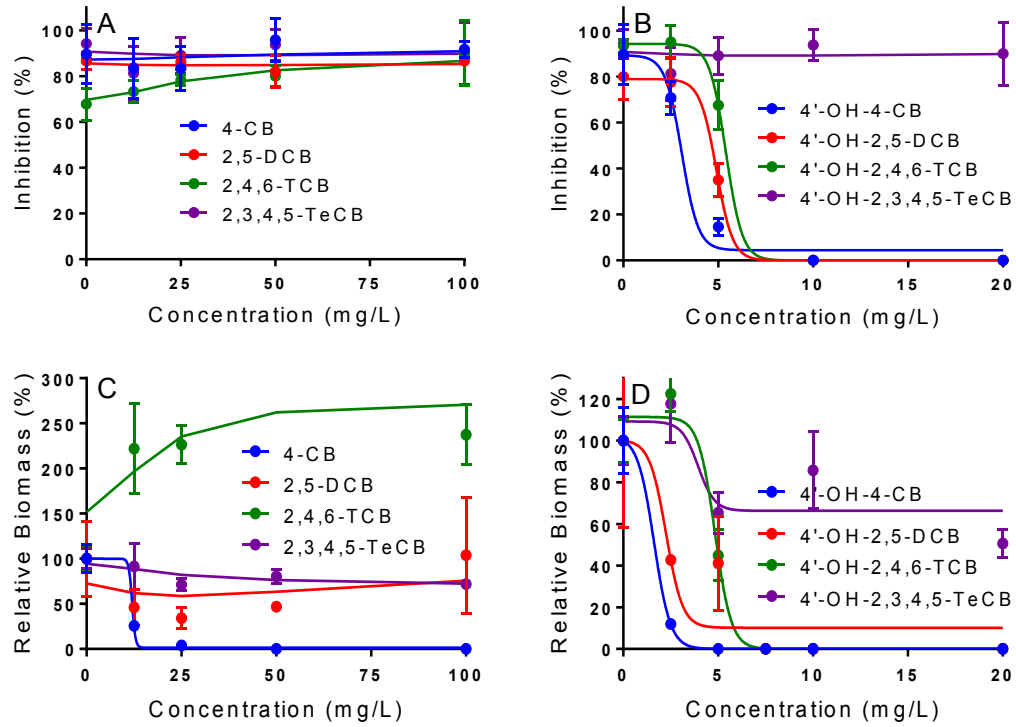


Figure 3.1 Dose-response curves of *A. thaliana* exposed to PCBs (panels A, C) and OH-PCBs (panels B, D) as determined through germination tests (panels A, B) and growth tests (panels C, D). Solid lines for significantly toxic compounds (4-CB, 4'-OH-4-CB, 4'-OH-2,5-DCB, and 4'-OH-2,4,6-TCB) were obtained by fitting to a 3-parameter sigmoidal inhibition model (Prism 5.04, Graphpad). Solid lines for other, non-toxic compounds were obtained by 2nd-order smoothing of experimental data (Prism 5.04, Graphpad). The error bars represent standard deviations between biological replicates.

Table 3.2 Toxicity of PCBs and OH-PCBs for A. thaliana as determined through germination and growth tests. IC50 were computed from the dose-response curves using a three-parameter sigmoidal model. IC50, 95%-confidence interval (CI 95%), coefficients of determination R²), and octanol-water partition coefficients (K_{ow}) are presented

PCBs & OH-PCBs	Abbreviation	Germination Tests			Growth Tests			
		IC50 (mg L ⁻¹)	CI 95% (mg L ⁻¹)	R ²	IC50 (mg L ⁻¹)	CI 95% (mg L ⁻¹)	R ²	logK _{ow}
3-Chlorobiphenyl	3-CB	ND ^a	ND	ND	ND	ND	ND	4.59
4-Hydroxy-3-	4-OH-3-CB	5.19	4.38-5.99	0.9	5.08	4.22-5.94	0.95	4.49
4-Chlorobiphenyl	4-CB	ND	ND	ND	12.02	11.76-12.27	1.00	4.60
4'-Hydroxy-4-	4'-OH-4-CB	3.08	1.73-4.42	0.9	1.62	1.62-1.63	1.00	4.50
2,4'-Dichlorobiphenyl	2,4'-DCB	ND	ND	ND	ND	ND	ND	5.11
4-Hydroxy-2,4'-	4-OH-2,4'-DCB	2.23	1.67-2.79	0.9	3.65	2.99 - 4.31	1.00	5.11
2,5-Dichlorobiphenyl	2,5-CDB	ND	ND	ND	ND	ND	ND	5.20
2'-Hydroxy-2,5-	2'-OH-2,5-DCB	10.74	8.90-12.58	0.9	5.25	4.52-5.97	0.99	4.88
3'-Hydroxy-2,5-	3'-OH-2,5-DCB	10.01	8.78-11.24	0.9	5.44	1.45-9.42	0.80	5.11
4'-Hydroxy-2,5-	4'-OH-2,5-DCB	4.90	4.78-5.02	1.0	2.47	0.54-4.40	0.89	5.11
3,4-Dichlorobiphenyl	3,4-DCB	ND	ND	ND	ND	ND	ND	5.19
4'-Hydroxy-3,4-	4'-OH-3,4-DCB	7.31	5.34-9.27	0.9	7.28	6.42-8.15	0.96	5.10
2,2',5-Trichlorobiphenyl	2,2',5-TCB	ND	ND	ND	NT ^b	NT		5.65
4'-Hydroxy-2,2',5'-	4'-OH-2,2',5'-TCB	8.05	0.00-20.84	0.9	NT	NT		5.44
2,4,6-Trichlorobiphenyl	2,4,6-TCB	ND	ND	ND	ND	ND	ND	5.97
2'-Hydroxy-2,4,6-	2'-OH-2,4,6-TCB	9.97	8.13-11.81	0.9	5.40	3.26-7.55	0.93	5.58
3'-Hydroxy-2,4,6-	3'-OH-2,4,6-TCB	5.07	4.02-6.12	0.9	4.60	3.87-5.33	0.99	5.87
4'-Hydroxy-2,4,6-	4'-OH-2,4,6-TCB	5.40	5.30-5.50	1.0	4.83	3.93-5.73	0.98	5.88
3,3',4-Trichlorobiphenyl	3,3',4-TCB	ND	ND	ND	ND	ND	ND	5.66
4'-Hydroxy-3,3',4-	4'-OH-3,3',4-TCB	ND	ND	ND	ND	ND	ND	5.48
2,2',5,5'-Tetrachlorobiphenyl	2,2',5,5'-TeCB	ND	ND	ND	ND	ND	ND	6.29
4'-Hydroxy-2,2',5,5'-	4'-OH-2,2',5,5'-TeCB	5.28	3.51-7.06	0.8	2.27	0.89-3.64	0.86	6.11
2,3,4,5-Tetrachlorobiphenyl	2,3,4,5-TeCB	ND	ND	ND	ND	ND	ND	6.55
2'-Hydroxy-2,3,4,5-	2'-OH-2,3,4,5-TeCB	ND	ND	ND	ND	ND	ND	6.24
3'-Hydroxy-2,3,4,5-	3'-OH-2,3,4,5-TeCB	ND	ND	ND	ND	ND	ND	6.46
4'-Hydroxy-2,3,4,5-	4'-OH-2,3,4,5-TeCB	ND	ND	ND	ND	ND	ND	6.46
3,3',4,5'-Tetrachlorobiphenyl	3,3',4,5'-TeCB	ND	ND	ND	ND	ND	ND	6.26
4'-Hydroxy-3,3',4,5'-	4'-OH-3,3',4,5'	ND	ND	ND	ND	ND	ND	6.09

Because higher-chlorinated PCBs and OH-PCBs have low water solubility, a homogenous dispersion was prepared by dissolution in acetone prior to addition to the hydroponic medium (OECD, 2006). The low volume of acetone stock solution added (< 1%) was not expected to significantly modify water solubility of the solutes (Schwarzenbach et al., 2016). Based on the germination tests, none of the parent PCBs exhibited a detectable or significant toxicity (i.e., IC_{50} non determined–ND) at the concentration of 100 mg L^{-1} , with germination rates ranging from 73 to 94% relative to non-exposed controls (Figure 3.1, Table 3.1). OH-PCBs with one to three chlorine atoms exhibited a recordable toxicity at the concentration of 20 mg L^{-1} or lower (except 4'-OH-3,3',4-TCB), with IC_{50} values ranging from 2.2 mg L^{-1} to 10.7 mg L^{-1} . Three OH-PCBs with four chlorine atoms showed no detectable toxicity at the concentration of 20 mg L^{-1} , with germination rates ranging from 77 to 100% relative to non-exposed controls. 4'-OH-2,2',5,5'-TeCB was shown toxic with IC_{50} equal to 5.3 mg L^{-1} (Figure 3.1, Figure 3.2).

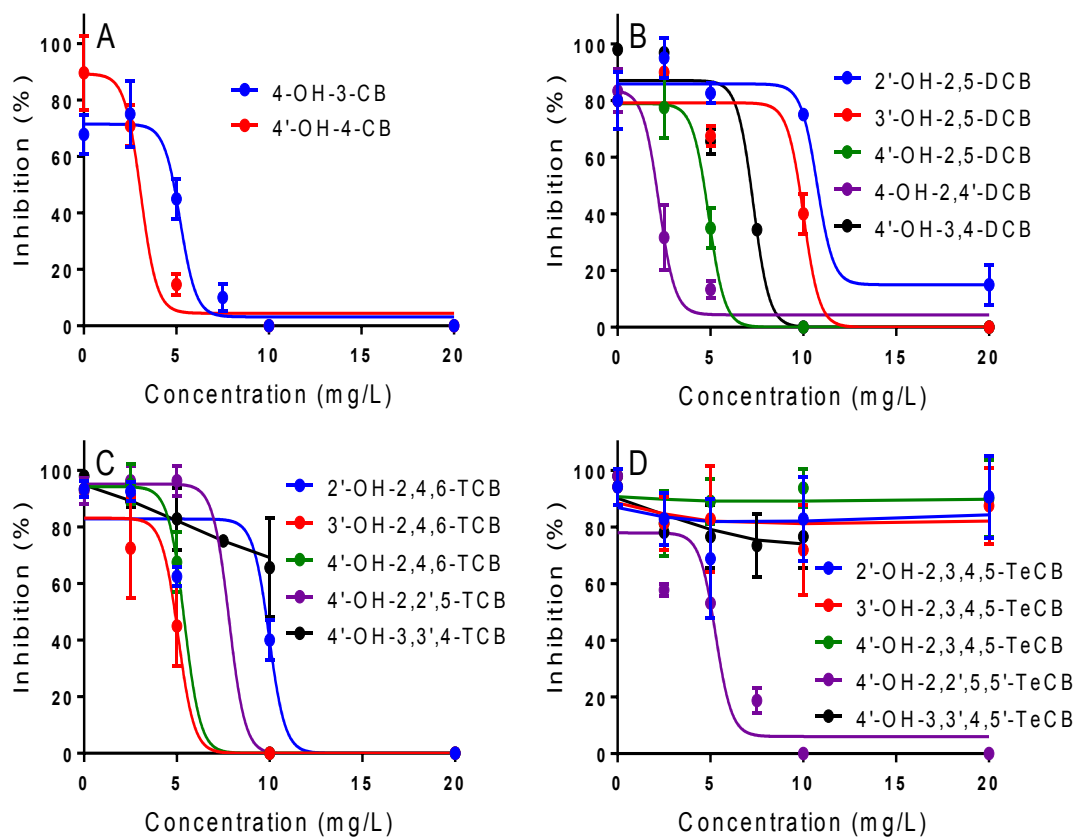


Figure 3.2 Dose-response curves of *A. thaliana* exposed to OH-PCBs

(panel A: mono-chlorinated congeners, panel B: di-chlorinated congeners, panel C: tri-chlorinated congeners, and panel D: tetra-chlorinated congeners) as determined through germination tests. The inhibitory effect of PCBs and OH-PCBs is presented as a percentage of the germination rate. Solid lines for significantly toxic compounds were obtained by fitting to a 3-parameter sigmoidal inhibition model (Prism 5.04, Graphpad). Solid lines for other, non-toxic compounds (4'-OH-3,3',4-TCB and tetra-chlorinated congeners, except 4'-OH-2,2',5,5'-TeCB) were obtained by 2nd-order smoothing of experimental data (Prism 5.04, Graphpad). The error bars represent the standard deviation between biological replicates.

Growth tests based on biomass were overall consistent with germination tests, showing no significant toxicity – and sometimes strong stimulation of the growth – with parent PCBs (except 2,4'-DCB) and tetra-chlorinated OH-PCBs (except 4'-OH-2,2',5,5'-TeCB) – biomasses after 21 days ranged from 59 to 237% relative to non-exposed controls (Figure 3.1, Table 3.2). 2,4'-DCB resulted in growth stimulation (227% of non-exposed control) at 25 mg L⁻¹ and complete (100%) inhibition at 50 mg L⁻¹ and higher. As with germination tests, mono-, di-, and tri-chlorinated OH-PCBs (except 4'-OH-3,3',4'-TCB) and one tetra-chlorinated OH-PCBs (4'-OH-2,2',5,5'-TeCB) resulted in significant growth inhibition with IC₅₀ values ranging from 1.6 mg L⁻¹ to 12.0 mg L⁻¹ (Figure 3.1, Figure 3.3).

The data fitted generally well the toxicity model, with coefficients of determination (R^2) ≥ 0.9 for most analyses.

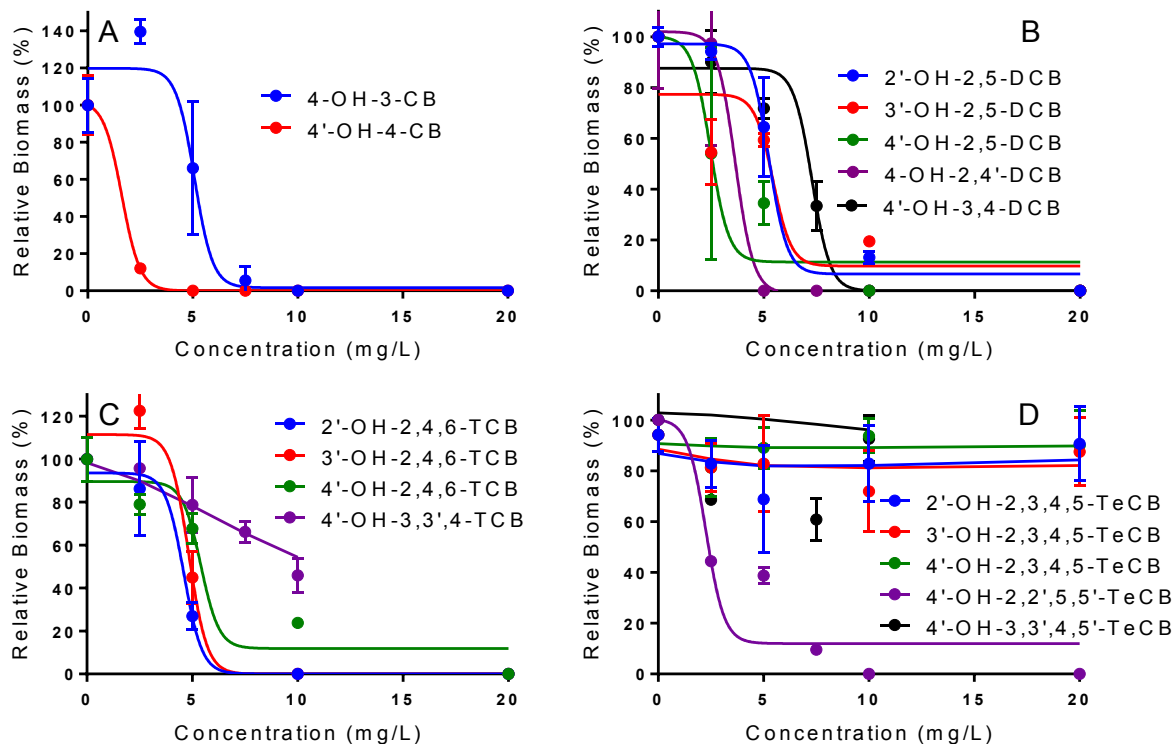


Figure 3.3 Dose-response curves of *A. thaliana* exposed to OH-PCBs (panel A: mono-chlorinated congeners, panel B: di-chlorinated congeners, panel C: tri-chlorinated congeners, and panel D: tetra-chlorinated congeners) as determined through biomass growth tests. The inhibitory effect of PCBs and OH-PCBs is presented as a percentage of the biomass in non-exposed controls. Solid lines for significantly toxic compounds were obtained by fitting to a 3-parameter sigmoidal inhibition model (Prism 5.04, Graphpad). Solid lines for other, non-toxic compounds (4'-OH-3,3',4-TCB and all tetra-chlorinated congeners, except 4'-OH-2,2',5,5'-TeCB) were obtained by 2nd-order smoothing of experimental data (Prism 5.04, Graphpad). The error bars represent the standard deviation between biological replicates.

Consistently with our results, several studies have shown that PCBs exert low to moderate toxicity toward terrestrial plants, except when exposed to high concentrations (Weber & Mrozek, 1979; Mahanty, 1986). For instance, Weber and Mrozek (Weber & Mrozek, 1979) observed that exposure of soybean plants to Aroclor 1254 for 26 days resulted in approx. 11%, 27%, and 22% growth inhibition (based on fresh weight) at the concentration of 10, 100, and 1,000 mg L⁻¹, respectively. In fescue plants, exposure to

Aroclor 1254 for 42 days resulted in growth stimulation at low concentration (10 – 100 mg L⁻¹) and 16% inhibition at 1,000 mg L⁻¹. Examining the phytoremediation capabilities of nine plant species growing in various soils contaminated with Aroclor 1260, Zeeb et al. (Zeeb et al., 2006) reported biomass reduction and toxic stress symptoms (e.g., chlorosis, leaf yellowing) in most plants growing in the highest contaminated soil (4,200 mg kg⁻¹), while plants growing in lower contaminated soils (90 and 250 mg kg⁻¹) showed no toxic effects. On the other hand, several studies have shown more severe effects of PCBs on plants at concentrations well below the maximum concentration (100 mg L⁻¹) used in our study. Jin et al. (Jin et al., 2011) exposed *Arabidopsis* plants – growing on agar plates and in soil – to increasing concentration of 2,2',3,3'-TeCB and observed that low concentrations (below 10 mg L⁻¹) resulted in growth stimulation (e.g., increase of root length and plant height), while higher concentration (40 to 100 mg L⁻¹) resulted in growth inhibition. Wang et al. (Wang, et al., 2017) recently showed that exposure of alfalfa seedlings to low concentration of 3,3',4,4'-TCB (3 mg L⁻¹) had a significant impact on plant growth (reduction of root and shoot biomass dry weight by 17.6 and 20.6%, respectively). In addition, PCB exposure caused reduction of the chlorophyll content and oxidative stress. Ahammed et al. (2013) investigated the effects of foliar application of Aroclor 1242 on tomato plants and observed that low concentrations (0.4, 2, and 10 µL L⁻¹) resulted in significant reduction of the plant biomass (reduction of root and shoot dry weight by 8.0, 33.0, and 38.4%, respectively). The authors also reported a negative effect on photosynthesis (e.g., chlorophyll content and CO₂ assimilation) and increase of lipid peroxidation and reactive oxygen species (ROS). Using hairy root culture of *Solanum nigrum*, Kucerova et al. (Kucerova et al., 2000) showed that exposure to 3 mg L⁻¹ of

various lower-chlorinated PCBs resulted in 21 to 53% inhibition of the biomass growth after 14 days. This rather high toxicity may be explained by the higher susceptibility of plant cell cultures as compared with whole plants. Exposure to 3,3',4,5'-TCB, which is coplanar, dioxin-like PCBs, did not result in noticeable toxicity. This result was expected because plants do not possess the aryl hydrocarbon receptor (AHR), which is the specific target of coplanar PCBs in mammals (Hahn, 1998). In several cases, hormesis (i.e., biphasic dose-response including metabolic stimulation at low exposure level and inhibition at higher level) was observed, as it was the case in our study. Hormesis has been described in plants, as well as other organisms, exposed to various types of stressors, including toxic chemicals (Kaveh et al., 2013; Jin, et al., 2011; Garcia-Sanchez et al., 2015). It is believed that low level of stress triggered cellular signaling pathways and defense mechanisms involving transcription factors, protective proteins, and antioxidant molecules, which have beneficial effects for the organisms (Balasubramaniyam, 2015).

Although not involving the model plant, *A. thaliana*, prior studies have shown that plants were capable to take up and translocate PCBs, which were then susceptible to induce phytotoxicity. For instance, in their study on PCB uptake and translocation by nine plant species (see above), Zeeb et al. (2006) reported that the PCB concentration in plant tissues varied widely depending on the species and the concentration in soil (from 90 to 4,200 mg kg⁻¹) and were higher in root tissues (from 47 to 6,500 mg kg⁻¹) than in shoot tissues (from 0.32 to 470 mg kg⁻¹). In a pilot-scale field study conducted at a PCB-contaminated site (Aroclor 1254/1260), Aslund et al. (2008) reported root concentrations of 66, 40, and 15 mg kg⁻¹ and shoot concentration of 13, 6.7, and 4.7 mg kg⁻¹ in sedge,

pumpkin, and tall fescue, respectively. Shoot bioaccumulation factors (BAFs) ranged from 0.1 (tall fescue) to 0.29 (sedge). Liu and Schnoor (2008) have reported that hybrid poplar trees (*Populus deltoides* × *nigra*) were capable to take up various PCBs with one to four chlorine atoms from the hydroponic solution. Concentrations of PCBs in root tissues decreased when the degree of chlorination increased (from 1.1 mg kg⁻¹ fresh weight with mono-chlorinated PCB to 0.17 mg kg⁻¹ with tetra-chlorinated PCB). Root concentration factors (RCFs) increased with the degree of chlorination (from 185 with mono-chlorinated PCB to 1965 with tetra-chlorinated PCB), likely reflecting different dosages in the hydroponic solution and differential sorption of PCBs to root tissues. As in other studies, no or low levels of PCBs were detected in aerial parts (stems and leaves), showing limited translocation of PCBs in plants. Results published in the literature suggest that uptake and toxic effects of PCBs are highly variable depending on the congeners and the plant species. Not only that different PCBs are characterized by different hydrophobicities – and bioavailabilities, but different congeners have different substitution patterns, potentially conferring distinct biological activities (e.g., dioxin-like versus non-dioxin-like PCBs). As generally observed in experimental toxicology, the different toxicities reported in the literature likely reflect different experimental conditions, including the route of exposure (e.g., medium), duration of the experiment, and detected endpoints (e.g., germination, biomass).

To the best of our knowledge, the toxicity of OH-PCBs to plants has not been previously investigated. Consistently with our observations, studies conducted in other organisms, including animals and bacteria, have also reported that OH-PCBs can be more toxic than the parent PCBs (Grimm et al., 2015; Montano et al., 2013; Bhalla, et al.,

2016). Even though hydroxylation of PCBs is generally regarded as a detoxification mechanism, *in vitro* studies have shown that OH-PCBs can be further hydroxylated, generating toxic species, such as quinones and reactive oxygen species (ROS), which can damage DNA and form adducts with proteins, lipids, and nucleic acids (Grimm et al., 2015). In fact, the toxicity of many halogenated contaminants, including PCBs, has been attributed to the formation of OH-metabolites (Grimm et al., 2015; Montano et al., 2013). The higher toxicity of OH-PCBs (expressed by the IC_{50}) as compared with their parent PCB could be explained partially by the higher solubility (expressed by the $\log K_{ow}$) and bioavailability of the former (Table 3.2) (Bhalla et al., 2016; Camara et al., 2004). Although well studied in humans and other animals (Grimm et al., 2015; Montano et al., 2013), the mechanisms of toxicity of PCBs and OH-PCBs in plants have received little attention.

Gene expression microarrays

The transcriptional response of *Arabidopsis* plantlets exposed to 2,5-DCB and 4'-OH-2,5-DCB was investigated using Affymetrix whole-genome expression microarrays. Concentration of 50 mg 2,5-DCB L⁻¹ and 5 mg 4'-OH-2,5-DCB L⁻¹ – which resulted in sub-inhibitory effects based on germination and growth tests – were chosen for microarray experiments. After filtering out low-quality and insignificant expression results – based on One-Way ANOVA ($p < 0.01$) –, 958 genes were shown to be differentially expressed by exposure to 2,5-DCB as compared with the non-exposed control, including 323 (33.7%) upregulated genes (change fold > 2.0) and 635 (66.3%) downregulated genes (change fold < 0.5). Exposure to 4'-OH-2,5-DCB resulted in

differential expression of 508 genes, including 167 (32.9%) upregulated genes and 341 (67.1%) downregulated genes. Two hundred fifty nine (259) genes were differentially expressed by exposure to both 2,5-DCB and 4'-OH-2,5-DCB, including 35 upregulated genes (10.8% of total upregulated genes) and 224 downregulated genes (35.3% of total downregulated genes). Many more genes were downregulated than upregulated in response to 2,5-DCB and 4'-OH-2,5-DCB, suggesting that gene expressions – and many related biological functions – were inhibited by the two compounds. Hierarchical clustering revealed that exposure to both 2,5-DCB and 4'-OH-2,5-DCB induced rather similar gene expression profiles as compared with control plants (Figure 3.4), which may be explained by the structural similarities between the two compounds or by the partial in vivo transformation of 2,5-DCB into 4'-OH-2,5-DCB.

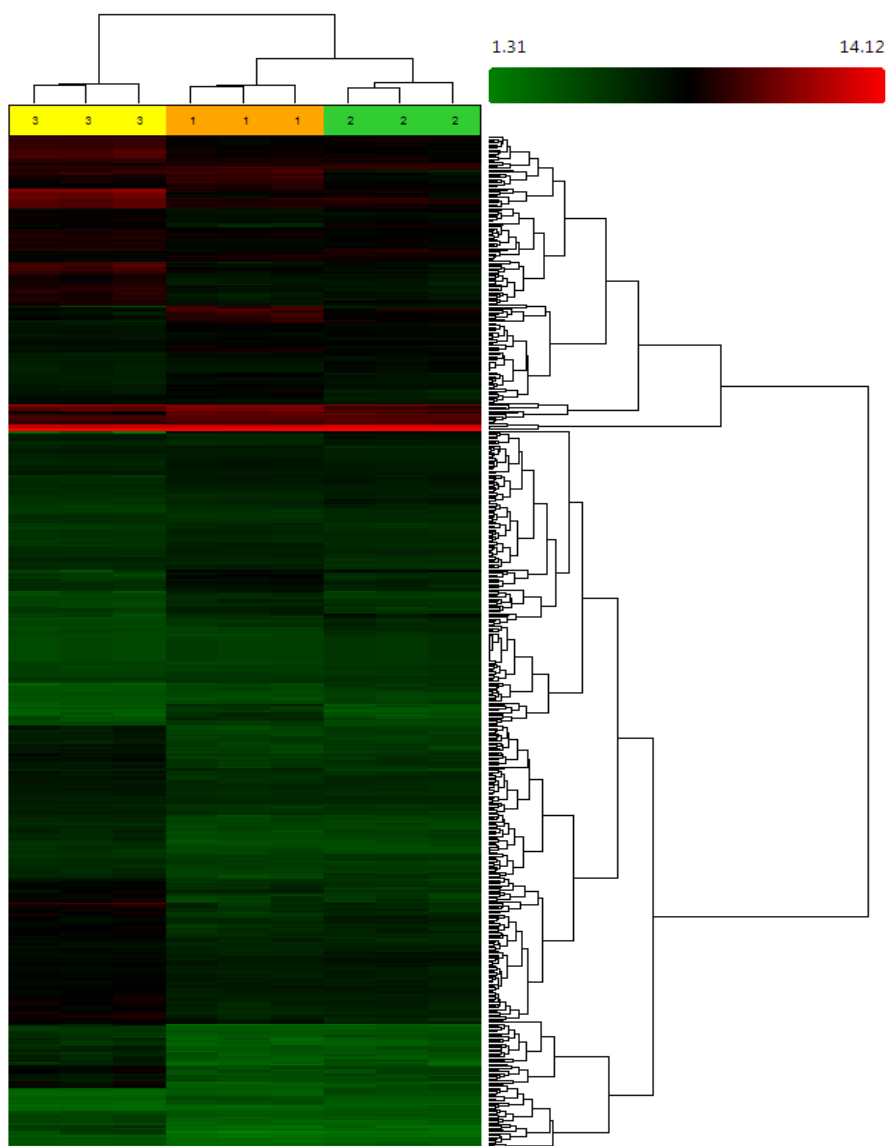
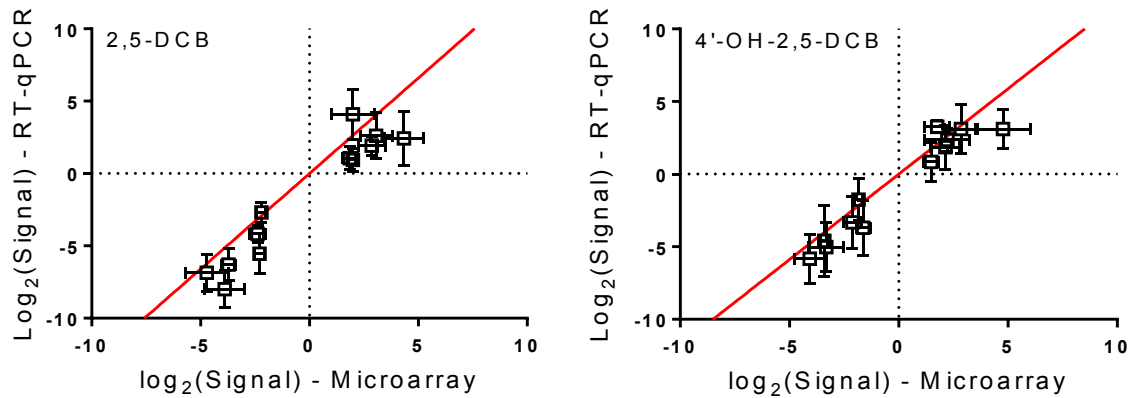


Figure 3.4 Hierarchical clustering of gene expression profiles of A. thaliana (Arabidopsis Gene 1.0 ST Arrays, Affymetrix) exposed to 2,5-DCB (orange), 4'-OH-2,5-DCB (green), and non-exposed controls (yellow). The analysis was performed on three biological using the Affymetrix Expression Console™.

In order to validate the microarray results, quantitative analysis of gene expression was performed using RT-qPCR on 12 selected genes, including genes down- and upregulated upon exposure to both compounds. Expression levels obtained with microarrays have

been plotted against expression levels obtained by RT-qPCR (Figure 3.5), showing satisfactory correlations (Pearson's correlation coefficient of 0.95 and 0.96 for exposure to 2,5-DCB and 4'-OH-DCB, respectively).



*Figure 3.5 Comparison of relative gene expression levels in *A. thalianae* exposed to 2,5-DCB (left) and 4'-OH-2,5-DCB (right) using reverse-transcription real-time PCR (RT-qPCR) and microarrays (*Arabidopsis* Gene 1.0 ST Arrays, Affymetrix). Error bars represent the standard deviations of three biological replicates.*

Functional categories of differentially expressed genes

The enrichment of transcripts in Gene Ontology (GO) categories was interrogated using the Remote Term Enrichment tool with Bonferroni correction (<http://amigo.geneontology.org/rte>) (Carbon et al., 2009). To avoid redundancy, only the most specific categories (i.e., at the lowest hierarchical level) were considered for the analysis (Table 3.3). Genes upregulated in response to 2,5-DCB showed strong enrichment in several Biological Processes related to the metabolism of toxic substances, including toxin catabolism, response to toxic substance, and response to oxidative stress, which likely reflect the phytotoxicity of 2,5-DCB. Exposure to 2,5-DCB also induced genes not directly related to toxic chemicals, such as genes involved in response to

oomycetes and bacteria. Many biotic and abiotic stresses result in similar cellular damages and, hence, similar plant responses, potentially explaining PCB-mediated induction of genes involved in different types of stress (Skipsey et al., 2011). Plants possess various mechanisms of xenobiotic sensing and it is difficult to distinguish between responses directly induced by the toxic compounds and indirectly induced by their deleterious effects (Ramel et al., 2012). Prior studies focusing on transcription factors in *Arabidopsis* showed overlap of genes expressed in response to different types of stresses (Singh et al., 2002). Toxic compounds have been reported to induce genes involved in response to oxidative stress and pathogens, which frequently produce toxins inside the host cells (Ramel et al., 2012; Jiang et al., 2012). Genes upregulated in response to 2,5-DCB showed also enrichment in Molecular Functions potentially involved in the PCB metabolism, including glutathione transferase activity, alkyl/aryl transferase activity, and transmembrane transporter activity (Table 3.3). Genes upregulated upon exposure to 4'-OH-2,5-DCB did not show significant enrichment in specific GO terms. On the other hand, genes downregulated upon exposure to both 2,5-DCB and 4'-OH-2,5-DCB showed enrichment in several Biological Processes involved in jasmonic acid (JA) and abscisic acid (ABA) signaling, along with genes involved in response to a range of biotic and abiotic factors not directly related to toxicity, such as cold, wounding, water deprivation, chitin, drought, and salt (Table 3.3). Stress response in plants involves complex signaling pathways which can act synergistically – as shown above – or antagonistically. For instance, response to flooding has been shown to reduce plant resistance to herbivores through negative cross-talk between ethylene and JA signaling (Nguyen, et al., 2016). Other examples of the negative effect of a type of stress

on tolerance to other stresses have been reported, including drought, toxic nanoparticles, and pathogens (Garcia-Sanchez et al, 2015; Ramegowda & Senthil-Kumar, 2015) ABA and JA are plant hormones involved in many plant processes, including response to biotic (JA) and abiotic (ABA) stresses (Fujita et al, 2006). The downregulation of JA and ABA signaling pathways by 2,5-DCB and 4'-OH-2,5-DCB is therefore consistent with the repression of genes involved in response to a variety of stresses and it can be interpreted as a plant attempt to prioritize protection against toxic compounds. Genes downregulated upon exposure to both compounds showed also enrichment in Molecular Functions involved in transcription, including transcription corepressor activity and transcription cofactor activity (Table 3.3). Inhibition of transcription is a common response to toxic stress and it is consistent with the larger number of genes downregulated than upregulated upon exposure to 2,5-DCB and 4'-OH-2,5-DCB. A remarkable difference between the two compounds is that exposure to 2,5-DCB, but not 4'-OH-DCB, resulted in a large enrichment of upregulated genes involved toxic response and detoxification reactions (see below).

Table 3.3 Enrichment analysis of genes up- and downregulated upon exposure to 2,5-DCB and 4'-OH-2,5-DCB based on Biological Processes and Molecular Functions.

GO terms with enrichment p -value < 0.01 are presented. Only the most specific GO terms (lowest hierarchical level) are shown. GO terms of special interest are underlined.

Response to 2,5-DCB					
Upregulated Genes			Downregulated Genes		
Biological Processes	Enrich	P -Value	Biological Processes	Enrich	P -Value
<u>Toxin catabolic process</u>	17.89	6.92E-06	<u>Regulation of jasmonic acid signaling</u>	12.18	5.13E-03
Defense response to oomycetes	17.68	3.22E-03	Cold acclimation	11.44	6.46E-05
<u>Response to toxic substance</u>	14.25	1.62E-10	Response to wounding	6.11	1.37E-09
Response to bacterium	4.15	2.54E-03	Response to chitin	5.98	1.35E-04
<u>Response to oxidative stress</u>	4.10	2.95E-03	Response to water deprivation	4.95	5.49E-08
Response to inorganic	2.97	6.14E-03	<u>Response to jasmonic acid</u>	4.18	2.66E-03
<u>Oxidation-reduction process</u>	2.88	1.39E-06	<u>Response to abscisic acid</u>	3.26	4.04E-05
			Hormone-mediated signaling	2.80	3.38E-05
			<u>Transcription, DNA-templated</u>	1.85	3.31E-03
			<u>Regulation of transcription</u>	1.71	8.57E-03
Molecular Function	Enrich	P -Value	Molecular Function	Enrich	P -Value
<u>Glutathione transferase activity</u>	16.72	8.03E-06	<u>Transcription corepressor activity</u>	11.71	4.32E-03
<u>Alkyl or aryl transferase activity</u>	8.22	8.06E-04	<u>Transcription factor activity</u>	1.90	3.92E-03
<u>Secondary transmembrane transporter activity</u>	5.32	5.42E-05			
Ion transmembrane transporter activity	3.19	3.43E-03			
<u>Oxidoreductase activity</u>	2.81	4.75E-06			

Table 3.3 (continued)

Response to 4'-OH-2,5-DCB					
Biological Process	Enrich.	P-Value	Biological Process	Enrich.	P-Value
<i>No significant enrichment</i>			<u>Regulation of jasmonic acid signaling</u>	23.78	5.84E-05
			Cold acclimation	20.12	2.53E-06
			Response to wounding	10.10	3.54E-12
			Response to water deprivation	9.68	5.75E-15
			Response to chitin	7.79	1.99E-03
			<u>Response to jasmonic acid</u>	6.72	8.27E-05
			Regulation of defense response	5.97	9.51E-04
			<u>Response to abscisic acid</u>	4.72	3.13E-06
			Cellular response to acid	4.07	3.34E-03
			Response to salt stress	3.74	5.31E-03
			Defense response	2.55	3.58E-04
			Signal transduction	2.29	2.45E-03
Molecular Function	Enrich.	P-Value	Molecular Function	Enrich.	P-Value
<i>No significant enrichment</i>			<u>Transcription corepressor activity</u>	22.87	4.96E-05

The transcriptomic profile of *Arabidopsis* exposed to 2,5-DCB and 4'-OH-2,5-DCB was then searched against the Arabidopsis expression microarray database, Genevestigator (genevestigator.com/gv/) (Hruz et al., 2008). The analysis was restricted to expression profiles recorded with wild-type *A. thaliana* and the *Perturbation Category, Chemicals*. The expression profile induced by 2,5-DCB (based on the 300 most upregulated genes), was most similar to the ones induced by various toxic organic and inorganic chemicals, including pesticides, metals, and ozone (Figure 3.6). Five out of the 10 expression profiles most similar to the one induced by 2,5-DCB – but not by 4'-OH-2,5-DCB – were associated with 5-(3,4-dichloro-phenyl)furan-2-yl)(piperidin-1-yl) methanethione (DFPM), 4-chloro-6-methyl-2-phenylpyrimidine (CMP), fenclorim, and

sulfomethuron methyl. Intriguingly, fenclorim, sulfomethuron methyl, and CMP are structurally related compounds involving a pyrimidine moiety with rather similar substitution patterns, suggesting that they act by binding the same receptor(s) (Figure 3.7). In addition, CMP and fenclorim are compounds known as plant safeners, which are non-toxic chemicals commonly applied to crops together with pesticides because of their protective effect on the plants (Skipsey et al., 2011; Riechers et al., 2010). Plant safeners are thought to act through the induction of detoxification enzymes, known as xenobiotic response genes (XRG). Best characterized are the cytochrome P-450 monooxygenases, glucosyltransferases, glutathione S-transferases, and ABC transporter proteins (Behringer et al., 2011). For instance, fenclorim was found to be a strong inducer of glutathione S-transferases in *Arabidopsis* (DeRidder et al., 2002). DFPM, although not structurally related to CMP, fenclorim, or sulfomethuron methyl, is a signaling molecule synthesized in plants in response to safeners, such as fenclorim and CMP (Rigal et al., 2014). On the other hand, the 4'-OH-2,5-DCB expression profile was most similar to the ones induced by the herbicides, norflurazon and benzothiadiazole, and the phytotoxic antibiotic, sulfamethoxazole (data not presented).

Dataset: 116 perturbations from data selection: AT_AFFY_ATH1-0
 Showing 297 measure(s) of 300 gene(s) on selection: AT-1

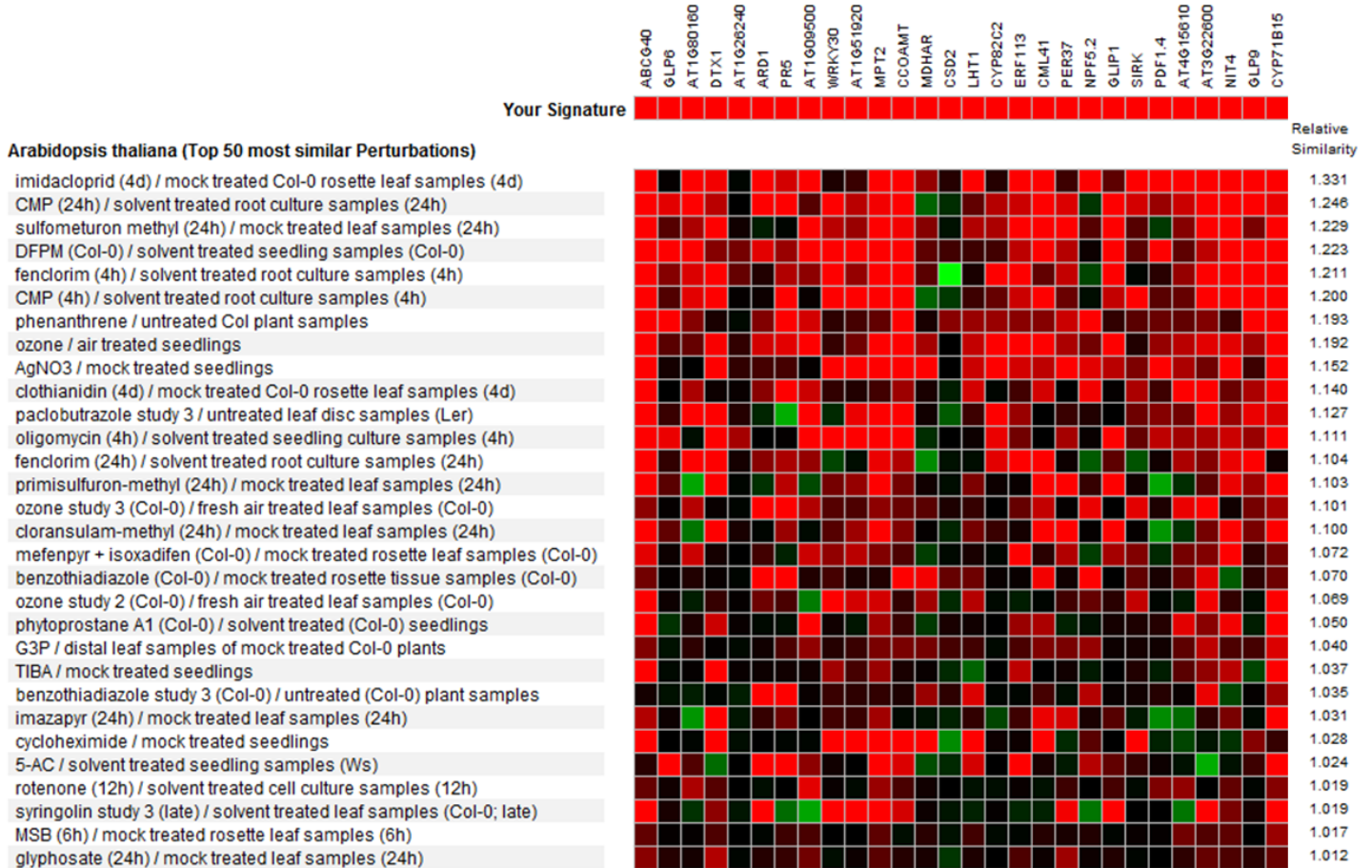
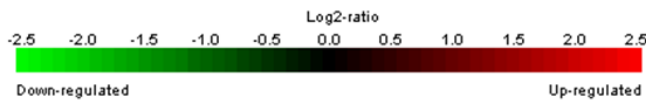


Figure 3.6 Comparison between gene expression profiles of *A. thaliana* exposed to 2,5-DCB and other chemicals.

The analysis has been conducted using Geneinvestigator 5-12-03 (Platform: Affymetrix Arabidopsis ATH1 Genome Array, genetic background: wild-type, perturbation: chemical). The relative similarity score was calculated by Geneinvestigator from Euclidean distance between the 2,5-DCB signature and each experiment of the selection.

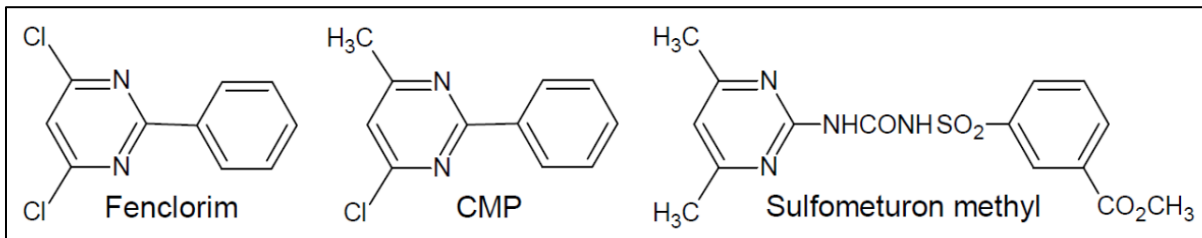


Figure 3.7 Chemical structure of fenclorim, 4-chloro-6-methyl-2 phenylpyrimidine (CMP), and sulfometuron methyl.

Table 3.4 Expression levels of potential xenobiotic response genes (XRGs) in Arabidopsis plants exposed to 2,5-DCB versus non-exposed controls (upper part) and 4'-OH-2,5-DCB versus non-exposed controls (lower part)

2,5-DCB versus Control		
TAIR ID	Fold Change	Description
AT1G15520	34.48	ABC transporter G family member 40
AT4G31970	7.08	Cytochrome P450, family 82, subfamily C, polypeptide 2
AT5G66690	5.60	UDP-glycosyltransferase 72E2
AT2G30140	5.58	UDP-glycosyltransferase 87A2
AT2G34500	4.94	Cytochrome P450 710A1
AT1G74590	4.76	Glutathione S-transferase TAU 10
AT1G22400	4.74	UDP-glycosyltransferase 85A1
AT1G69930	4.56	Glutathione S-transferase TAU 11
AT2G37770	4.29	Aldo-keto reductase family 4 member C9
AT3G10320	4.21	Glycosyltransferase family 61 protein
AT1G69920	3.91	Glutathione S-transferase TAU 12
AT3G11340	3.68	UDP-dependent glycosyltransferase 76B1
AT1G60750	3.61	Probable aldo-keto reductase 6
AT4G37370	3.44	Cytochrome P450, family 81, subfamily D, polypeptide 8
AT1G02930	3.21	Glutathione S-transferase 6
AT5G05340	3.16	Peroxidase 52
AT2G47800	3.13	ABC transporter C family member 4
AT4G34135	2.99	UDP-glucosyltransferase 73B2
AT3G53480	2.96	ABC transporter G family member 37
AT3G14680	2.94	Cytochrome P450, family 72, subfamily A, polypeptide 14
AT2G29420	2.87	Glutathione S-transferase tau 7
AT5G44990	2.81	Glutathione S-transferase family protein
AT3G09270	2.78	Glutathione S-transferase TAU 8
AT2G15490	2.69	UDP-glycosyltransferase 73B4
AT4G37520	2.69	Peroxidase 50
AT5G20400	2.62	Oxidoreductase, 2OG-Fe(II) oxygenase family protein
AT5G37600	2.60	Glutamine synthetase 1;1
AT1G60730	2.52	Probable aldo-keto reductase 5
AT2G29490	2.52	Glutathione S-transferase TAU1
AT5G02780	2.50	Glutathione transferase lambda 1
AT2G37760	2.47	Aldo-keto reductase family 4 member C8
AT1G17170	2.47	Glutathione S-transferase TAU 24
AT3G14620	2.42	Cytochrome P450, family 72, subfamily A, polypeptide 8
AT5G67400	2.42	Peroxidase 73
AT4G31870	2.38	Glutathione peroxidase 7
AT4G37530	2.27	Peroxidase 51
AT2G43820	2.18	UDP-glucosyltransferase 74F2
AT2G24180	2.13	Cytochrome P450 71B6
AT1G05240	2.13	Peroxidase; Peroxidase superfamily protein
AT1G78380	2.07	Glutathione S-transferase TAU 19
AT3G03470	2.05	Cytochrome P450, family 87, subfamily A, polypeptide 9
AT2G02390	2.04	Glutathione S-transferase zeta-class 1
AT4G01660	2.04	ABC transporter I; hypothetical protein
AT1G05670	-2.05	UDP-Glycosyltransferase superfamily protein
AT3G14630	-2.08	Cytochrome P450, family 72, subfamily A, polypeptide 9
AT1G10360	-2.36	Glutathione S-transferase TAU 18
AT5G06530	-2.95	ABC transporter G family member 22
AT2G29450	-3.73	Glutathione S-transferase tau 5
AT2G06050	-3.81	12-oxophytodienoate reductase 3
AT3G48520	-4.27	Cytochrome P450, family 94, subfamily B, polypeptide 3

Table 3.4 (continued)

4'-OH-2,5-DCB versus Control		
TAIR ID	Fold Change	Description
AT4G36430	4.09	Peroxidase 49
AT2G38390	4.01	Peroxidase 23
AT1G17180	2.97	Glutathione S-transferase TAU 25
AT5G64100	2.54	Peroxidase 69
AT5G20400	2.42	Oxidoreductase, 2OG-Fe(II) oxygenase family protein
AT4G11290	2.37	Peroxidase 39
AT5G02780	2.23	Glutathione transferase lambda 1
AT4G20240	2.22	Cytochrome P450, family 71, subfamily A, polypeptide 27
AT4G15500	2.19	UDP-glycosyltransferase 84A4
AT5G48000	2.14	Cytochrome P450 708A2
AT4G37410	2.02	Cytochrome P450, family 81, subfamily F, polypeptide 4
AT2G06050	-3.20	12-oxophytodienoate reductase 3
AT2G29450	-3.32	Glutathione S-transferase tau 5
AT3G48520	-3.96	Cytochrome P450, family 94, subfamily B, polypeptide 3

Consistently with these observations, exposure to 2,5-DCB resulted in upregulation (fold-change > 2.0) of 38 genes encoding potential XRGs, while exposure to 4'-OH-2,5-DCB induced only 11 potential XRGs (Table 3.4). XRGs overexpressed in response to 2,5-DCB include genes possibly involved in the three phases of 'green liver model' (Sanderman, 1994), including initial activation, conjugation with plant molecules, and sequestration in plant organelles (e.g., vacuole) or structures (e.g., cell wall). Cytochrome P450 monooxygenases and peroxidases have been suggested to be involved in initial hydroxylation of PCBs (Phase I) (Chroma et al., 2003), glutathione S-transferases and glycosyltransferases are known to be involved in conjugation of several chlorinated xenobiotic compounds (Phase II) (Sanderman, 1994), and ABC transporter proteins are known to be involved in vacuolar excretion of xenobiotic conjugates (Phase III) (Tommasini et al., 1998). A prior study focusing on the transcriptomic response of *Arabidopsis* exposed to 2,2',3,3'-TeCB similarly reported overexpression of genes potentially involved in the three phases of the green liver model, including cytochrome P-450 monooxygenases, UDP-glucuronosyltransferases, and transporter proteins (Jin et al,

2011). Based on the observations above, we hypothesize that the differentiated induction of detoxification enzymes in response to the parent PCB, 2,5-DCB, explains its lower toxicity as compared with its OH-metabolite, 4'-OH-2,5-DCB.

It is noteworthy that our gene expression study only focused on one single PCB congener (out of 208) and one single mono-OH-PCB congener (out of 837). Other PCBs and OH-PCBs – even isomers – are likely to induce different plant responses and gene expression profiles. The goal of this study was to show that hydroxylation of a model PCB molecule, which is part of a detoxification sequence, could result in dramatic increase of toxicity, partially explained at the molecular level – for instance by changing the interaction with specific receptors and subsequent expression of specific transcription factors. As mentioned earlier, coplanar, dioxin-like PCBs exhibit high toxicity toward mammals because of their defined stereochemistry, allowing binding the aryl hydrocarbon receptor (AHR) (Hahn, 1998). Similarly, selected para-OH PCBs exert higher endocrine disruption activity – as compared with ortho- or meta-OH isomers – because of their capability to specifically bind estrogen receptor (Arulmozhiraja et al., 2005). Many studies consider PCBs in mixtures because they have been released in the environment as complex commercial formulations (e.g., Aroclor). However, one must keep in mind that each PCB and OH-PCB congener is a distinct compound, with specific chemical and physical properties, potentially resulting in different biological activities and toxicities.

Further understanding of the metabolism of PCBs in plants, which may have important implications for human health and the environment, will require additional research to identify the xenobiotic receptors and transcription factors involved in the

plant response to PCBs and their metabolites. Studying the transcriptomic profiles developing in response to various PCBs and their derivatives will help identify the structural elements necessary to activate specific receptors and trigger the detoxification sequence (i.e., comparative toxicogenomics).

3.6 Acknowledgements

This work was funded by the Iowa Superfund Basic Research Program, National Institute of Environmental Health Sciences, Grant P42ES013661. The authors want to thank Hans-Joachim Lehmler (University of Iowa) for providing some PCBs and OH-PCBs used in this study, and Sasha Eisenman (Temple University) for valuable discussion on plant hormones.

CHAPTER 4 TRANSCRIPTOMIC RESPONSE OF *ARABIDOPSIS THALIANA* EXPOSED TO HYDROXYLATED POLYCHLORINATED BIPHENYLS (OH-PCBS)

The sections presented in this chapter have been published in Subramanian S., Tehrani R. and Van Aken B. “Transcriptomic response of Arabidopsis thaliana exposed to hydroxylated polychlorinated biphenyls (OH-PCBs)”, International Journal of Phytoremediation

This chapter appertains to **Specific Aim 2**, which focuses on understanding the regulation of *A. thaliana* response to PCBs and OH-PCBs at the transcriptomic level.

The transcriptomic response was investigated using whole-genome microarrays. These results were consistent with the toxicity testing results. The three OH-derivatives generated similar gene expression data and their expression was distinct from the gene expression profiles induced by the parent PCB and non-exposed controls.

4.1 Abstract

Hydroxylated polychlorinated biphenyls (OH-PCBs) are toxic contaminants produced via biotic or abiotic transformation of PCBs. In this study, we have tested the toxicity of 2,5-dichlorobiphenyl (2,5-DCB) and three of its OH-derivatives, 2'-OH-, 3'-OH-, and 4'-OH-2,5-DCB toward the model plant, *Arabidopsis thaliana*. Toxicity tests showed that the parent 2,5-DCB (5 mg L⁻¹) had little effect on the plants, while all three OH-metabolites (5 mg L⁻¹) exhibited a significant toxicity, with 4'-OH-2,5-DCB being the most potent (inhibition concentration 50%–IC₅₀ in germination tests = 9.8 mg L⁻¹ for 2'-OH-2,5-DCB, 9.5 mg L⁻¹ for 3'-OH-2,5-DCB, and 4.8 mg L⁻¹ for 4'-OH-2,5-DCB). Whole-genome expression microarrays (Affymetrix) showed that exposure to the three OH-PCBs resulted in rather similar expression patterns, which were distinct from the one developing in response to 2,5-DCB. Searching an *Arabidopsis* microarray database (Genevestigator) revealed that, unlike the parent compound, the three OH-derivatives induced expression profiles similar to inhibitors of brassinosteroid synthesis (i.e., brassinazole, propiconazole, and uniconazole), resulting in severe iron deficiency in exposed plants. Our results suggest that the higher phytotoxicity of OH-derivatives as compared to 2,5-DCB is at least partly explained by the inhibition of the brassinosteroid pathway.

4.2 Introduction

Hydroxylated polychlorinated biphenyls (OH-PCBs) have been widely detected in the environment, including air, water, sediments, and animal tissues (Kawano et al., 2005; Tehrani and Van Aken, 2014; Awad et al., 2016). OH-PCBs have raised environmental

concerns because they are in some cases more toxic than the parent PCBs (Grimm et al., 2015; Montano et al., 2013). OH-PCBs are formed by the biological or abiotic transformation of PCBs. The metabolism of PCBs in higher organisms is often initiated by hydroxylation reactions mediated by oxidative enzymes, such as the cytochrome P-450 monooxygenase (Grimm et al., 2015). OH-PCBs have also been suggested to be co-contaminants in commercial formulations and/or be formed in the atmosphere through reaction with the hydroxyl radical (Anderson and Hites, 1996; Marek et al., 2013).

As many organic contaminants, PCBs are susceptible to be taken up and, to some extent, metabolized by plants (Sanderman, 1994; Schnoor et al., 1995; Van Aken et al., 2010). Within plant tissues, PCBs are thought to be metabolized through a three-step process known as 'green liver model' (Sanderman, 1994), which is typically initiated by oxidation to OH-derivatives (Chroma et al., 2003; Van Aken et al., 2010). Different studies have shown that PCBs exert moderate to severe effects on plants, depending on the PCB congener and the plant species (Weber and Mozek, 1979; Mahanty, 1986).

Even though OH-PCBs are widespread in the environment, little information is available about their toxicity for plants. Understanding the effects of PCBs and OH-PCBs on plants is significant because plants are the basis of the terrestrial food web and can be used for soil remediation (i.e., phytoremediation). In a prior publication, we reported that a suite of lower-chlorinated OH-PCBs were highly toxic for the model plant, *Arabidopsis thaliana*, while most parent PCBs did not show significant effects (Subramanian et al., 2017). Gene expression analysis using 2,5-dichlorobiphenyl (2,5-DCB) and its OH-derivative, 4'-OH-2,5-DCB, showed that the parent compound – unlike the OH-derivative – induced multiple xenobiotic response genes, such as cytochrome P-450 and glutathione

S-transferases, potentially involved in the PCB metabolism, which may explain the lower phytotoxicity of PCBs as compared with their OH-derivatives.

The objective of the present study is to understand further the toxicity of PCB and OH-PCBs by comparing the effects of three OH-isomers of 2,5-DCB, 2'-OH-2,5-DCB, 3'-OH-2,5-DCB, and 4'-OH-2,5-DCB, on *Arabidopsis* plants. We used whole-genome microarrays (Affymetrix) to explain why different OH-PCB isomers have different toxic effects on plants.

4.3 Materials & Methods

Toxicity tests

A. thaliana, ecotype Columbia (Col-0/Redei-L211497, Ohio State University, Columbus, OH) was grown as we described in Subramanian et al. (2017). In short, surface-sterilized seeds were germinated in Petri dishes containing semi-solid, half-strength Murashige & Skoog (MS) medium (0.3% sucrose) supplemented with increasing concentrations of 2,5-DCB, 2'-OH-, 3'-OH-, and 4'-OH-2,5-DCBs. The toxicants were added to the medium as an acetone solution (5,000-mg L⁻¹) to final concentrations from 0.0 to 20 mg L⁻¹ for OH-2,5-DCBs and 0.0 to 100 mg L⁻¹ for 2,5-DCB. Control seeds were grown in the nutrient medium supplemented with the solvent carrier only (acetone, ≤ 1% v/v). Seeds were incubated at 25°C under white (cool) fluorescent light (0.4 ± 0.05 W ft⁻²) with a 16-h light/8-h dark photoperiod. After 7 days, the germination rate was determined by visual observation (plantlets with two visible green leaves were counted as germinated). After 21 days, surviving plantlets were removed from the medium, washed and weighed to determine the fresh biomass. Three replicate dishes containing at least 20

seeds per dish were used for each treatment. The phytotoxic effect of PCBs and OH-PCBs was expressed by the inhibition concentration 50% (IC₅₀) obtained by plotting the experimental dose – response curve (percent inhibition vs. contaminant concentration) and computing a 3-parameter sigmoidal regression (Prism 6.0, GraphPad, La Jolla, CA).

Gene expression analysis using microarrays

A. thaliana was grown in 10 × 10-cm Magenta boxes as described above. Plantlets were exposed to sub-inhibitory concentration of 2,5-DCB, 2'-OH-, 3'-OH-, and 4'-OH-2,5-DCB (5 mg L⁻¹). Control plantlets were grown in the presence of the solvent carrier (acetone) only. Six boxes containing five plantlets each were used for each treatment. After 21 days of growth, plantlets were removed from the medium, treated with RNAlater™ (Ambion, Foster City, CA) and stored at -80°C until RNA extraction. RNA was extracted from the whole plants using TRIzol® Plus RNA Purification kit with on-column PureLink® DNase treatment (ThermoFisher, Waltham, MA) as described in Subramanian et al. (2017). RNA was analyzed by the absorbance ratios OD (optical density) ₂₆₀/OD₂₈₀ and OD₂₆₀/OD₂₃₀ (NanoDrop™ ND-2000, Vernon Hills, IL). RNA integrity numbers (RIN) (Agilent 2100 Bioanalyzer, Santa Clara, CA) were between 6.6 and 7.4. RNA was labeled and hybridized to the Arabidopsis Gene 1.0 ST Arrays according to the manufacturer's instructions (Affymetrix, Santa Clara, CA). Three biological replicates per treatment were utilized. Scanned microarray images were analyzed using the Expression Console™ and Transcriptome Analysis Console™ version 3.0 (Affymetrix). Analysis of gene expression level was conducted using One-Way Between-Subject ANOVA (unpaired) with *p*-value < 0.05.

Reverse-transcription real-time PCR

Quantitative analysis of gene expression was performed for a subset of genes using reverse-transcription real-time PCR (RT-qPCR) as described in Subramanian et al. (2017). Six genes – three upregulated and three downregulated across all treatments – were selected for the analysis. The internal standard was the 18S ribosomal DNA (rDNA) gene. RT-qPCRs were conducted using the same RNA as used for the microarray experiments. RNA was reverse-transcribed into cDNA using SuperScript[®] III First-Strand Synthesis system and oligo-dT primers (Invitrogen, Foster City, CA). Negative controls were generated by running the reactions without reverse-transcriptase. Gene sequences were retrieved from The Arabidopsis Information Resource (TAIR) database (www.arabidopsis.org/) and used to design gene-specific real-time primers using PrimerQuest (IDT, Coralville, IA) (Table 4.1). Real-time PCR quantification of cDNA was performed on a StepOnePlus[™] Real-Time PCR System using SYBR[®] Green PCR Master Mix (Applied Biosystems, Foster City, CA). CT (cycle threshold) values were computed by the StepOnePlus[™] Software (version 2.1; Applied Biosystems).

Table 4.1 List of primers used for the reverse-transcription real-time PCR (RT-qPCR) of selected genes

TAIR ID	Gene Description	Fold Change		Primer Sequences (5' → 3')
AT1G47400	Hypothetical protein	9.57 – 11.57	Forward	GGAGGCGACCCATGTATTTAG
			Reverse	TAGTACTAGTCGTGCCAGTGT
AT5G59570	Homeodomain-like superfamily protein	4.80 – 6.63	Forward	GTGTCTCCTCTACCCTTCCTAA
			Reverse	CAGCTCAACTAAGTCCCATGA A
AT1G47395	Hypothetical protein	6.37 – 9.90	Forward	GTGCTTCCGTGGTGTATGTT
			Reverse	CATAGCCACTGTCATCGTCAT C
AT1G07050	CCT motif family protein	6.08 – 6.2	Forward	GAAGAGGAGCGAACGTATAT GG
			Reverse	CGACAGCGGATGAGTAGATTT
AT2G23130	Lysine-rich arabinogalactan-protein (AGP)	-2.80 – -3.95	Forward	CACCGATCCATTCTCCTTCTAC
			Reverse	AGCCTCTACAGGTGCTTCTA
AT1G50040	Formin-like protein	-3.8 – -3.95	Forward	GGTTTCAGGTTACGCTTGATTT
			Reverse	CCGACCCGGACTTCTTATTATT
AT5G24150	FAD/NAD(P)-binding oxidoreductase family protein	-3.20 – -3.29	Forward	GACGGTGCTACTGACGTTATC
			Reverse	GTTCTCTCAGGTCCCTCTCTAT
AT5G08030	PLC-like phosphodiesterases superfamily protein	-3.17 – -3.78	Forward	CAGGTCCATCCATACACATAC C
			Reverse	CAAACCATCAACACCGATCTT ATT
AT3G41768	18S Ribosomal DNA (rDNA)		Forward	GGTGGTGCATGGCCGTTCTTA G
			Reverse	GGGCATCACAGACCTGTTAT

MIAME compliance

This article is written in compliance with the Minimum Information About a Microarray Experiment (MIAME) guidelines (<http://www.mged.org/miame>). Microarray data have been submitted to the Gene Expression Omnibus (<http://www.ncbi.nlm.nih.gov/geo>).

4.4 Results and discussion

Toxicity testing

The toxicity of 2,5-DCB and its three OH-derivatives, 2'-OH-, 3'-OH-, and 4'-OH-2,5-DCB, for *A. thaliana* was determined based on germination and growth tests conducted over 7 and 21 days, respectively. Based on both germination and growth tests, the three OH-derivatives exhibited a significant toxicity at the concentration of 5 mg L⁻¹ and higher (Figure 4.1). On the other hand, exposure to the parent 2,5-DCB did not exhibit significant effects at concentration up to 100 mg L⁻¹ (data not presented). In both germination and growth tests, 4'-OH-2,5-DCB exhibited a significantly higher toxicity than 2'-OH- and 3'-OH-2,5-DCB: inhibition concentration 50% (IC₅₀) in germination tests = 4.8 mg L⁻¹ (confidence interval–CI 95% = 4.2 – 5.5 mg L⁻¹) for 4'-OH-2,5-DCB vs. 9.8 and 9.5 mg L⁻¹ (CI 95% = 9.5 – 10.1 mg L⁻¹ and 8.0 – 11.0 mg L⁻¹) for 2'-OH- and 3'-OH-2,5-DCB, respectively. The data fitted generally well the toxicity model, with coefficients of determination (R²) ranging from 0.80 to 0.99.

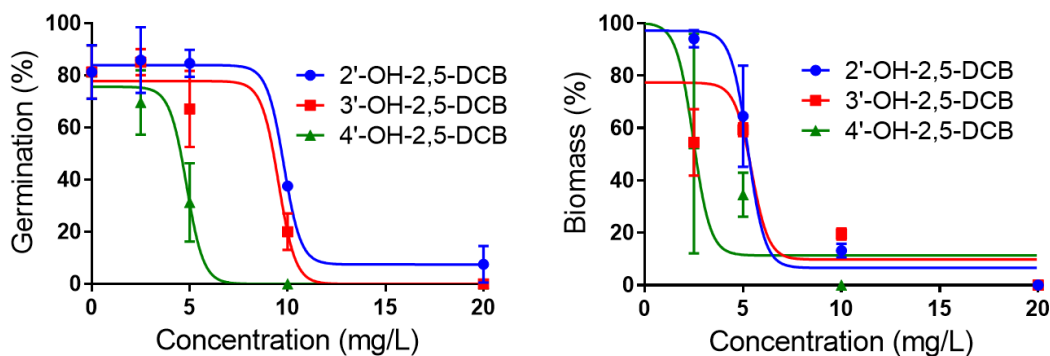


Figure 4.1 Dose-response curves of *A. thaliana* exposed to OH-PCBs

(panel A: mono-chlorinated congeners, panel B: di-chlorinated congeners, panel C: tri-chlorinated congeners, and panel D: tetra-chlorinated congeners) as determined through biomass growth tests.

Consistently with our results, several studies have shown that PCBs exert low to moderate toxicity toward terrestrial plants, except when exposed to high concentrations (Weber and Mozek, 1979; Mahanty, 1986). For instance, exposure of soybean plants to Aroclor 1254 for 26 days resulted in approx. 11%, 27%, and 22% growth inhibition at concentration of 10, 100, and 1,000 mg L⁻¹, respectively. In fescue plants, exposure to Aroclor 1254 for 42 days resulted in growth stimulation at low concentration (10 – 100 mg L⁻¹) and 16% inhibition at high concentration (1,000 mg L⁻¹) (Weber and Mozek, 1979). On the other hand, several studies have reported more severe effects of PCBs on plants at concentrations well below the maximum concentration (100 mg L⁻¹) used in our study (Jin et al., 2011; Ahammed et al. 2013; Wang et al., 2017). For instance, exposure of Arabidopsis plants to increasing concentration of 2,2',3,3'-tetrachlorobiphenyl resulted in growth stimulation low concentrations (≤ 10 mg L⁻¹) and growth inhibition at higher levels (40 to 100 mg L⁻¹) (Jin et al., 2011).

Although higher organisms are known to metabolize PCBs into OH-derivatives (Van Aken et al., 2010; Chroma et al., 2002), little information is available about the effects of OH-PCBs on plants. In a prior study, we tested the toxicity of 17 mono-hydroxylated PCBs and 11 parent compounds carrying one to four chlorine atoms toward *A. thaliana* (Subramanian et al., 2017). In this prior study, we observed none of the parent PCBs tested (except one congener) were significantly toxic at concentration up to 100 mg L⁻¹, which is consistent with the results presented here. On the other hand, all OH-PCBs with

one to three chlorine atoms exhibited a recordable toxicity at the concentration of 20 mg L⁻¹ or lower (IC50 values ranging from 2.2 mg L⁻¹ to 10.7 mg L⁻¹).

Studies conducted in other organisms, including animals and bacteria, also reported that OH-PCBs can be more toxic than the parent PCBs. The higher toxicity of OH-PCBs could be explained partially by their higher solubility and bioavailability (Bhalla et al., 2016). On the other hand, OH-PCBs are known to be further oxidized *in vivo* into toxic products, such as quinones, and generate reactive oxygen species (ROS), which can damage DNA and form adducts with proteins, lipids, and nucleic acids (Grimm et al., 2015).

Gene expression microarrays

The transcriptional response of Arabidopsis plantlets exposed to 2,5-DCB and its three OH-derivatives, 2'-OH-, 3'-OH-, and 4'-OH-2,5-DCB, was investigated using Affymetrix whole-genome expression microarrays. After filtering out low-quality and non-significant expression results – based on One-Way ANOVA ($p < 0.05$), 387 genes were shown to be differentially expressed by exposure to 2,5-DCB (as compared with non-exposed controls), including 252 (65.1%) upregulated genes (defined as genes showing an expression level at least two times higher in exposed plants than in untreated controls: i.e., fold change > 2.0) and 135 (34.9%) downregulated genes (similarly as defined genes showing an expression level at least two times lower in exposed plants than in untreated controls: i.e., fold change < 0.5). Exposure to the three OH-derivatives, 2'-OH-, 3'-OH-, and 4'-OH-2,5-DCB, resulted in differential expression of 214, 162, and 172 genes, including 133 (62.1%), 46 (28.4%), and 72 (41.9%) upregulated genes, and 81

(37.9%), 116 (71.6%), and 100 (58.1%) downregulated genes, respectively. Thirty seven (37) genes were differentially expressed by exposure to all four compounds (representing 12.1 – 29.0% of the total differentially-expressed genes, depending on the congener). Fifty one (51) genes were differentially expressed by exposure to all three OH-derivatives (representing 23.8 – 31.5% of the total differentially-expressed genes). Hierarchical clustering showed good consistency between replicate microarray results associated with each treatment (Figure 4.2). It also revealed that exposure to the three OH-derivatives, 2'-OH-, 3'-OH-, and 4'-OH-2,5-DCB, induced rather similar gene expression profiles as compared with the plants exposed to the parent 2,5-DCB and the control, non-exposed plants. This suggests that hydroxylation of 2,5-DCB resulted in distinct transcriptomic responses, as indicated by the toxicity testing.

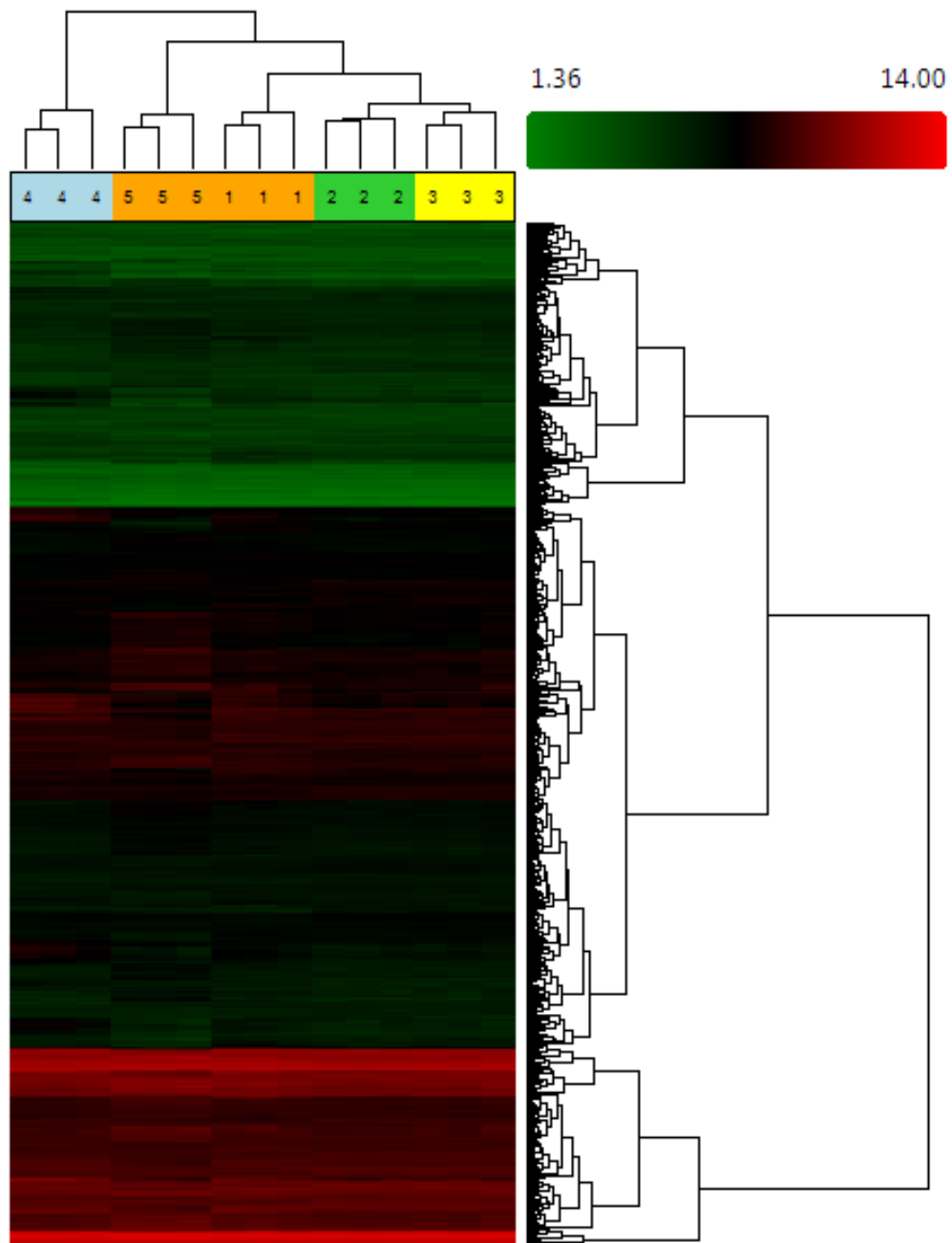


*Figure 4.2 Hierarchical clustering of gene expression profiles of *A. thaliana* (*Arabidopsis* Gene 1.0 ST Arrays, Affymetrix) exposed to 2,5-DCB (blue – 4), 2'-OH-2,5-DCB (orange – 1), 3'-OH-2,5-DCB (green – 2), 4'-OH-2,5-DCB (yellow – 3), and non-exposed controls (orange – 5). The analysis was performed on three biological replicates using the Affymetrix Expression Console™.*

In order to validate the microarray results, quantitative analysis of gene expression was performed using RT-qPCR on six selected genes, including three downregulated and

three upregulated genes upon exposure to each compound. Because the purpose of the RT-qPCR was solely to confirm the microarrays results, these genes were not selected based on their biological significance. Expression levels obtained by microarrays were plotted against expression levels obtained by RT-qPCR (Figure 4.3), showing good correlations (Pearson's correlation coefficients = 0.95, 1.00, 0.92, and 0.73 for exposure to 2,5-DCB, 2'-OH-, 3'-OH-, and 4'-OH-2,5-DCB, respectively).

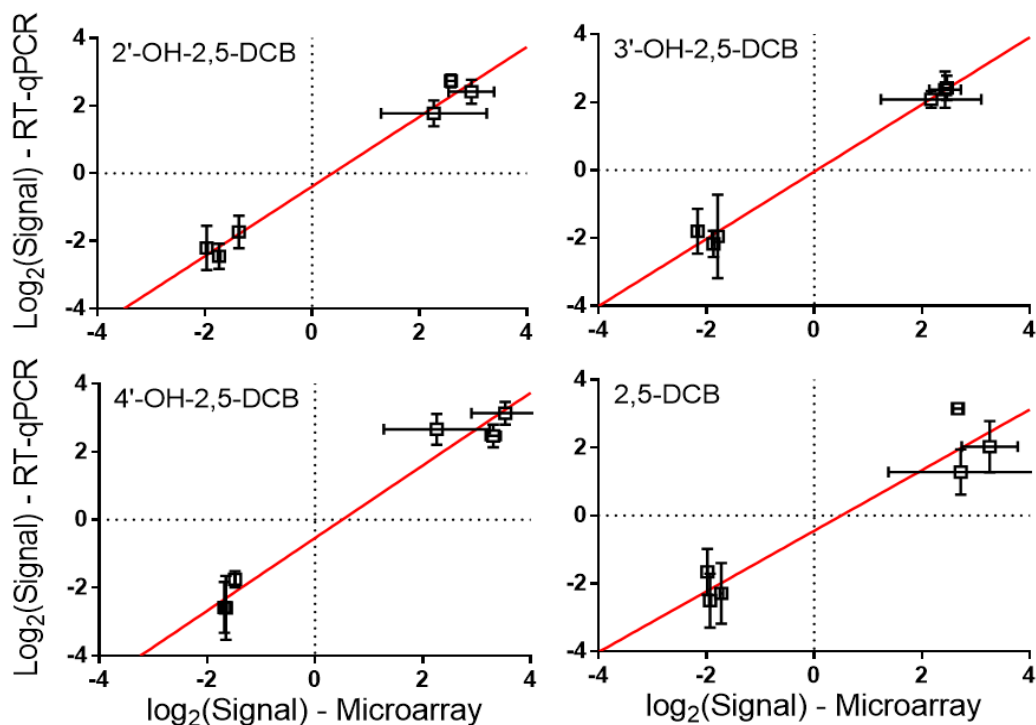


Figure 4.3 Expression levels obtained by microarrays plotted against expression levels obtained by RT-qPCR

Functional categories of differentially expressed genes

The enrichment of transcripts in different Gene Ontology (GO) categories was interrogated using the Remote Term Enrichment tool with Bonferroni's correction (<http://amigo.geneontology.org/rte>). To avoid redundancy, only the most specific

categories (i.e., at the lowest hierarchical level) were considered for the discussion (Table 4.2). Genes upregulated in response to 2,5-DCB and its OH-derivatives showed strong enrichment in several *Biological Processes* related to response to abiotic stresses (e.g., high light intensity, salt, osmotic stress, water deprivation, cold, oxidative stress) and biotic stresses (e.g., nematodes, chitin, fungus), indicating the deleterious effects of the compounds for plants. Exposure to 2,5-DCB and its OH-derivatives induced stress-response genes not directly related to toxic chemicals. Different types of biotic and abiotic stresses may cause similar cellular damages and therefore induce similar plant responses. This may explain why PCBs activated genes involved in different types of stresses. Xenobiotic sensing by plant cells may occur directly by recognition of toxic molecules or indirectly by detection its deleterious effects (Singh et al., 2002; Ramel et al., 2012). For instance, toxic compounds can activate genes similar to the ones involved in response to oxidative stress and pathogens, which frequently cause accumulation of toxins inside the host cells (Ramel et al., 2012). Unlike the three OH-derivatives, exposure to 2,5-DCB resulted in enrichment of genes involved in regulation and hormone signaling, including jasmonic acid, abscisic acid, and ethylene (Table 4.2). Jasmonic acid, abscisic acid, and ethylene are plant hormones involved in many plant processes, including response to biotic and abiotic stresses (Singh et al., 2002; Cao et al., 2007; Ramel et al., 2012; Ramegowda and Senthil-Kumar, 2015). The induction of genes involved in jasmonic acid, abscisic acid, and ethylene signaling pathway by 2,5-DCB may in turn stimulate toxic response genes, which are capable to counteract the deleterious effects of the compound. On the contrary, the failure of the OH-derivatives, 2'-OH-, 3'-OH-, and 4'-OH-2,5-DCB, to induce such signaling cascade may explain their

much higher toxicity to the plants. Although limited information is available about the toxic mechanisms of PCBs on plants, several studies have shown that exposure to PCBs resulted in decrease of plant biomass associated with photosynthesis inhibition (e.g., reduction of chlorophyll content and CO₂ assimilation), lipid peroxidation, and oxidative stress (e.g., generation of reactive oxygen species–ROS) (Ahammed et al., 2013; Wang et al., 2017).

Table 4.2 Enrichment analysis of genes up- and down regulated upon exposure to 2,5-DCB and 4'-OH-2,5-DCB based on Biological Processes and Molecular Functions. Only gene ontology (GO) terms of special interest are shown.

GO biological process	Enrich.	P-value	GO biological process	Enrich.	P-value
2'-OH-2,5-DCB			2,5-DCB		
Cellular response to iron ion starvation	67.41	3.20E-05	Protein autoubiquitination	28.98	2.79E-06
Hyperosmotic salinity response	11.83	9.48E-05	Response to chitin	17.12	8.63E-26
Transition metal ion homeostasis	10.97	5.87E-06	Photosynthesis, light harvesting in photosystem I	16.38	2.88E-05
Response to nematode	9.23	2.81E-04	Jasmonic acid biosynthetic process	16.38	2.88E-05
Response to chitin	8.17	9.80E-06	Response to high light intensity	9.54	2.67E-07
Response to cold	5.75	3.85E-08	Response to blue light	8.81	1.95E-06
Response to water deprivation	5.33	1.71E-06	Cold acclimation	8.19	5.37E-04
Response to wounding	5.09	2.38E-04	Negative regulation of defense response	7.24	8.98E-04
Response to oxidative stress	3.93	3.93E-05	Response to wounding	7.11	3.81E-11
Response to osmotic stress	3.05	2.66E-04	Response to red light	6.85	3.66E-04
Defense response to other organism	2.84	8.83E-05	Response to water deprivation	6.64	6.86E-15
3'-OH-2,5-DCB			Ethylene-activated signaling pathway	5.2	6.90E-06
GO biological process			Response to reactive oxygen species	5.08	2.01E-05
Photosynthesis, light harvesting in photosystem I	Enrich.	P-value	Response to heat	4.29	8.57E-05
Cellular response to salt stress	30.08	1.66E-05	Immune system process	3.53	4.10E-05
Response to red light	20.35	6.66E-05	Response to bacterium	3.01	8.51E-05
Response to blue light	15.72	3.75E-06	Response to auxin	2.8	4.57E-04
Cellular response to light stimulus	13.48	8.60E-06	Response to fungus	2.79	5.77E-05
Response to cold	10.64	1.41E-06	Response to salt stress	2.63	1.87E-04
Oxidation-reduction process	4.61	8.25E-05	Response to abscisic acid	2.61	2.04E-04

Table 4.2 (continued)

4'-OH-2,5-DCB	Enrich.	P-value
GO biological process		
Cellular response to iron ion starvation	3.12	9.11E-07
Iron ion homeostasis	> 100	4.41E-11
Response to cold	27.54	1.64E-09
Response to water deprivation	6.04	1.43E-07
Response to light stimulus	4.43	2.57E-04
Response to abiotic stimulus	3.24	1.39E-04
	2.98	3.70E-09

Comparison between 2'-OH-, 3'-OH-, 4'-OH-2,5-DCB, and 2,5-DCB

Exposure of Arabidopsis plants to the parent compound 2,5-DCB and the three OH-derivatives, 2'-OH-, 3'-OH-, and 4'-OH-2,5-DCB, resulted in overexpression of many genes involved in response to stress, including toxin catabolic processes (e.g., copper/zinc superoxide dismutase 2–AT2G28190), oxidative stress (e.g., superoxide dismutase–AT1G08830, peroxidase– AT1G49570), osmotic stress (e.g., low-temperature-responsive protein 78/desiccation-responsive protein 29A–AT5G52310, stress-induced protein KIN2–AT5G15970), defense response to organisms (e.g., defensin-like protein 4–AT2G02120), and transcription factors involved in abiotic stress response (e.g., dehydration-responsive element-binding protein 2A–AT5G05410). Overall, genes involved in response to stress accounted for 13.9 – 21.7% of the total upregulated genes and 7.4 – 13.6% of the total downregulated genes by exposure to 2,5-DCB and OH-DCBs. In addition, the parent 2,5-DCB – and not its OH-derivatives – resulted in upregulation of multiple genes involved in response to hormones, including

ethylene-responsive elements (e.g., ethylene-responsive transcription factor ERF109–AT4G34410, ethylene responsive element binding factor 6–AT4G17490), genes responsive to jasmonic acid stimulus (e.g., ethylene-responsive transcription factor 13–AT2G44840, calcium-binding protein CML38–AT1G76650), and genes responsive to abscisic acid stimulus (e.g., E3 ubiquitin-protein ligase ATL31–AT5G27420, putative WRKY transcription factor 40–AT1G80840). Overall, genes involved in response to ethylene accounted for 21.8% of the upregulated genes by 2,5-DCB (vs. 1.5 – 4.3% of the upregulated genes by OH-DCBs) and 1.5% of the downregulated genes by 2,5-DCB (vs. 2.5 – 5.0% of the downregulated genes by OH-DCBs). Jasmonic acid, abscisic acid, and ethylene are plant hormones involved in response to many types of biotic and abiotic stresses (Singh et al., 2002; Ramel et al., 2012; Ramegowda and Senthil-Kumar, 2015).

Looking at the OH-derivatives of 2,5-DCB, we observed that exposure to the most toxic congeners, 4'-OH-2,5-DCB, resulted in expression of specific genes not significantly up- or down-regulated by the two other isomers, 2'-OH-2,5-DCB and 3'-OH-2,5-DCB: among the 40 genes the most overexpressed by exposure to 4'-OH-2,5-DCB, only five were induced by this compound and not by the two other isomers; four of these genes are involved in response to iron deficiency: transcription factor bHLH100 (AT5G04150, fold change 7.36), transcription factor ORG2 (AT3G51560, fold change 6.29), transcription factor ORG3 (AT3G56980, fold change 5.55), and zinc ion binding protein (AT1G74770, fold change 2.54) (Sivitz et al., 2012; Kobayashi and Nishizawab, 2014). This observation is consistent with the enrichment analysis, showing that the two Biological Process categories with the highest enrichment values are cellular response to iron ion starvation (enrichment > 100) and iron ion homeostasis (enrichment 27.54). The

second gene the most downregulated by exposure to 4'-OH-2,5-DCB (and not by the two other isomers) is a rubredoxin family protein (AT5G17170, fold change -4.28) involved in iron ion binding (Kobayashi and Nishizawab, 2014). The reduction of rubredoxin synthesis may constitute an attempt by the plant to limit iron uptake in biological molecules, which would further lower iron availability. Genes involved in iron deficiency and homeostasis were also differentially regulated in response to the 2'-OH- and 3'-OH-2,5-DCB, but to a lesser extent, possibly explaining their lower toxicity as compared with 4'-OH-2,5-DCB.

Table 4.3 Enrichment analysis of genes up- and down regulated upon exposure to 2,5-DCB, 2'-OH-, 3'-OH-, and 4'-OH-2,5-DCB based on Biological Processes. Only the most specific gene ontology (GO) terms (lowest hierarchical level) are shown.

GO biological process	Enrich.	P-value	GO biological process	Enrich.	P-value
2'-OH-2,5-DCB			2,5-DCB		
Cellular response to iron ion starvation	67.41	3.20E-05	Protein autoubiquitination	28.98	2.79E-06
Hyperosmotic salinity response	11.83	9.48E-05	Stamen filament development	25.12	0.000449
Circadian rhythm	11.78	1.52E-07	Response to chitin	17.12	8.63E-26
Response to sucrose	11.42	1.10E-04	Photosynthesis, light harvesting in photosystem I	16.38	2.88E-05
Transition metal ion homeostasis	10.97	5.87E-06	Jasmonic acid biosynthetic process	16.38	2.88E-05
Response to karrikin	9.55	7.96E-07	Response to desiccation	15.7	3.44E-05
Response to nematode	9.23	2.81E-04	Regulation of organ growth	15.07	0.00025
Response to chitin	8.17	9.80E-06	Negative regulation of cell death	11.16	0.000689
Response to cold	5.75	3.85E-08	Circadian rhythm	10.97	4.59E-11
Response to water deprivation	5.33	1.71E-06	Response to high light intensity	9.54	2.67E-07
Response to wounding	5.09	2.38E-04	Response to blue light	8.81	1.95E-06
Response to oxidative stress	3.93	3.93E-05	Cold acclimation	8.19	5.37E-04
Response to osmotic stress	3.05	2.66E-04	Negative regulation of defense response	7.24	8.98E-04
Defense response to other organism	2.84	8.83E-05	Response to wounding	7.11	3.81E-11
3'-OH-2,5-DCB			Response to red light	6.85	3.66E-04
GO biological process	Enrich.	P-value	Response to water deprivation	6.64	6.86E-15
Photosynthesis, light harvesting in photosystem I	30.08	1.66E-05	Response to karrikin	6.53	2.19E-06
Cellular response to salt stress	20.35	6.66E-05	Phloem or xylem histogenesis	6.06	2.41E-04
Xyloglucan metabolic process	16.02	2.30E-05	Ethylene-activated signaling pathway	5.2	6.90E-06
Response to red light	15.72	3.75E-06	Response to reactive oxygen species	5.08	2.01E-05
Response to blue light	13.48	8.60E-06	Regulation of flower development	4.46	2.86E-04
Circadian rhythm	11.76	3.52E-06	Response to heat	4.29	8.57E-05
Response to karrikin	10.9	1.19E-06	Immune system process	3.53	4.10E-05
Cellular response to light stimulus	10.64	1.41E-06	Response to bacterium	3.01	8.51E-05
Response to cold	4.61	8.25E-05	Response to auxin	2.8	4.57E-04
Oxidation-reduction process	3.12	9.11E-07	Response to fungus	2.79	5.77E-05
Response to acid chemical	2.71	1.37E-04	Response to salt stress	2.63	1.87E-04
			Response to abscisic acid	2.61	2.04E-04
			Transcription, DNA-templated	2.07	1.88E-06
			Regulation of transcription, DNA-templated	1.83	1.62E-05

Table 4.3 (continued)

4'-OH-2,5-DCB		
GO biological process	Enrich.	P-value
Cellular response to iron ion starvation	> 100	4.41E-11
Iron ion homeostasis	27.54	1.64E-09
Circadian rhythm	14.14	3.22E-08
Response to karrikin	10.19	1.96E-06
Response to cold	6.04	1.43E-07
Response to water deprivation	4.43	2.57E-04
Response to light stimulus	3.24	1.39E-04
Response to abiotic stimulus	2.98	3.70E-09

Comparison of expression profile of 2,5-DCB and OH-2,5-DCBs with other chemicals

The transcriptomic profiles of *Arabidopsis* exposed to 2,5-DCB, 2'-OH-, 3'-OH-, and 4'-OH-2,5-DCB were then searched against the *Arabidopsis* expression microarray database, Genevestigator (genevestigator.com/gv/). The analysis was restricted to expression profiles recorded with wild-type *A. thaliana* and the Perturbation Category, Chemicals. Searching expression profiles similar to the ones induced by the three OH-derivatives (based on the 25 most upregulated genes for each treatment) returned a suite of 13 chemicals, which were all among the 20 highest hits for each compounds (Table 4.4). (Only two of these 13 chemicals were among the 20 highest hits for 2,5-DCB). For each OH-derivatives, the two highest hits – based on the similarity of transcription profiles – were two compounds (referred to as '7606596' and '5929745') described as 'albino chemicals' because they induce an albino phenotype in exposed plants. This is consistent with the observation that exposure to OH-derivatives resulted in enrichment of genes involved with response to high light intensity. Unfortunately, no more information can be found about compounds '7606596' and '5929745'.

Three other compounds inducing expression profiles similar to the OH-derivatives are brassinazole, propiconazole, and uniconazole, which all are characterized by a triazole

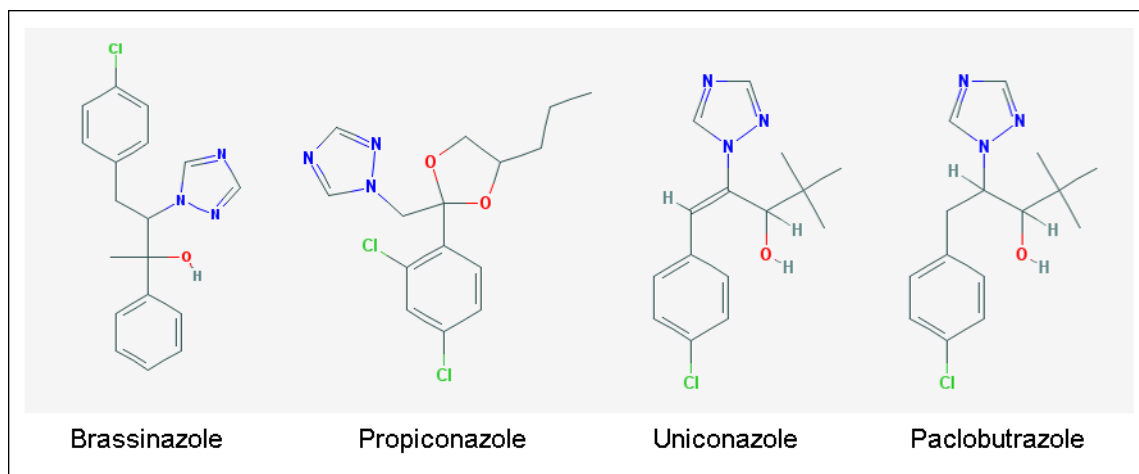


Figure 4.4 Structure of Brassinazole, Propicanazole, Uniconazole and Paclobutrazole group and a chlorinated benzylic ring.

The expression profile developing in response to 2'-OH-2,5-DCB is in addition similar to paclobutrazole, which is characterized by a similar structure (Figure 4.4). These four compounds, brassinazole, propiconazole, uniconazole, and paclobutrazole, are inhibitors of the brassinosteroid synthesis. Brassinosteroids are signaling molecules involved in many plant functions, such as extreme dwarfism, delayed senescence, male sterility, and constitutive photomorphogenesis in the dark (Mussig et al., 2002). Interestingly, it has been demonstrated that the structural elements responsible for the inhibitory activity include not only the triazole ring and chlorinated benzylic ring, but also an hydroxyl group – or, in the case of propiconazole, a dioxlane group (Hartwig et al., 2012) (Figure 4.4). None of these compounds were shown to induce an expression profile similar to the parent PCB, which also lacks the hydroxyl (or dioxlane) group (Table 4.4). Consistently with these observations, exposure to all three OH-derivatives

resulted in strong downregulation of several genes responsive to brassinosteroid stimulus or involved in brassinosteroid synthesis: e.g., phosphate-responsive 1 family protein (AT4G08950), ethylene-responsive transcription factor ERF012 (AT1G21910) and ERF013 (AT1G77640), xyloglucan endotransglucosylase/hydrolase protein 22 (AT5G57560), 24-methylenesterol C-methyltransferase 3 (AT1G76090), probable pectinesterase/pectinesterase inhibitor 41 (AT4G02330) (Table 4.3). All these six genes were most strongly repressed in plants exposed to 4'-OH-2,5-DCB, which is also the most toxic of the OH-derivatives under study. On the contrary, none of these genes were downregulated in plants exposed to the parent compound. Most interestingly, brassinosteroids have been found to be involved in iron uptake and homeostasis (Brumbarov et al., 2014). Indeed, many genes involved in response to iron starvation were upregulated in plants exposed to the three OH-derivatives (e.g., copper/zinc superoxide dismutase 2–AT2G28190, transcription factor bHLH100–AT5G04150, bHLH transcription factor POPEYE–AT3G47640) (Table 4.4). Conversely, many genes involved in iron binding and homeostasis were downregulated in plants exposed to the three OH-derivatives (e.g., NEET group protein–AT5G51720, metal-nicotianamine transporter YSL3–AT5G53550, glutamyl-tRNA reductase 1–AT1G58290). On the other hand, only very few genes involved in iron metabolism were differentially expressed by exposure to the parent 2,5-DCB (Table 4.4).

Table 4.4 Genes involved in brassinosteroid and iron response differentially expressed in response to 2'-OH-, 3'-OH-, 4'-OH-2,5-DCB, and 2,5-DCB.

Tair #	Description	Biological function	Fold change		
			2'-OH-	3'-OH-	4'-OH-
At2g28190	Copper/zinc superoxide dismutase	Response to iron deficiency	4.38	2.34	
At5g04150	bhlh100	Response to iron deficiency	4.17		5.44
At3g51560	ORG2	Response to iron deficiency			
At3g56980	ORG3	Response to iron deficiency			5.55
At3g18290	Putative E3 ligase BRUTUS	Response to iron deficiency	2.30		2.70
At3g47640	bhlh Transcription factor POPEYE	Response to iron deficiency	2.09		2.15
At4g11280	1-Aminocyclopropane-1-carboxylate synthase	Response to iron	2.02		
At1g08830	Superoxide dismutase [Cu-Zn]	Response to iron		2.34	
At1g74770	Zinc ion binding protein	Response to iron deficiency			2.54
At3g14940	Phosphoenolpyruvate carboxylase	Response to iron deficiency			2.24
At5g51060	Respiratory burst oxidase homolog protein c	Iron binding/homeostasis			2.23
At4g13310	Cytochrome p450 71A20	Iron binding	2.06		
At5g51720	NEET group protein	Iron binding/homeostasis	-2.06	-2.04	-2.58
At5g53550	Metal-nicotianamine transporter YSL3	Iron binding/homeostasis	-2.09		
At1g58290	Glutamyl-trna reductase	Response to iron	-2.24	-2.51	-3.91
At5g52570	Beta-carotene hydroxylase	Iron binding/homeostasis	-2.57		-3.17
At1g33720	Cytochrome P450, family 76	Iron binding/homeostasis	-2.82		
At1g44446	Chlorophyllide a oxygenase	Iron binding/homeostasis		-2.03	
At1g02205	Protein eceriferum	Iron binding/homeostasis		-2.07	
At2g34770	Fatty acid hydroxylase	Iron binding/homeostasis		-2.27	
At5g23980	Ferric reduction oxidase	Iron binding/homeostasis		-2.61	
At5g25130	Cytochrome P450 71B12	Iron binding/homeostasis			-2.03
At3g48310	Cytochrome P450 71A22	Iron binding/homeostasis			-2.31
At4g04770	ATP binding cassette protein	Response to iron			-2.43
At5g17170	Rubredoxin family protein	Iron binding/homeostasis			-4.28
At4g08950	Phosphate-responsive 1 family protein	Response to brassinosteroid	-2.55	-2.35	-2.80
At1g21910	Ethylene-responsive transcription factor ERF012	Response to brassinosteroid	-2.73	3.29	-4.10
At1g77640	Ethylene-responsive transcription factor ERF013	Response to brassinosteroid	-2.75	-2.17	-3.18
At5g57560	Xyloglucan endotransglucosylase/hydrolase	Response to brassinosteroid		-2.92	-2.78
At1g76090	24-methylenesterol C-Methyltransferase	Brassinosteroid biosynthesis			-2.22
At4g02330	Probable pectinesterase/pectinesterase inhibitor	Response to brassinosteroid			-2.43

Besides iron deficiency, the inhibition of brassinosteroid synthesis is likely to have additional effects on plants. For instance, brassinosteroid deficiency is also known to repress genes involved in cell elongation and resistance to stress factors, such as response to cold (Mussig et al., 2002). Indeed, exposure to OH-2,5-DCBs downregulated expansins genes (e.g., expansin-like A1–AT3G45970, expansin-like A2–AT4G38400). Also, enrichment analysis has shown that exposure to the three OH-derivatives resulted in enrichment of genes involved in response to cold (Table 4.4). Besides, brassinosteroids have been shown to play a role in plant responses to a variety of biotic and abiotic stresses, including pathogens, drought, heavy metals, organic pollutants, and nanomaterials (Ahammed et al., 2013). Intriguingly, brassinosteroids have been shown to alleviate the specific toxicity of PCBs on plants (Ahammed et al., 2013; Wang et al., 2017). The inhibition of brassinosteroids by OH-derivatives of PCBs is therefore expected to increase to toxicity for the plants.

Other chemicals inducing expression profiles similar to the OH-derivatives include broad-spectrum herbicides and pesticides (e.g., glyphosate, imazapyr, rotenone, sulfometuron methyl), plant growth regulators (aminoethoxyvinylglycine–AVG, prohexadione, benzothiadiazole), inducers of systemic acquired resistance (dichloroisoicotinic acid–INA, $MgCl_2$ +glycerol-3-phosphate–G3P), and various phytotoxic compounds (e.g., syringolin, *N*-octyl-3-nitro-2,4,6-trihydroxybenzamide–PNO8, ibuprofen, dexamethasone, phenanthrene) (Table 4.5). This suggests that OH-derivatives of 2,5-DCB act on plants through various mechanisms in addition to inhibition of brassinosteroid synthesis.

As it was reported in a prior publication (Subramanian et al., 2017), we observed that exposure to 2,5-DCB resulted in an expression profile similar to plant safeners (e.g., 4-chloro-6-methyl-2-phenylpyrimidine–CMP, fenclorim, isoxadifen, menadione sodium bisulphite–MSB). Safeners are non-toxic chemicals used to protect crops against deleterious effects of herbicides and pesticides (Skipsey et al., 2011; Behringer et al., 2011) (Table 4.5). Safeners are thought to act through the induction of detoxification enzymes, known as xenobiotic response genes (XRGs), such as cytochrome P-450 monooxygenases, glucosyltransferases, glutathione S-transferases, and ABC transporter proteins (DeRidder et al., 2002; Behringer et al., 2011), therefore further explaining the low toxicity of 2,5-DCB for plants (Subramanian et al., 2017). Other compounds inducing expression profiles similar to 2,5-DCB include a radio-protective agent (4-thiazolidinone/acetic acid), an inhibitor of the response to indole acetic acid (triodobenzoic acid– TIBA), a flowering agent (furyl acrylate ester), and an antifungal antibiotic (*trichostatin A*) (Table 4.5).

Table 4.5 Chemicals resulting in expression profiles most similar to 2'-OH-, 3'-OH-, 4'-OH-2,5-DCB, and 2,5-DCB.

The list was obtained searching the Arabidopsis microarray database, Genevestigator, using the 'signature' function. Only the 20 highest hits for each compound are shown.

2'-OH-2,5-DCB	3'-OH-2,5-DCB	4'-OH-2,5-DCB	2,5-DCB
7606596	7606596	7606596	Clothianidin
5929745	5929745	5929745	4-thiazolidinone/acetic acid
Glyphosate	Imazapyr	Arsenate	Furyl acrylate ester
Brassinazole	Glyphosate	Brassinazole	Fenclorim
Syringolin	Syringolin	Bleomycin +	
Arsenate	Uniconazole	INA	AgNO ₃
PNO8	Benzothiadiazole	Glyphosate	Ozone
Propiconazole	Brassinazole	PNO8	TIBA
Ibuprofen	Dexamethasone	Phenanthrene	Imidacloprid
CMP	INA	Propiconazole	CMP
INA	Ozone	Ibuprofen	Arsenate
MG132	Propiconazole	Syringolin	Chitin
Imazapyr	Paclobutrazole	Imazapyr	Bleomycin + INA
Uniconazole	Rotenone	INA	MSB
Dexamethasone	Ibuprofen	G3P	Mefenpyr/isoxadifen
Oligomycin	Sulfometuron methyl	Oligomycin	5-AC
AVG	Rotenone	Rotenone	Selenate
Prohexadione	Gabaculin	Uniconazole	Oligomycin
AgNO ₃	PNO8	MG132	Sulfometuron methyl
Rotenone	CMP	Uniconazole	Trichostatin A
	AgNO ₃	Dexamethasone	PNO8

5-AC: deoxycytidine; AgNO₃: silver nitrate; AVG: aminoethoxyvinylglycine; CMP: 4-chloro-6-methyl-2-phenylpyrimidine; G3P: glycerol-3-phosphate; INA: dichloroisoicotinic acid; MSB: menadione sodium bisulphite; MG132: carbobenzoxyl-leucinyl-leucinyl-leucinal; PNO8: *N*-octyl-3-nitro-2,4,6-trihydroxybenzamide; TIBA: triiodobenzoic acid.

The results presented here increase our understanding of the effects of PCBs and OH-PCBs on plants, which may have important implications for human health and the environment. It is noteworthy that the major findings of this study were obtained using

resource of a microarray database, emphasizing the importance of standardizing transcriptomic data and developing searchable databases. However, the evidence presented in this article is entirely based on the analysis of transcriptomic results. Biochemical analyses are warranted to confirm the toxic mechanism of OH-PCBs through the inhibition of brassinosteroid synthesis. Further investigation is also needed to identify the xenobiotic receptors and transcription factors that are involved in the plant response to PCBs and OH-PCBs.

4.5 Acknowledgements

This work was funded by the Iowa Superfund Basic Research Program, National Institute of Environmental Health Sciences (NIEHS), Grant P42ES013661.

CHAPTER 5 *ARABIDOPSIS THALIANA* BIOMASS ASSESSMENT FOR BIOFUEL GENERATION USING FTIR-ATR

*This chapter relates to Specific Aim 3: "To determine the change in the biomass composition of *A. thaliana* upon exposure to different PCBs and OH-PCBs."*

Prior evidence obtained by us and others have suggested that exposure of plants to environmental contaminants may lead to a change of the biomass composition, especially an increased in the lignin content. This could be a challenge in the case the plants would be used for biofuel production. In pursuance of this aim, *A.thaliana* plants were exposed to sub-inhibitory concentrations of parent PCBs and their hydroxylated congeners for a period of 21 days. The whole plants were then analyzed for lignin and cellulose content using FTIR-ATR spectroscopy. The lignin and cellulose peaks were determined by reference to authentic standards. Significant changes in the lignin and cellulose content of the treated samples were compared against untreated controls. Only samples exposed to 2,3,5,6-TeCB showed a significant increase in the cellulose content compared to the control. None of the other treated samples showed a significant increase or decrease in the cellulose content, though qualitative changes were observed. Among the samples exposed to PCBs, 3,4-DCB, 2,4,6-TCB and 2,3,5,6-TeCB induced a significant decrease in the lignin content in the plants. Of all the OH-PCBs, only 2-OH-3'4',-DCB and 4-OH-2',3',5'-TCB caused a significant decrease in the lignin content in exposed samples.

5.1 Introduction

Environmental pollution affects land, water, atmosphere and biosphere, and has been a cause of concern for a few decades. PCBs are characterized to be highly toxic,

carcinogenic and persistent in the environment (Desforges, 2018). Due to their high chemical stability and resistant nature to natural degradation, they persist in the soil for many years (Zhang, 2013). Their ability to bioaccumulate is of great health concern to humans and other organisms (Rahuman et al., 2000; Carpenter, 2006). Though they were banned in the 70s, due to improper disposal and leakages, a large quantity was released into the environment, and subsequently accumulated in soils and sediments. Their potential health and environmental risks call for effective remediation strategies (Salimizadeh, 2018).

Traditional cleanup technologies such as incineration, soil excavation and landfills are expensive and are also met with high public resistance (Zeeb, 2006). Also as these methods are not capable of treating large amounts of contamination, there is an increasing need to look for remediation techniques that are more environment friendly, less expensive and widely accepted by the general public (Zeeb, 2006).

Phytoremediation, an emerging technology, has shown that plants and associated bacteria and fungi, are capable of uptake of contaminants (Van Aken et al., 2010; Sharma et al., 2018). Singer et al. (2003) have shown significant reduction of PCBs in soils planted vs non-planted soils. Plants such as Giant Reed and Castor Bean have been shown to produce bioethanol on exposure to contaminated substrates (Prasad et al., 2016).

Cell walls of plants are an important complex structure that play a key role throughout the life cycle of the plant. They help in various functions ranging from maintaining structural integrity to acting as a barrier towards pathological and environmental stresses (Houston, 2016). However, the cell wall also contains variable

amounts of lignin, which constitutes the major technical obstacle to lignocellulosic biomass digestibility and conversion into bioethanol (Demartini and Wyman, 2011). The plant lignin content is susceptible to change when exposed to toxic chemicals, which would affect the biomass digestibility. Digestion of lignocellulosic biomass currently proceeds through the enzymatic breakdown of lignin, cellulose, and hemicellulose followed by the fermentation of resulting single sugars to produce ethanol, which can be substituted for fossil fuels. Therefore, the quantity of lignin and cellulose determines the amount of ethanol that can be produced by plants.

Prior research has shown that exposure to environmental stresses, including environmental contaminants, can modify the lignin and cellulose content in feedstock plants (Zhu et al., 2012). Plants have been shown to take up toxic chemicals, such as TNT and PCBs, which results in transcriptional changes that ultimately may affect the production of cell wall components (Zhu et al., 2012). Studies have shown that plants accumulate toxic trace metals in the cell wall, and that this accumulation causes a change in the cell wall structure (Krzeslowska, 2011). Both enhancement and inhibition of growth rate have been observed in plants upon exposure to toxic contaminants. Moreover, as a defense mechanism against external stressors, plants have been shown to respond by increasing the lignin content of the cell wall.

Several investigators have quantified lignin and cellulose by extraction through biochemical processes, which is time consuming and results in destruction of the plant material (Imadi and Kazi, 2015). Another option is the use of Fourier transform infrared (FTIR) spectroscopy coupled with fiber optics has been used to evaluate the composition of organic materials and tissues, including plants (Huck, 2014). In FTIR attenuated total

reflectance (ATR) mode, compositional data can be collected within seconds without destruction of the plant.

FTIR spectroscopy is a technique based on identifying molecular composition by investigating the fundamental vibration modes of various molecular functional groups (Muller et al., 2009; Luz, 2006). Each functional group is capable of producing a characteristic redistribution of spectral absorption features such as stretches, wags and scissoring. For use of FTIR with respect to biological specimen, the widely used spectral regions correspond to the fingerprint region ($600\text{-}1450\text{ cm}^{-1}$), the amide I/II region ($1500\text{-}1700\text{ cm}^{-1}$) and the high wave number region ($2550\text{-}3500\text{ cm}^{-1}$). The higher wavenumber region is specific to S-H, C-H, N-H and O-H stretching vibrations (Baker et al., 2014).

Lahlai et al. (2014), investigated the impact of heat stress on lipids and protein in pea pollen grains using FTIR-ATR. They were able to characterize the secondary protein structure between two different cultivars. FTIR-ATR has also been successfully applied to the quantification of sugar content in different varieties of honey (Anjos et al., 2015).

This study focuses on the use of FTIR spectroscopy for evaluation of the composition of *A. thaliana* biomass in response to exposure to PCBs and hydroxylated PCBs (OH-PCBs). *A. thaliana* is a model plant that has been well studied for phytoremediation (Cobbett and Meagher, 2002). It has a short growth cycle, which makes it ideal for laboratory based experiments and rapid characterization (Meineke et al., 1998). It has been used in several studies to understand changes occurring in cell wall composition and the genes associated with these changes. Schmidt et al. (2010) successfully demonstrated the use of *A. thaliana* as a very good model for the cell wall probing. In that study, they were able to characterize the spatial distribution of the cell

wall polymers in *A. thaliana*, without destruction of the lignocellulosic components using the technique of Raman spectroscopy.

In the current study, our goal was to characterize the effects of PCBs and their hydroxylated derivatives on *A. thaliana* biomass composition, for the purpose of phytoremediation and biofuel production. This goal was achieved by using FTIR spectroscopy to quantify the changes in lignin and cellulose content in the cell wall of exposed plants versus control plants (non-exposed).

5.2 Materials and Methods

Lignin and cellulose were obtained from Sigma Aldrich, St. Louis, MO. These standards were lyophilized for 12 hours to remove water. *A. thaliana*, ecotype Columbia (Col-0/Redei-L211497, Ohio State University, Columbus, OH) were grown as described in Kaveh et al. (2013). Briefly, the seeds were surface sterilized and then placed in petri-dish containing sterile semi-solid nutrient medium (0.5-strength MS nutrient solution with 0.3% sucrose and 0.7% phytoagar, pH 7.2. The semi-solid media was cooled and then supplemented with PCBs and OH-PCBs as acetone stock solutions (5,000-mg L⁻¹). The concentrations of the PCBs and OH-PCBs used were determined based on the growth and germination tests as described in Chapters 3 and 4. The PCBs and OH-PCBs used in this study are indicated in Table 5.1. Although many PCBs are of interest to study, we were able to obtain these parent PCBs with matched hydroxylated derivatives. For control plants, the nutrient media was supplemented with only the solvent carrier, acetone ($\leq 1\%$ w/v). The plants were grown for a period of 3 weeks under white (cool) fluorescent light ($0.38 \pm 0.02 \text{ W ft}^{-2}$) with a 16-h light/8-h dark photoperiod, at a temperature of 25°C. After 21 days, surviving plantlets were removed from the medium,

washed with water and dried by blotting. The period of 21 days was chosen, as it is the longest phase we can expose *A. thaliana* plants, without entering the flowering state. The plants were then stored at $\leq -80^{\circ}\text{C}$ until analysis. The frozen samples were thawed and blotted to remove water. They were lyophilized for a period of 24 hours to remove any further water content.

Table 5.1 PCB compounds and hydroxylated PCBs tested on A. thaliana plants

PCBs used (50 mg/ml)	OH-PCBs used (5 mg/ml)
4-Chlorobiphenyl	4-OH-4'-Chlorobiphenyl
3,4-Dichlorobiphenyl	2-OH-3',4'-Dichlorobiphenyl
2,3,5-Trichlorobiphenyl	2-OH-2',3',5'-Trichlorobiphenyl
2,4,6- Trichlorobiphenyl	2-OH-2',4',6'-Trichlorobiphenyl
2,3,5,6- Tetrachlorobiphenyl	Not Tested

FTIR ATR data collection and processing

ATR spectra were collected from standards (pure lignin and pure cellulose powder, Sigma Aldrich, Sr. Louis MO) and plant material using a Thermo Fisher Nicolet iS5 spectrometer with an ID7 diamond crystal, in the spectral region $440\text{--}4000\text{ cm}^{-1}$, with 8 cm^{-1} spectral resolution and 64 co-added scans. Air was used as background and 128 co-added scans were collected.

For the standards data were collected using $\sim 1\text{ mg}$ of each powder. Spectra were collected in triplicates.

Spectra were analyzed with Unscrambler 10.4.1 software (Unscrambler®- Camo Software, Norway). Raw spectra were pre-processed with a 13 point Savitzky–Golay smoothing window and, in order to amplify the separation of overlapping peaks, second derivative spectra were obtained. The pure component spectra were examined for peaks that were specific to the individual components.

Spectra in the mid infrared (MIR) region were acquired for both lignin and cellulose in powdered lyophilized form. MIR was used for measuring the lignin and cellulose content, as the MIR region is the gold standard to identify fundamental absorption bands and molecular fingerprints. Second derivative spectra were used to resolve the raw spectra and to better aid in identifying the peaks unique to lignin and cellulose. *A. thaliana* ATR data were acquired using a Thermo Nicolet iS5 FT-IR Spectrometer with an ID7 ATR crystal accessory at 8 cm^{-1} spectral resolution and 64 co-added from $440\text{--}4000\text{ cm}^{-1}$. Since *A. thaliana* is a small plant, the average size being $\sim 40\text{ mm}$ after 3 weeks of exposure, the entire organism was used for analyzing the changes in lignin and cellulose composition in the cell wall. To understand how individual plant components changed with PCB and OH-PCB concentrations, absorbance intensity unique to lignin (1532 cm^{-1}) and to cellulose (1322 cm^{-1}) were calculated using second derivative spectra. These were inverted to make peaks positive. These absorbances were ratioed to the matrix peak (1014 cm^{-1}), which arises from absorbances of all structural components in the plant, including pectin and hemicellulose (Senthil-Kumar et al., 2017; Alonso-Simon et al., 2011). These vibrations arise from C-O, C-N and C-OH stretches.

Statistical Analysis:

JMP Pro 13 (SAS Institute, Cary, NC) was used to calculate average values and standard

deviations of the ATR-calculated lignin and cellulose content of control and exposed plants. Significant differences among average values were assessed using one-way Analysis of Variance (ANOVA), followed by a Dunnett's post hoc test with significance set at $p < 0.05$.

5.3 Results

Pure component spectral data:

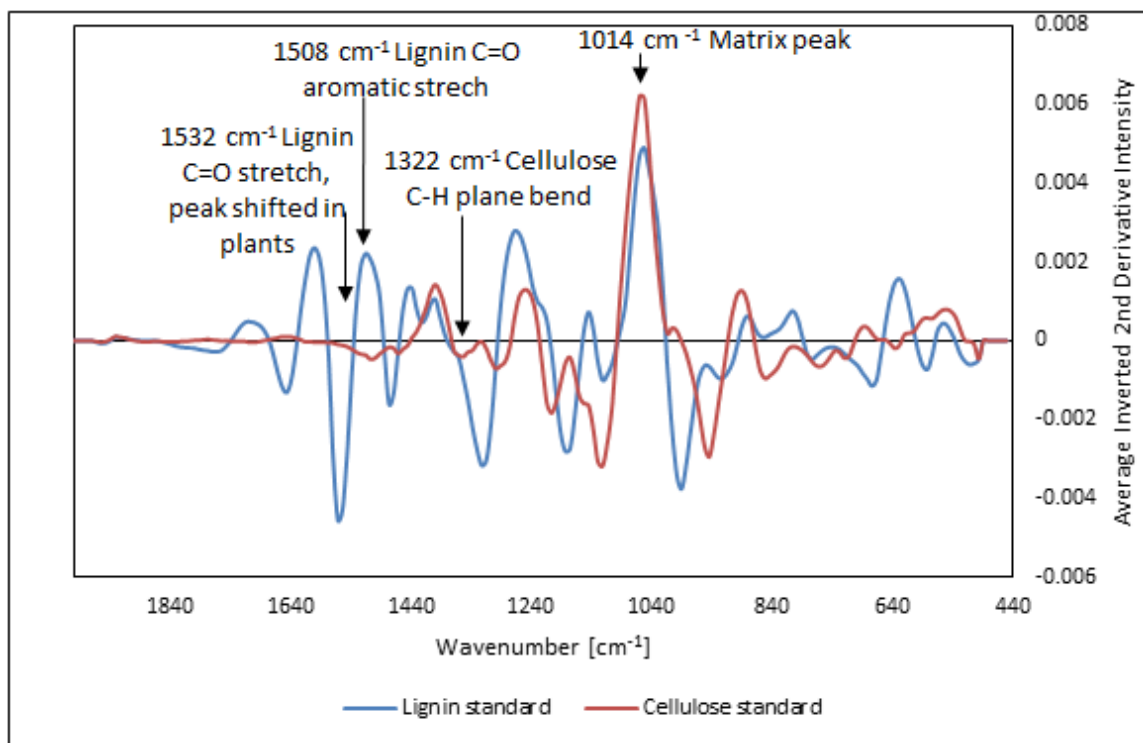


Figure 5.1 Second derivative inverted average (n=3) spectra of lignin and cellulose standards obtained in the MIR region using FTIR.

From Figure 5.1, it can be seen that lignin and cellulose show unique peaks at 1508 cm^{-1} and 1322 cm^{-1} respectively. The changes in these peaks were evaluated in the control plants and plants treated with PCBs and OH-PCBs. The lignin peak showed a shift in the plants to 1532 cm^{-1} , attributed to the C=O stretching (Marshall et al., 2005). The peak at 1014 cm^{-1} is used as a reference, or "matrix" peak.

Spectral data of non-exposed controls and exposed samples:

The general shape of the spectra appear to be similar between the control and the treated samples, but the treated samples showed variation in the amount of cellulose and lignin based on intensity of the peaks specific to those components.

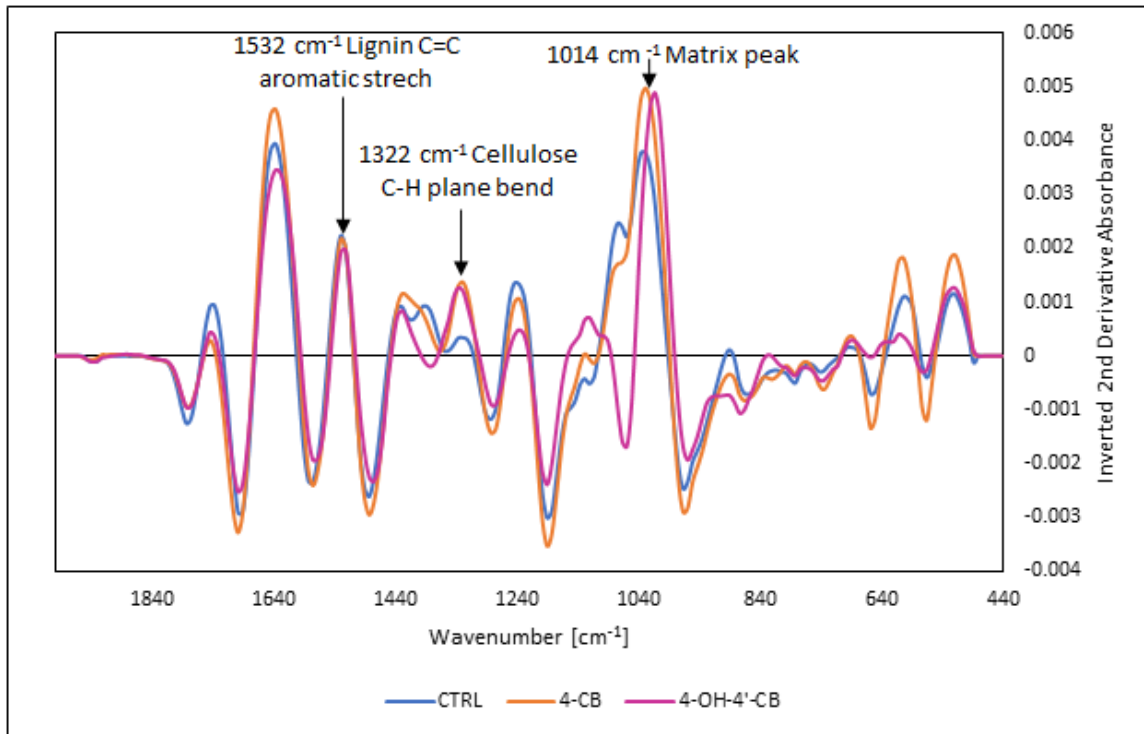


Figure 5.2 Second derivative average (n=3) spectra of samples exposed to 4-CB and 4-OH-4'-CB compared to control

Samples exposed to 4-CB and 4-OH-4'-CB did not show any significant change in the lignin or cellulose content (Figure 5.2).

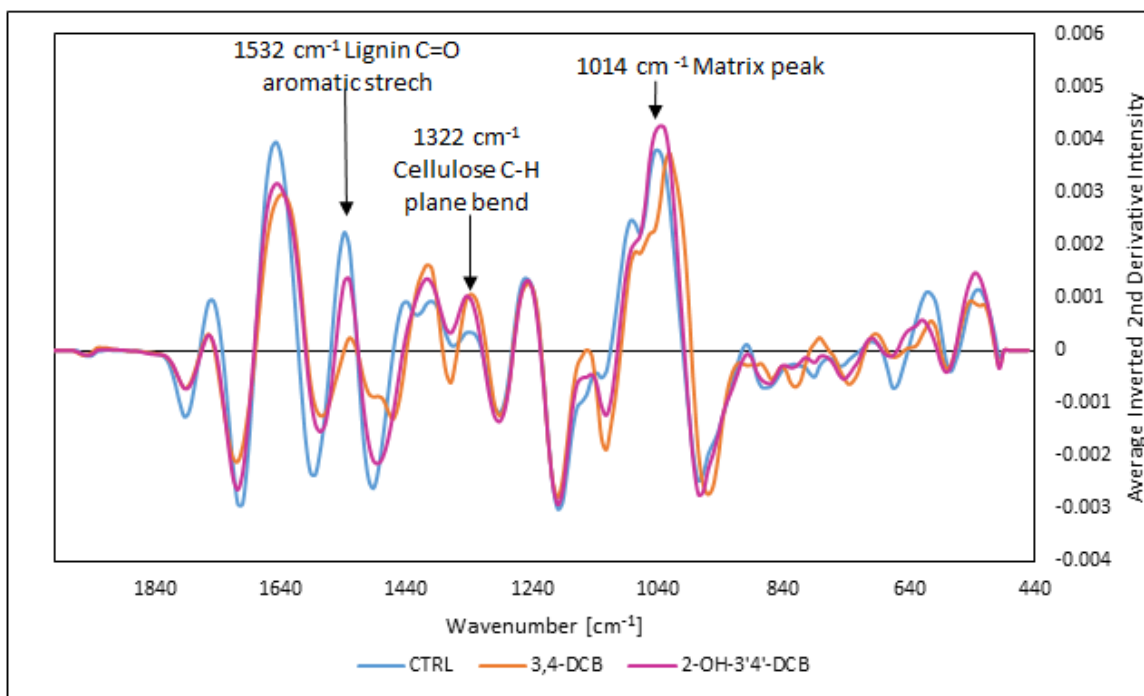


Figure 5.3 Second derivative average (n=3) spectra of samples exposed to 3,4-DCB and 2-OH-3',4'-DCB compared to control

For samples contaminated with 3,4-DCB, there was a statistically significant reduction in the lignin content as compared to controls (Figure 5.3). The plants exposed to 2-OH-3',4'-DCB, also showed a small insignificant decrease in the amount of lignin.

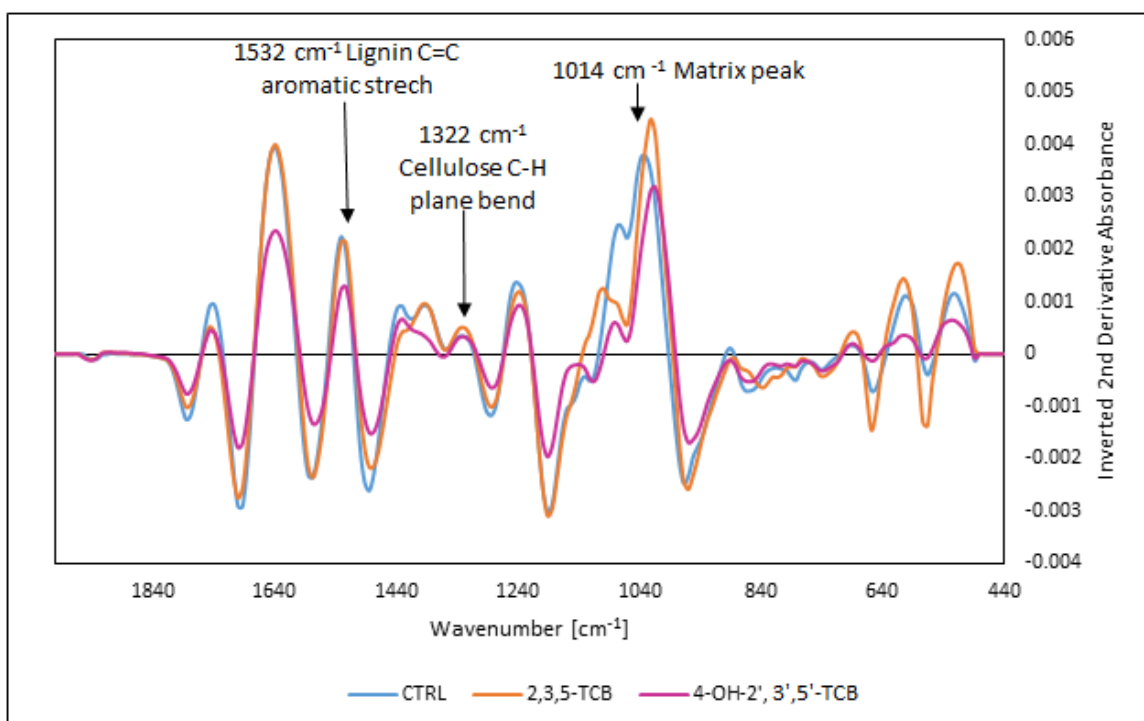


Figure 5.4 Second derivative average (n=3) spectra of samples exposed to 2,3,5-TCB and 2-OH-2',3',5'-TCB compared to control

Samples exposed to 2,3,5-TCB did not result in a significant change in the lignin or cellulose content, however samples exposed to the OH-congener resulted in a significant decrease in the lignin content (Figure 5.4).

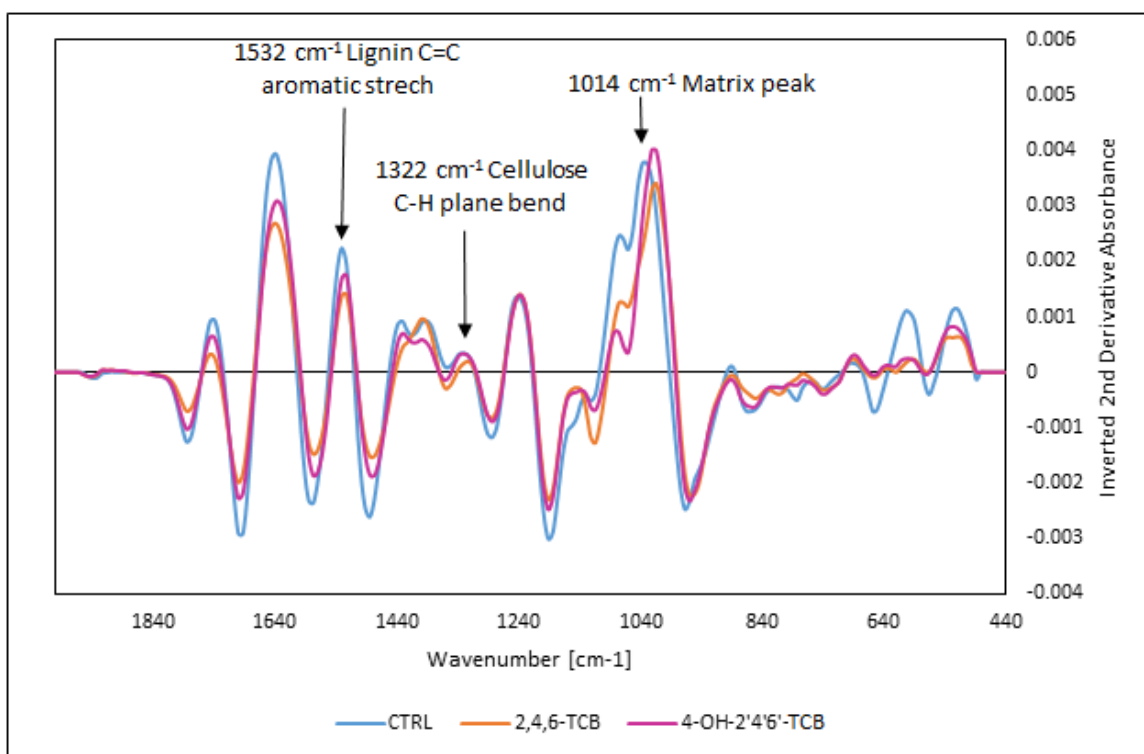


Figure 5.5 Second derivative average (n=3) spectra of samples exposed to 2,4,6-TCB and 4-OH-2',4',6'-TCB compared to control

Samples exposed to 2,4,6-TCB resulted in a significant decrease in the lignin content, but not difference was observed with exposure to the OH-congener (Figure 5.5).

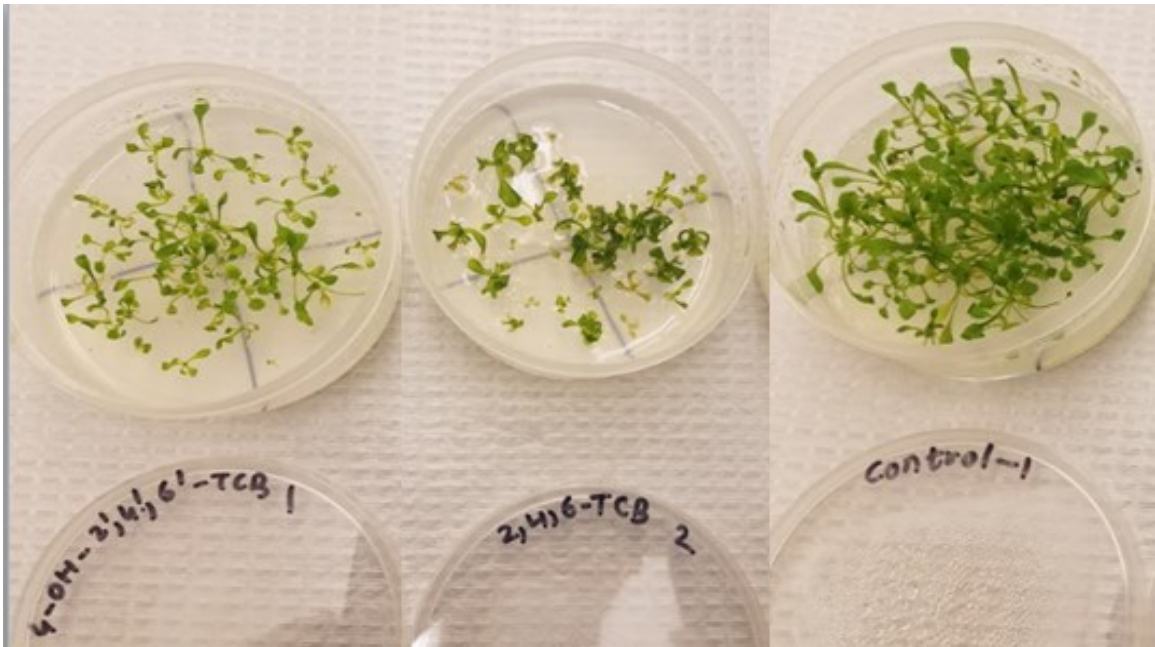


Figure 5.6 *A. thaliana* plants exposed to Control, 2,4,6-TCB and 4-OH-2',4',6'-TCB

Figure 5.6 shows the difference in the size and number of plants between exposure to control, 2,4,6-TCB and 4-OH-2',4',6'-TCB. We can observe that the PCB and OH-congener cause a reduction in the size and biomass of the *A. thaliana* plants.

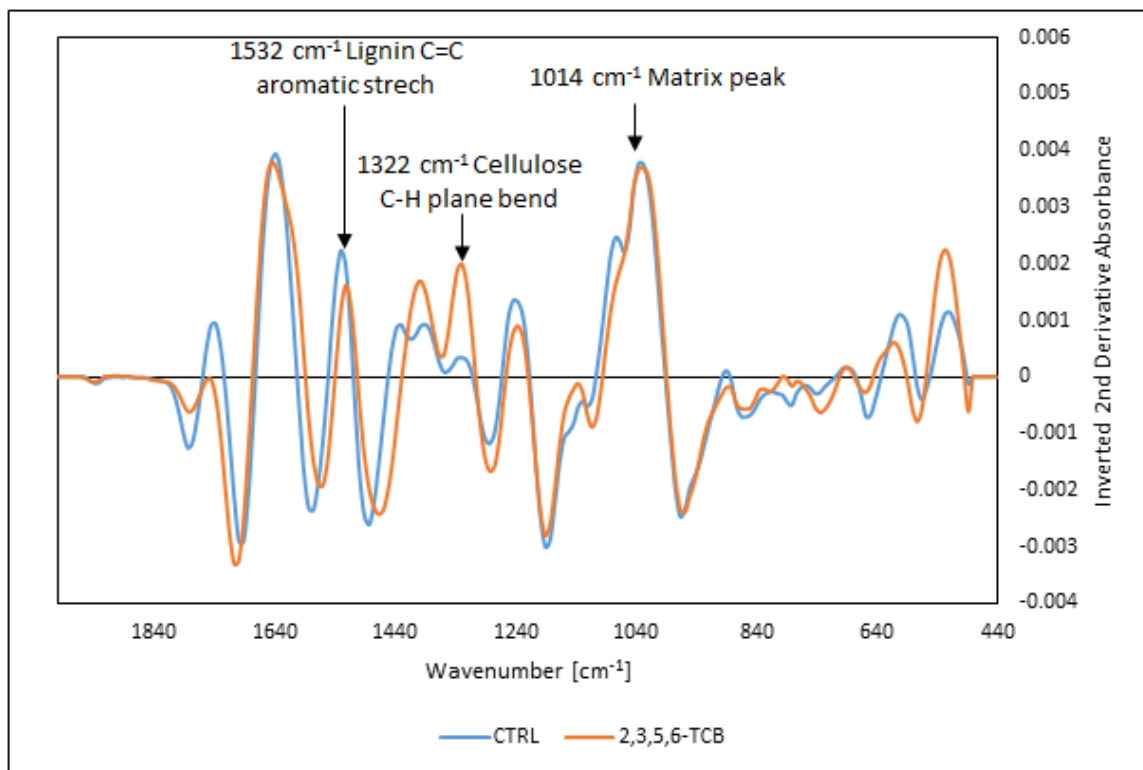


Figure 5.7 Second derivative average (n=3) spectra of samples exposed to 2,3,5,6-TCB compared to control

Plant samples exposed to 2,3,5,6-TeCB resulted in a significant decrease in the lignin content. Exposure to these PCBs did not result in a significant change in the cellulose content (Figure 5.7).

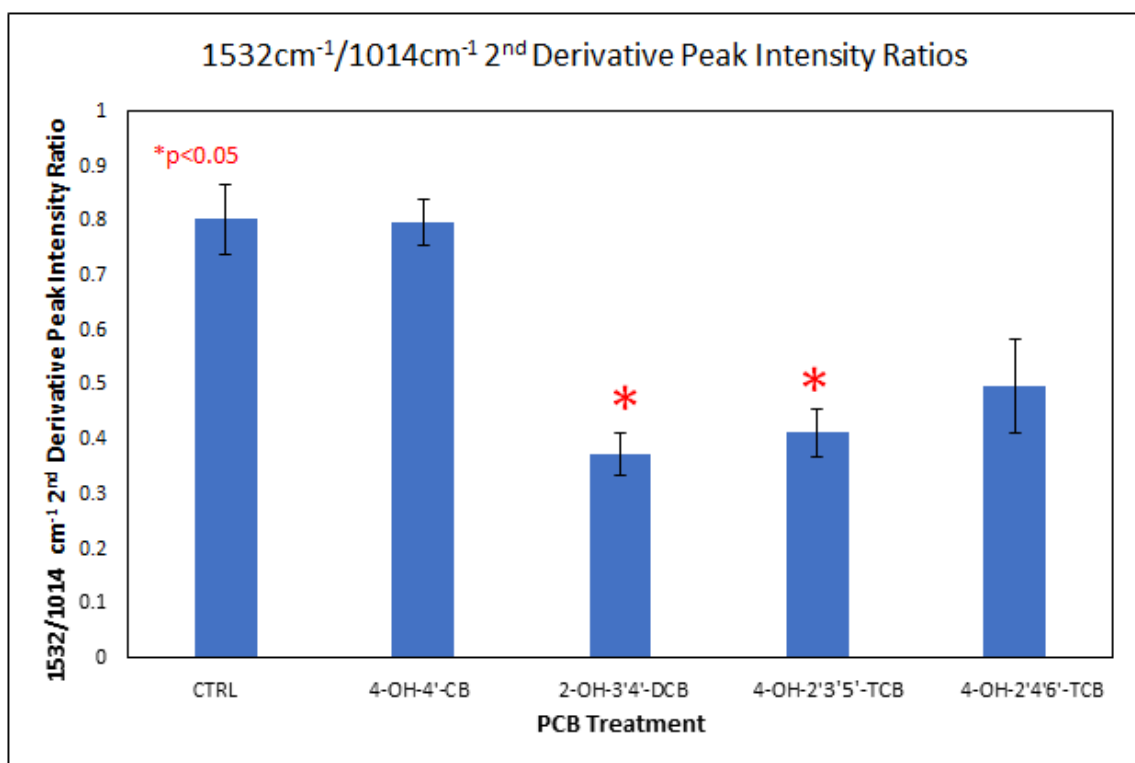


Figure 5.8 The ratio of area under the lignin and matrix peaks in plants exposed to OH-PCBs and non-exposed control plants. The error bars represent the standard deviation among three replicates. The asterisk represents the groups that are significantly different from the control ($p < 0.05$).

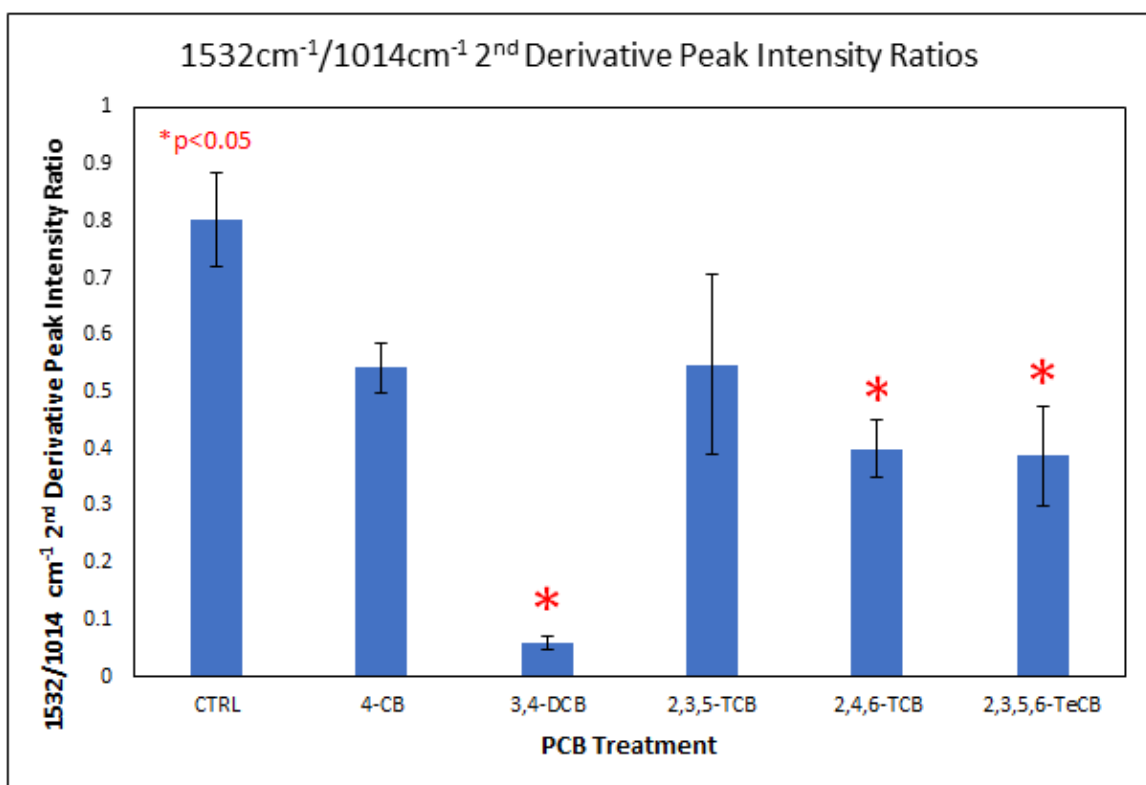


Figure 5.9 The ratio of area under the lignin and matrix peaks in plants exposed to PCBs and non-exposed control plants. The error bars represent the standard deviation among three replicates. The asterisk represents the groups that are significantly different from the control ($p < 0.05$).

From Figure 5.8, it can be observed that the hydroxylated congeners of 3',4'-DCB and 2',3',5'-TCB cause a significant decrease in lignin as compared to the control. In plants exposed to parent PCBs (Figure 5.9), only 3,4-DCB, 2,4,6-TCB and 2,3,5,6-TeCB causes a significant decrease in lignin compared to the controls.

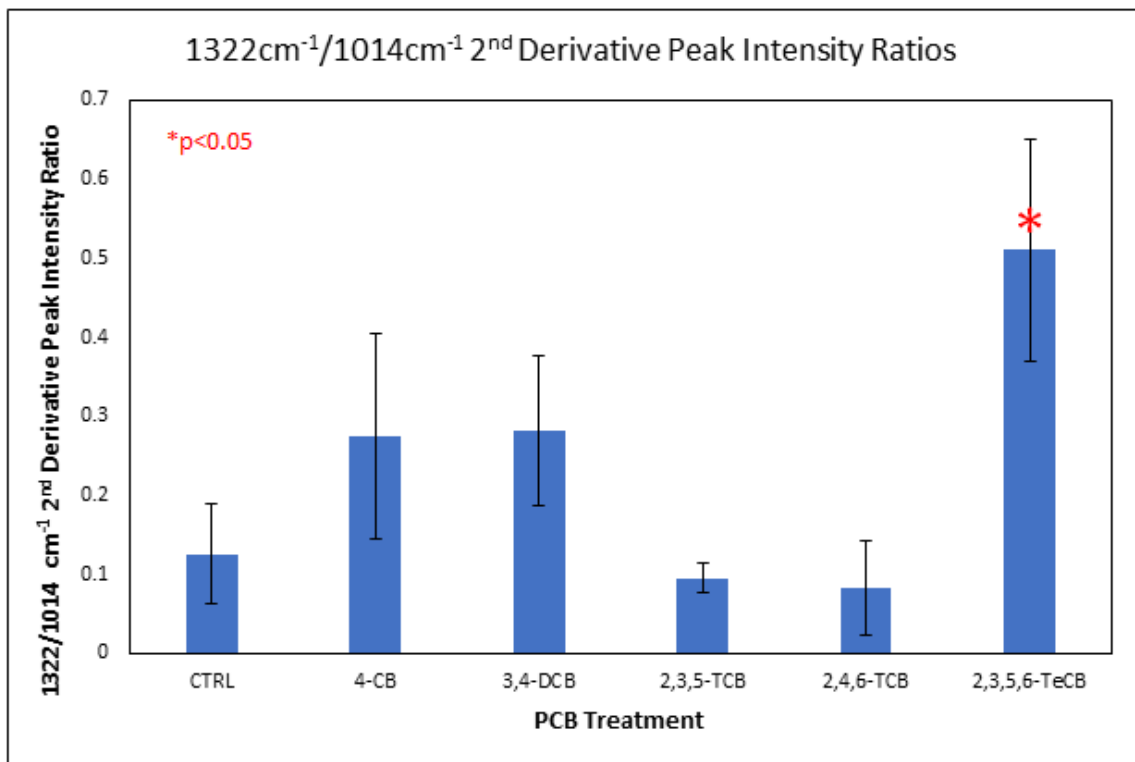


Figure 5.10 The ratio of area under the cellulose and matrix peaks in plants exposed to PCBs and non-exposed control plants. The error bars represent the standard deviation among three replicates. The asterisk represents the groups that are significantly different from the control ($p < 0.05$).

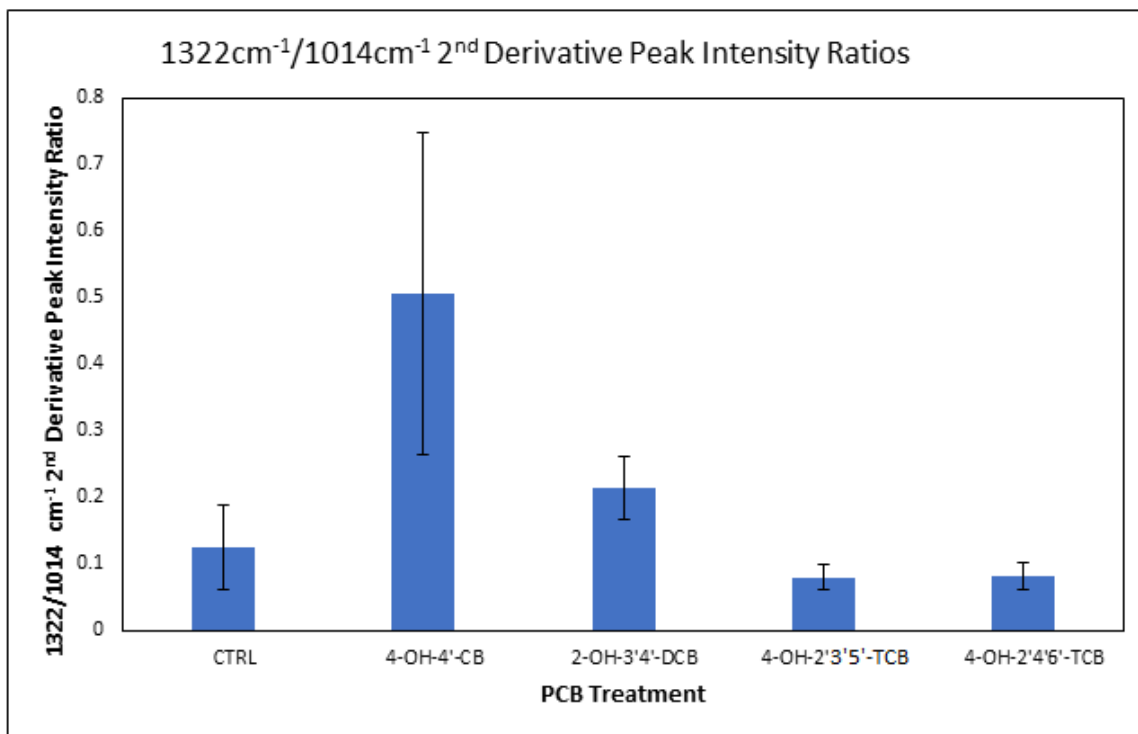


Figure 5.11 The ratio of area under the cellulose and matrix peaks in plants exposed to OH-PCBs and non-exposed control plants. The error bars represent the standard deviation among three replicates. There is no treatment significantly different from the control ($p < 0.05$).

From Figure 5.10 and 5.11, we can observe that only exposure to 2,3,5,6-TeCB results in a significant increase in the cellulose content. Exposure to 2,3,5-TCB and 2,4,6-TCB resulted in a decrease and exposure to 4-CB and 3,4-DCB resulted in an increase in cellulose content, though both these changes are not significant. None of the samples exposed to hydroxylated PCBs resulted in a significant change in the cellulose content.

5.4 Discussion

From the data presented above it can be concluded that infrared spectroscopy is sensitive for detection of the effects of contaminants on the lignocellulose composition in *A. thaliana*. The data shows that a change in lignin and cellulose composition occurred in *A. thaliana* plants exposed to PCBs and hydroxylated PCBs. Spectral data allowed for

understanding the amount of change in the cell wall components. Lignin and cellulose are two key components playing a role in bioethanol generation; therefore, it was essential to identify peaks unique to them in pure component form and compare those peaks to control and contaminated plants. Further, the identification of unique lignin and cellulose peaks by pure component spectra allowed for tracking of those peaks in contaminated plants.

Lignin, is an amorphous, high-molecular weight structure conferring the cell wall rigidity and chemical and physical strength (Demartini, 2011; Ruquia, 2014). To extract cellulose, lignin must be removed, therefore, having smaller amounts of lignin allows for greater accessibility to the sugars that are necessary for biofuel generation (Fu, 2011). In order to understand how the lignin and cellulose composition changed compared to the rest of the components in *A. thaliana*, second derivative was used to compare intensities of lignin and cellulose signals in different treatments compared to the control. These results help to understand the potential impact of environmental contaminants on biomass productivity and digestibility in bioenergy feedstock plants.

Also an increasing trend can be observed in the cellulose starting at the monochlorinated compound, with continuous qualitative decrease as the degree of chlorination increases. This is in correlation with the trend in cellulose content as analyzed in the plants exposed to OH-PCBs. Based on these results, OH-PCBs, with the exception of 4-OH-4'-CB and 4-OH-2',4',6'-TCB, exhibits a significant decrease in the lignin content. This may indicate higher toxicity of OH-PCBs towards plants as previous studies have displayed a decrease in lignin content on exposure to stress conditions such a water deficit and high temperatures (Olenichenko and Zagoskina, 2005; Zwiazek , 1991). This is also consistent

with previous studies conducted by our group where OH-PCBs resulted in higher toxicities towards growth and germination in *A. thaliana* plants, as compared to parent PCBs (Subramanian et al., 2017; Subramanian et al., 2018). The Dunnett's test also indicates significant decrease in lignin content in 3,4-DCB compared to 4-OH-4'-DCB. Though we may not be able to correlate this decrease to a specific mechanism or change, this indicates that different treatments lead to different changes in the lignin content in the *A. thaliana* plants. Previous literature also suggests that the uptake and toxicity of different PCBs are variable and may be governed by the level of chlorination and the substitution patterns (Subramanian et al., 2017). The toxicities also depend on the plant species, experimental conditions, and the length of exposure.

5.5 Conclusion

We believe that this is the first work that shows the effect of differently chlorinated PCBs and their hydroxylated derivatives on the lignin and cellulose content in plants. As observed, OH-PCBs induce a significant reduction in lignin content. This could be attributed to higher toxicity of OH-PCBs as they are susceptible of further hydroxylation inside the plant tissues and may lead to the formation of reactive oxygen species (ROS). These ROS have been reported to cause damage to DNA, proteins, lipids and nucleic acid (Subramanian et al., 2017; Tehrani et al., 2014; Grimm et al., 2015). Tehrani and Van Aken (2014) have reviewed the toxicities of PCBs and OH-PCBs. They describe the solubilities of different PCBs and their hydroxylated congeners. Based on the values of the log K_{ow} (octanol-water partitioning coefficient), OH-PCBs display a higher solubility

than their parent PCBs, and thus are more bioavailable for uptake (Bhalla et al., 2014; Zeeb et al., 2006).

Cheng et al. (2017) in their review article also describe the uptake and translocation of different contaminants in plants based on different chemical parameters. They report a positive correlation between the K_{ow} value of the contaminant and the final concentration of the contaminant found in the plants. This may also explain the higher toxicity of OH-PCBs as they have a high K_{ow} value compared to the parent PCBs. Though PCBs display a lower K_{ow} and in turn lower toxicity, they can still be absorbed by the plants through passive or active uptake (Inui et al., 2008; Cheng et al., 2017).

Cheng et al., (2017) have also hypothesized that organic pollutants such as PCBs and OH-PCBs can be translocated to the stems and the leaves. In the leaves, they display an effect on the cell structure, cell biosynthesis, and cell DNA. Since lignin and cellulose play an integral part of the cell structure, it is but right to hypothesize that exposure to organic contaminants results in changes in the lignin and cellulose content. Also, since the production of lignin and cellulose depends on the cellular enzymes and pathways, their biosynthesis is thus bound to be affected on exposure to contaminants and stress conditions (Cheng et al., 2017; Moore and Harris, 1974; Moore and Roberts, 1998; Brain et al., 2010). In the future, through genome-wide transcriptomic analysis, the molecular basis of the mechanisms by which contaminants affect the biomass growth and lignocellulose composition is recommended to be investigated. This would allow to further understand how the PCBs and their metabolites impact the production of cellulose and lignin at the molecular level. In conjunction with the spectral method, genomic analysis

would help to further assess plant composition, which can be useful to optimize biofuel production.

CHAPTER 6 CONCLUSION

In order to understand the uptake and translocation of PCBs and OH-PCBs in plants, it is first important to determine the toxicity threshold of these contaminants for *A. thaliana* plants. In Specific Aim 1, the potential toxicity of a suite of 11 parent PCBs and their 17 hydroxylated (OH) congeners was evaluated by exposing *A. thaliana* plants to sub-inhibitory concentrations of the contaminants (this was discussed in Chapter 3). The germination rate and biomass growth rate after 21 days of exposure were used to test the difference in toxicity between selected parent PCBs and their hydroxylated derivatives. Generally speaking, exposure to parent PCBs did not result in significant toxicity. In the case of OH-PCBs, the mono-, di- and tri-chlorinated OH-PCBs (with the exception of 4'-OH-3,3',4-TCB) resulted in significant toxicity. As discussed in Chapter 4, *A. thaliana* plants were also exposed to 2,5-DCB and three of its hydroxylated derivatives (for the purpose both of testing the toxicity and investigating the toxic mechanisms at the molecular level by conducting whole-genome transcriptomic analysis – see Specific Aim 2).

The underlying hypothesis being tested in Specific Aim 1 was that OH-PCBs display a higher toxicity compared to their parent PCBs. This could be attributed to the lower log K_{ow} of the OH-PCBs, as compounds with a lower log K_{ow} show higher uptake by the plants as they are more soluble and bioavailable. However, based on transcriptomic analyses, this higher toxicity of OH-PCBs also originates from different molecular response induced by PCBs and OH-PCBs (Specific Aim 2).

Besides PCBs, it is important to study the effects of OH-PCBs on plants as they have been detected in a broad spectrum of environmental samples (Ueno et al., 2007; Tehrani and Van Aken, 2014).

Thus it is also highly important to study the toxicity mechanisms and metabolic pathways of PCBs and OH-PCBs in plants, which may further help to understand the pathways affected by OH-PCBs and PCBs in plants and potential impacts on humans. This was performed in Specific Aim 2 (Chapter 3 and 4) using both toxicity testing and whole-genome transcriptomic analyses.

A. thaliana plants were exposed to sub-inhibitory concentrations of 2,5-DCB and its three hydroxylated congeners (2-OH-, 3-OH- and 4-OH-2',5'-DCB), as described in Chapter 3 and 4. Using genome wide expression microarrays, we studied the transcriptional response of *A. thaliana* plants to the above-mentioned contaminants. Our results have shown that exposure to the parent PCBs and its hydroxylated derivatives resulted in multiple differentially expressed genes as compared to the controls. A range of 12.1 to 29% genes were found to be differentially expressed amongst all four treatments.

Exposure to 2,5-DCB showed expression profiles similar to those associated with plant safeners, which are compounds used in combination with herbicides (Chapter 3). These safeners act as crop protectors without affecting the capacity of the herbicide. Safeners are known to induce a xenobiotic response in plants, and this corresponds with our finding that 38 genes related to xenobiotic response are upregulated upon exposure to 2,5-DCB. Exposure to 2,5-DCB further resulted in an upregulation of genes involved in jasmonic acid, abscisic acid and ethylene, which are mediating multiple stress responses in plants. The up-regulation of these genes may explain the reduced toxicity of PCBs

towards plants, whereas the exposure to OH-PCBs did not induce such a response and thus trigger a higher toxicity towards plants.

As shown in Chapter 4, exposure to the OH-PCBs (but not the parent PCBs) also induced an expression profile similar to those of inhibitors of brassinosteroid synthesis, which induce severe iron deficiency in the plants. This in turn may partially explains the higher toxicity of hydroxylated PCBs as compared to the parent PCB.

As plants used for phytoremediation of toxic compounds, such as PCBs, are not suitable for human or animal consumption, they would be usable for production of biofuel. Second generation bioethanol is obtained from lignocellulosic biomass. Its production depends on the cellulose hydrolysis into fermentable sugars and it would be impaired by high levels of lignin. However, it has been shown by our group and others, that the lignin content in plants may be affected by exposure to environmental contaminants. In Specific Aim 3 (Chapter 5), we tested the hypothesis that exposure of *A. thaliana* plants to PCBs and OH-PCBs would ultimately result in a change in the cell wall composition. Since lignin and cellulose are the primary constituents of the cell wall, we investigated the effect of uptake of the contaminants on the lignin and cellulose content in exposed *Arabidopsis* plants. Spectra from exposed plants and controls, were collected in the mid-IR region, using FTIR-ATR and compared against spectra from the lignin and cellulose standards. The peaks corresponding to lignin and cellulose in the plant samples were compared between exposed plants and non-exposed controls. Overall, exposure to hydroxylated PCBs resulted in a decrease in lignin as compared to the parent PCBs. Exposure to PCBs also showed a decrease in the lignin content. These results are

consistent with results from the prior two Specific Aims, in which we observed that OH-PCBs induce a higher toxicity in *A. thaliana* plants compared to the parent PCBs.

Although this study helped us understand the basic aspects involved in the physiological and transcriptomic changes occurring in *A. thaliana* plants upon exposure to selected PCBs and OH-PCBs, there are certain limitations associated with the study, as stated below:

- a) Due to time and space limitations, the research was carried out on a small scale. A small sample size resulted in higher standard deviations. In order to progress further in this research, larger sample sizes and multiple time points would allow deepen the analysis.
- b) Also using actual soil contaminated with PCBs and OH-PCBs would help evaluating toxicity in a more practical manner as most of the PCB contaminations have been found in soil and sediments
- c) Since *A. thaliana* are small plants, the entire plant had to be collected for the analyses. It would be also useful to study transcriptomic changes and changes in the cell wall composition separately each tissue of the plant.

We used *A. thaliana*, which is not a crop plant and thus the results obtained may not be directly translated to larger plants with potential for phytoremediation, such as switchgrass or brassica. Keeping in mind these limitations, the results of this research successfully demonstrated the use of molecular techniques in understanding the toxic response and metabolic changes occurring in *A. thaliana* plants upon exposure to PCBs and OH-PCBs. Exposure to PCBs and OH-PCBs resulted in a dose-dependent response on the germination and biomass. Using molecular techniques such as microarrays and

RT-qPCR helped compare the pathways and genes up-regulated and down-regulated upon exposure to 2,5-DCB and its hydroxylated congeners. Further application of the FTIR technique to understand the changes in lignin and cellulose content in the cell wall provided evidence that IR spectroscopy can be a valuable tool in studying plant response to exposure to contaminants and stress conditions.

The results obtained from this research lays the foundation of further future perspectives. This research was carried out in fundamental, lab-scale settings using sterile media. Long-term exposure of *A. thaliana* plants to PCBs and OH-PCBs on contaminated soil will give a real world understanding on the effects of these contaminants on plants. The response of living organisms, including plants, to xenobiotic pollutants is known to be primarily regulated at the transcriptional level. Regulation of gene expression is mediated by complex interactions between signaling cascades, transcription factors, and gene promoters. To develop a deeper understanding, epigenetic modifications of the DNA, including DNA methylation, histone modification, and RNA interference (RNAi), that regulate gene expression in mammals and plants, would need to be investigated. In higher plants, the epigenetic changes induced by environmental factors are known to be sometimes retained after the exposure, allowing a faster and more efficient response during recurring events. This 'epigenetic memory' is therefore believed to contribute to plant adaptation to environmental perturbations

It would further be beneficial to use more biofuel oriented, larger plant species, such as soybean and switchgrass, to understand the changes occurring in the lignin and cellulose composition in the cell wall. Also more advanced transcriptomic analysis methods, such as RNA sequencing, could shed more light on the pathways and genes up and down regulated, which are involved in lignin and cellulose synthesis.

Although FTIR analysis helped us identify the peaks characterizing changes in lignin and cellulose composition upon exposure to the contaminants, additional analytical

techniques such as spectrometric and biochemical methods would help confirm the FTIR results.

REFERENCES

Ahamed, G., Ruan, Y., Zhou, J., Xia, X., Shi, K., Zhou, Y., Yu, J., “Brassinosteroid alleviates polychlorinated biphenyls-induced oxidative stress by enhancing antioxidant enzymes activity in tomato”, *Chemosphere*, pp 2645-2653, 2013.

Anderson, P., Hites, R., “OH radical reactions: The major removal pathway for polychlorinated biphenyls from the atmosphere”, *Environmental Science & Technology*, pp 1756-1763, 1996.

Anjos, O., Campos, M. G., Ruiz, P. C., Antunes, P., “Application of FTIR-ATR spectroscopy to the quantification of sugar in honey”, *Food Chem.*, pp 218-23, 2015.

Arulmozhiraja, S., Shiraishi, F., Okumura, T., Iida, M., Takigami, H., Edmonds, J., Morita, M., “Structural requirements for the interaction of 91 hydroxylated polychlorinated biphenyls with estrogen and thyroid hormone receptors”, *Toxicol. Sci.*, 84, 49-62, 2005.

Aslund, M.L.W., Zeeb, B.A., Rutter, A., Reimer, K.J., “In Situ Phytoextraction of Polychlorinated biphenyls- PCB contaminated soil”, *Science of The Total Environment*, pp 1-12, 2007.

ATSDR Agency for Toxic Substances and Disease Registry Toxic Substances Portal- Polychlorinated Biphenyls. [online].

Awad, A., Martinez, A., Marek, R., Hornbuckle, K., “Occurrence and Distribution of Two Hydroxylated Polychlorinated Biphenyl Congeners in Chicago Air”, *Environmental Science & Technology Letters*, pp 47-51, 2016.

Baker, M.J., Trevisan, J., Bassan, P., Bhargava, R., Butler, H.J., Dorling, K.M., Fielden, P.R., Fogarty, S.W., Fullwood, N.J., Heys, K.A., Hughes, C., Lasch, P., Martin-Hirsch, P.L., Obinaju, B., Sockalingum, G.D., Sulé-Suso, J., Strong, R.J., Walsh, M.J., Wood, B.R., Gardner, P., Martin, F.L., “Using Fourier transform IR spectroscopy to analyze biological materials”, *Nat. Protoc.*, pp 1771–1791, 2014.

- Balasubramaniam, A., “Hormetic dose response as the paradigm of plant response to stress”, *Int. J. Plant Biol. Res.*, pp 1037, 2015.
- Balciunas, J.K., Grodowitz, M.J., Cofrancesco, A.F., Shearer, J.F., “Hydrilla. In: Van Driesche R et al (eds)”, *Biological Control of Invasive Plants in the Eastern United States*, USDA Forest Service Publication FHTET-2002-04, 413 p, 2002.
- Behringer, C., Bartsch, K., Schaller, A., “Safeners recruit multiple signalling pathways for the orchestrated induction of the cellular xenobiotic detoxification machinery in *Arabidopsis*”, *Plant Cell Environ.*, 34, 1970–1985, 2011.
- Bevan, M., Walsh, S., “The *Arabidopsis* Genome: A Foundation for plant research”, *Cold Spring Harbor Laboratory Press*, pp 1632-1642, 2005.
- Beyer, A., Biziuk, M., “Environmental Fate and Global Distribution of Polychlorinated Biphenyls”, *Reviews of Environmental Contamination and Toxicology*, pp 137-158, 2009.
- Bhalla, R., Tehrani, R., Van Aken, B., “Toxicity of hydroxylated polychlorinated biphenyls (HO-PCBs) using the bioluminescent assay Microtox (R)”, *Ecotoxicology* 25(7):1438-1444, 2016.
- Blanchet, S., “The use of molecular tools in invasion biology: An emphasis on freshwater ecosystems”, *Fisheries Manag. Ecol.*, pp 120-132, 2012
- Blanco, C.A., Koornneef, M., “Naturally occurring variation in *Arabidopsis*: an underexploited resource for plant genetics”, *Trends Plant Science*, pp 22-29, 2000.
- Block, T.A., Rhoads, A.F., “Aquatic Plants of Pennsylvania: A Complete Reference Guide”, *University of Pennsylvania Press, Philadelphia*, 2011.
- Bloom, M.S., Vena, J.E., Olson, J.R., Kostyniak, P.J., “Assessment of polychlorinated biphenyl congeners, thyroid stimulating hormone, and free thyroxine among New York

State anglers”, *International Journal of Hygiene and Environmental Health*, pp 599-611, 2009.

Bollati, V., Baccarelli, A., Hou, L., Bonzini, M., Fustinoni, S., Cavallo, D., “Changes in DNA methylation patterns in subjects exposed to low-dose benzene”, *Cancer Res.*, pp 876-880, 2007.

Brain, R.A., Solomon, K. R., Brooks, B. W., “Targets, effects and risks in aquatic plants exposed to veterinary antibiotics”, *Acs Symposium Series*, pp 169–189, 2010.

Brumbarova, T., Bauer, P., Ivanov, R., “Molecular mechanisms governing Arabidopsis iron uptake”, *Trends Plant Sci.*, 20(2):124-33, 2015.

Buckman, A., Wong, C., Chow, E., Brown, S., Solomon, K., Fisk, A., “Biotransformation of polychlorinated biphenyls (PCBs) and bioformation of hydroxylated PCBs in fish”, *Aquatic Toxicology*, 78, 176-185, 2006.

Camara, B., Herrera, C., Gonzalez, M., Couve, E., Hofer, B., Seeger, M., “From PCBs to highly toxic metabolites by the biphenyl pathway”, *Environ. Microbiol.*, pp 842-850, 2004.

Cao, W.H., Liu, J., He, X.J., Mu, R.L., Zhou, H.L., Chen, S.Y., Zhang, J.S., “Modulation of ethylene responses affects plant salt-stress responses”, *Plant Physiol*, 143(2):707-19, 2007.

Carbon, S., Ireland, A., Mungall, C.J., Shu, S., Marshall, B., Lewis, S., Davis, A.P., Dolinski, K., Dwight, S.S., Eppig, J.T., Harris, M.A., Hill, D.P., Issel-Tarver, L., Kasarskis, A., Lewis, S., Matese, J.C., Richardson, J.E., Ringwald, M., Rubin G.M., Sherlock, G., “AmiGO: Online access to ontology and annotation data”, AmiGO Hub, Web Presence Working Group. *Bioinformatics*, 25, 288-9, 2009.

Carpenter, D.O., “Polychlorinated biphenyls (PCBs): routes of exposure and effects on human health”, *Rev. Environ. Health*, 21 (1), 1-23, 2006.

Cary SC, Hicks BJ, Crawford NJ, Coyne K (2006). *A sensitive genetic-based detection capability for Didymosphenia geminata*. Interim Report. CBER Contract Report 45. MAF Biosecurity New Zealand.

Cary, C., Hicks, B.J., Coyne, K., Rueckert, A., Gemmill, C.E.C., Barnett, C.M.E., “*A Sensitive Genetic-Based Detection Capability for Didymosphenia geminata (Lyngbye) Schmidt*”, *CBER Contract Report*, pp 62, 2007.

Cary, S., Coyne, K., Rueckert, A., Wood, S., Kelly, S., Gemmill, C., Vieglais, C., Hicks, B., “Development and validation of a quantitative PCR assay for the early detection and monitoring of the invasive diatom *Didymosphenia geminata*”, *Harmful Algae*, **36**:63-70, 2014.

CBOL Plant Working Group, “A DNA barcode for land plants”, *Proc. Natl. Acad. Sci. USA*, pp 12794-12797, 2009.

Center for Aquatic and Invasive Plants-CAIP, “*Hydrilla verticillata*”, University of Florida, IFAS Extension. <http://plants.ifas.ufl.edu/node/183>, 2001a.

Center for Aquatic and Invasive Plants-CAIP, “*Myriophyllum spicatum*”, University of Florida, IFAS Extension. <http://plants.ifas.ufl.edu/node/278>, 2001b.

Chen, H., Ferrari, C., Angiuli, M., Yoa, J., Raspi, C., Bramanti, E., “Qualitative and quantitative analysis of wood samples by Fourier transform infrared spectroscopy and multivariate analysis”, *Carbohydrate Polymers*, pp 772–778, 2010.

Chinnusamy, V., Zhu, J. “Epigenetic regulation of stress responses in plants RID B-9079”, *Curr. Opin. Plant Biol.* 12:133-139, 2009.

Chroma, L., Moeder, M. Kucerova, P., Macek, T., Mackova, M., “Plant enzymes in metabolism of polychlorinated biphenyls”, *Fresen. Environ. Bull.*, pp 291-295, 2003.

Cobbett, C.S., Meagher, R.B., “*Arabidopsis* and the genetic potential for the phytoremediation of toxic elemental and organic pollutants”, *Arabidopsis Book*, 2002.

Connor, K., Ramamoorthy, K., Moore, M., Mustain, M., Chen, I., Safe, S., Zacharewski, T., Gillesby, B., Joyeux, A., Balagner, P., “Hydroxylated Polychlorinated Biohenyls (PCBs) as Estrogens and Antiestrogens : Structure-Activity Relationships”, *Toxicology and Applied Pharmacology*, pp 111-123, 1997.

Coyne, K.J., Handy, S.M., Demir, E., Whereat, E.B., Hutchins, D.A., Portune, K.J., Doblin, M.A., Cary, S.C., “Improved quantitative real-time PCR assays for enumeration of harmful algal species in field samples using an exogenous DNA reference standard”, *Limn. Ocean. Meth.*, pp 381-391, 2005.

Luz, da B.R., “Attenuated total reflectance spectroscopy of plant leaves: a tool for ecological and botanical studies”, *New Phytol.*, pp 305-18, 2006.

Dejean, T., Valentini, A., Miquel, C., Taberlet, P., Bellemain, E., Miaud, C., “Improved detection of an alien invasive species through environmental DNA barcoding: The example of the American bullfrog *Lithobates catesbeianus*”, *J. Appl. Ecol.*, pp 953-959, 2012.

Demartini, J.D., Wyman, C. E., “Composition and hydrothermal pretreatment and enzymatic saccharification performance of grasses and legumes from a mixed-species prairie”, *Biotechnol Biofuels*, 4, 52, 2011.

DeRidder, B., Dixon, D., Beussman, D., Edwards, R., Goldsbrough, P., “Induction of glutathione S-transferases in *Arabidopsis* by herbicide safeners”, *Plant Physiology*, 130(3):1497-1505, 2002.

Desforges, J.P., Hall, A., McConnell, B., Rosing-Asvid, A., Barber, J.L., Brownlow, A., De Guise, S., Eulaers, I., Jepson, P.D., Letcher, R.J., Levin, M., Ross, P.S., Samarra, F., Vikingson, G., Sonne, C., Dietz, R., “Predicting global killer whale population collapse from PCB pollution”, *Science*, pp 1373-1376, 2018.

EPA- Learn about Polychlorinated Biphenyls. [online].

- Flöder, S., Kilroy, C., “*Didymosphenia geminata* (Protista, Bacillariophyceae) invasion, resistance of native periphyton communities, and implications for dispersal and management”, *Biodivers. Conserv.*, pp 3809–3824, 2009.
- Fujita, M., Fujita, Y., Noutoshi, Y., Takahashi, F., Narusaka, Y., Yamaguchi-Shinozaki, N., Shinozaki, K., “Crosstalk between abiotic and biotic stress responses: A current view from the points of convergence in the stress signaling networks”, *Curr. Opin. Plant Biol.*, pp 436-442, 2006.
- Garcia-Sanchez, S., Bernales, I., Cristobal, S., “Early response to nanoparticles in the *Arabidopsis* transcriptome compromises plant defence and root-hair development through salicylic acid signaling”, *BMC Genomics*, 16, 341, 2015.
- Hahn, M., “The aryl hydrocarbon receptor: A comparative perspective”, *Comp. Biochem. Physiol. C Pharmacol. Toxicol. Endocrinol.*, 121, 23-53, 1998.
- Hamsher, S.E., Evans, K.M., Mann, D.G., Poulíčková, A., Saunders, G.W., “Barcoding diatoms: Exploring alternatives to COI-5P”, *Protist.*, pp 405-422, 2011.
- Hartwig, T., Corvalan, C., Best, N.B., Budka, J.S., Zhu, J.Y., Choe, S., Schulz, B., “Propiconazole is a specific and accessible brassinosteroid (BR) biosynthesis inhibitor for *Arabidopsis* and maize”, *PLoS One*, 7(5):e36625, 2012.
- Hoffmann, M.H., “Biogeography of *Arabidopsis thaliana* (L.) Heynh. (Brassicaceae),” *Journal of Biogeography*, 29:125-134, 2002.
- Hooper, S., Pettigrew, C.A., Sayler, G., “Ecological fate, Effects and Prospects for the Elimination of Environmental Polychlorinated Biphenyls (PCBs)”, *Environmental Toxicology and Chemistry*, pp 655-667, 1999.
- Houston, K., Tucker, M.R., Chowdhury, J., Shirley, N., Little, A., “The Plant Cell Wall: A Complex and Dynamic Structure As Revealed by the Responses of Genes under Stress Conditions”, *Front. Plant Sci.*, pp 984, 2016.

Hruz, T., Laule, O., Szabo, G., Wessendorp, F., Bleuler, S., Oertle, L., et al., "Genevestigator v3: A reference expression database for the meta-analysis of transcriptomes", *Adv. Bioinformatics*, 420747, 2008.

Huck, C.W., "Advances of vibrational spectroscopic methods in phytomics and bioanalysis", *J. Pharm. Biomed. Anal.*, pp 26-35, 2014.

Imadi, S., Kazi, A., "Extraction of Lignin from Biomass for Biofuel Production", *Agricultural Biomass Based Potential Materials*, 2015.

Inui, H., Wakai, T., Gion, K., Kim, Y. S., Eun, H., "Differential uptake for dioxin-like compounds by zucchini subspecies", *Chemosphere*, pp 1602-7, 2008.

Invasive Species Advisory Committee-ISAC, "Validation of PCR-Based Assays and Laboratory Accreditation for Environmental Detection of Aquatic Invasive Species", US Department of the Interior, Office of the Secretary (OS/SIO/NISC), pp 9, 2012.

Invasive.org, "Early Detection and Rapid Response (EDRR)", <http://www.invasive.org/edrr/>, 2013

Jaramillo, A., Osman, D., Caputo, L., Cardenas, L., "Molecular evidence of a *Didymosphenia geminata* (Bacillariophyceae) invasion in Chilean freshwater systems", *Harmful Algae*, pp 117-123, 2015.

Jensen, C. S., "Report of a new chemical hazard", *New Sci.*, 32:612, 1966.

Jiang, R., Tyler, B., VanAlfen, N., Leach, J., Lindow, S., "Mechanisms and evolution of virulence in oomycetes", *Annu. Rev. Phytopathol.*, pp 295-318, 2012.

Jin, X.F., Shuai, J.J., Peng, R.H., Zhu, B., Fu, X.Y., Tian, Y.S., Zhao, W., Han, H.J., Chen, C., Xu, J., "Identification of candidate genes involved in responses of Arabidopsis to polychlorinated biphenyls based on microarray analysis", *Plant Growth Regulation*, pp 127-135, 2011.

Johnson, R.L., Blossey, B., “Eurasian Watermilfoil. In: Van Driesche R et al (eds)”, *Biological Control of Invasive Plants in the Eastern United States*, USDA Forest Service Publication FHTET-2002-04, pp 413, 2002.

Kaveh, R., Li, Y.S., Ranjbar, S., Tehrani, R., Van Aken, B., Bruek, C.L., “Changes in *Arabidopsis thaliana* Gene Expression in Response to Silver Nanoparticles and Silver Ions”, *Environmental Science and Technology*, pp 10637-10644, 2013.

Kawano, M., Hasegawa, J., Enomoto, T., Onishi, H., Nishio, Y., Matsuda, M., Wakimoto, T., “Hydroxylated polychlorinated biphenyls (OH-PCBs): Recent advances in wildlife contamination study”, *Environ. Sci.*, pp 315-324, 2005.

Khan, A.G., “Mycorrhizoremediation – An Enhanced Form of Phytoremediation”, *Journal of Zhejiang University SCIENCE B*, pp 503-514, 2006.

Kilroy, C., “*A new Alien Diatom, Didymosphenia geminata (Lyngbye) Schmidt: Its Biology, Distribution, Effects and Potential Risks for New Zealand Fresh Waters*”. NIWA, Christchurch, New Zealand, 2004.

Kimbrough, R.D., “Polychlorinated Biphenyls (PCBs) and Human Health: An Update”, *Critical Reviews in Toxicology*, pp 133-163, 1995.

Kinoshita, T., Seki, M., “Epigenetic memory for stress response and adaptation in plants”, *Plant and Cell Physiology*, pp 1859-1863, 2014.

Kobayashi, T., Nishizawa, N.K., “Iron sensors and signals in response to iron deficiency”, *Plant Sci.*, 224:36-43, 2014.

Kress, W., Wurdack, K., Zimmer, E., Weigt, L., Janzen, D., “Use of DNA barcodes to identify flowering plants”, *Proc. Natl. Acad. Sci. U.S.A.*, pp 8369-8374, 2005.

Krzyszowska, M., “The cell wall in plant cell response to trace metals: polysaccharide remodeling and its role in defense strategy”, *Acta. Physiologiae Plantarum*, pp 35, 2011.

Kucerova, P., Mackova, M., Chroma, L., Burkhard, J., Triska, J., Demnerova, K., Macek, T., “Metabolism of polychlorinated biphenyls by *Solanum nigrum* hairy root clone SNC-90 and analysis of transformation products”, *Plant Soil*, 225, 109-115, 2000.

Lahaye, R., Van der Bank, M., Bogarin, D., Warner, J., Pupulin, F., Gigot, G., Maurin, O., Duthoit, S., Barraclough, T.G., Savolainen, V., “DNA barcoding the floras of biodiversity hotspots”, *Proc. Natl. Acad. Sci. U.S.A.*, pp 2923-2928, 2008.

Lahlali, R., Jiang, Y., Kumar, S., Karunakaran, C., Liu, X., Borondics, F., Hallin, E., Bueckert, R., “ATR-FTIR spectroscopy reveals involvement of lipids and proteins of intact pea pollen grains to heat stress tolerance”, *Front. Plant Sci.*, pp 747, 2014.

Largo-Gosens, Asier, “Fourier Transform Mid Infrared Spectroscopy Applications for Monitoring the Structural Plasticity of Plant Cell Walls”, *Frontiers in Plant Science*, pp 303, 2014.

Lee, I., Fletcher, J.S., “Involvement of mixed-function oxidase systems in polychlorinated biphenyl metabolism by plant-cells”, *Plant Cell Rep.*, pp 97-100, 1992.

Liu, J., Schnoor, J.L., “Uptake and Translocation of Lesser Chlorinated polychlorinated Biphenyls (PCBs) in Whole Hybrid Poplar Plants after Hydroponic Exposure”, *Chemosphere*, pp 1608-1616, 2008.

Macek, T., Pavlikova, D., Mackova M., “Phytoremediation of Metals and Inorganic Pollutants”, *Applied Bioremediation and Phytoremediation*, pp 135-157, 2004.

Mahanty, H.K., “Polychlorinated biphenyls: Accumulation and effects upon plants”, *PCBs and the Environment*, pp 1-8, 1986.

Marek, R., Martinez, A., Hornbuckle, K., “Discovery of Hydroxylated Polychlorinated Biphenyls (OH-PCBs) in Sediment from a Lake Michigan Waterway and Original Commercial Aroclors”, *Environmental Science & Technology*, pp 8204-8210, 2013.

- Meerts, I.A., Letcher, R.J., Howing, S., Marsh, G., Bergman, A., Lemmen, J.G., Burg, B., Browner, A., “In vitro Estrogenicity of Polybrominated Diphenyl Ethers, Hydroxylated PDBEs and Polybrominated bisphenol A Compounds”, *Environmental Health Perspective*, pp 399-407, 2001.
- Meyerowitz, E.M., Pruitt, R.E., “Arabidopsis thaliana and Plant Molecular Genetics”, *Science*, 1214-8, 1985.
- Montano, M., Gutleb, A., Murk, A., “Persistent Toxic Burdens of Halogenated Phenolic Compounds in Humans and Wildlife”, *Environmental Science & Technology*, pp 6071-6081, 2013.
- Moore, K., Roberts, L.J., “Measurement of lipid peroxidation”, *Free Radical Research*, pp 659–671, 1998.
- Moore, S.A., Harriss, R.C., “Differential sensitivity to PCB by phytoplankton”, *Marine Pollution Bulletin*, pp 174–176, 1974.
- Müller, G., Christian, S., Vos, H., Alireza, K., Andrea, P., “FTIR-ATR spectroscopic analyses of changes in wood properties during particle and fibreboard production of hard and softwood trees”, *BioResources*, pp, 49-71. 2009
- Müssig C., Fischer S., Altmann T., “Brassinosteroid-regulated gene expression”, *Plant Physiol.*, pp 1241-51, 2002.
- New York Invasive Species Information-NYIS.INFO, “Rock Snot, *Didymo (Didymosphenia geminata)*”, *The New York Invasive Species Clearinghouse Cornell Cooperative Extension Invasive Species Program*, Retrieved July 06, 2012, from http://www.nyis.info/index.php?action=invasive_detail&id=40, 2011.
- Nguyen, D., Rieu, I., Mariani, C., van Dam, N., “How plants handle multiple stresses: Hormonal interactions underlying responses to abiotic stress and insect herbivory”, *Plant Mol. Biol.*, pp 727-740, 2016.

Olenichenko, N.A., Zagoskina, N.V., “Response of winter wheat to cold: production of phenolic compounds and L-phenylalanine ammonia-lyase activity”, *Prikl. Biokhim. Mikrobiol.*, pp 681-5, 2005.

Organisation for Economic Co-operation and Development–OECD/OCDE, “*Lemna sp.* growth inhibition test. OECD guidelines for the testing of chemicals”, pp 221, 2006.

Page, D.R., Grossniklauss, U., “The Art and Design of Genetic Screens: *Arabidopsis thaliana*”, *Nature Reviews Genetics*, pp 124-136, 2002.

Pal, D., Weber, J.B., Overcash, M.R., Gunther, A.F., Gunther, J.D., “Fate of Polychlorinated Biphenyls (PCBs) in soil plant systems”, *Residue reviews: Residues of pesticides and Other Contaminants in the Total Environment*, pp 45-98, 1980.

Polychlorinated Biphenyls- EPA United States [online].

Prasad, M.N.V., Nakbanpote, W., Phadermrod, C., Rose, D., Suthari, S., “Mulberry and ventiver for phytostabilization of mine overburden: cogeneration of economic products”, *Bioremediation and bioeconomy*, pp 295-328, 2016.

Rahaman, M., Triferio, F.L., Pistone, “Destruction Technologies for Polychlorinatedbiphenyls (PCBs), proceedings of expert group meetings on POPs and pesticides contamination: remediation technologies (April 2000) and on clean technologies for the reduction and elimination of POPs, (May 2000)”, *ICS-UNIDO*, 2000.

Ramegowda, V., Senthil-Kumar M., “The interactive effects of simultaneous biotic and abiotic stresses on plants: Mechanistic understanding from drought and pathogen combination”, *Journal of Plant Physiology*, pp 47-54, 2015.

Ramel, F., Sulmon, C., Serra, A., Gouesbet, G., Couee, I., “Xenobiotic sensing and signalling in higher plants”, *J. Exp. Bot.* 63: 3999–4014, 2012.

Rezek, J., Macek, T., Mackova, M., Triska, J., Ruzickova K., “Hydroxy-PCBs, Methoxy –PCBs and Hydroxy-Methoxy –PCBs: Metabolites of Polychlorinated Biphenyls Formed

In Vitro by Tobacco Cells”, *Environmental Science and Technology*, pp 5746-5751, 2008.

Riechers, D.E., Kreuz, K., Zhang, Q., “Detoxification without Intoxication: herbicide safeners activate plant defense gene expression”, *Plant Physiol.*, 153, 3–13, 2010.

Rigal, A., Ma, Q., Robert, S., “Unraveling plant hormone signaling through the use of small molecules”, *Front. Plant Sci.*, 5, 373, 2014.

Safe, S.H., “Polychlorinated biphenyls (PCBs): Environmental Impact, Biochemical and Toxic Responses, and Implications for Risk Assessment”, *Critical Reviews in Toxicology*, pp 87-149, 1994.

Salimizadeh, M., Shirvani, M., Shariatmadari, H., Nikaeen, M., Leili Mohebi Nozar, S., “Coupling of bioaugmentation and phytoremediation to improve PCBs removal from a transformer oil-contaminated soil”, *Int. J. Phytoremediation*, pp 658-665, 2018.

Sanderman, H.Jr., “Higher plant metabolism of xenobiotics: The "green liver" concept”, *Pharmacogenetics*, pp 225-241, 1994.

Schmidt, M., Schwartzberg, A.M., Carroll, A., Chaibang, A., Adams, P.D., Schuck, P.J., “Raman imaging of cell wall polymers in *Arabidopsis thaliana*”, *Biochem. Biophys. Res. Commun.*, pp 521-3, 2010.

Schnoor, J.L., Licht, L.A., McCutcheon, S.C., Wolfe, N.L., Carreira, L.H., “Phytoremediation of organic and nutrient contaminants”, *Environ. Sci. Technol.*, 29(7):318A-23A, 1995.

Schwarzenbach, R.P., Gschwend, P.M., Imboden, D.M., “*Environmental Organic Chemistry*”, 3rd ed.; 2016.

Sharma, J.K., Gautam, R.K., Nanekar, S.V., Weber, R., Singh, B.K., Singh, S.K., Juwarkar, A.A., “Advances and perspective in bioremediation of polychlorinated biphenyl-contaminated soils”, *Environ. Sci. Pollut. Res. Int.*, pp 16355-16375, 2018.

Silldorff, E.L., “Status Update on 2012 Didymo Bloom in the Delaware River (Updated & Revised)”, 14-May-2012. Retrieved July 06, 2012, from http://www.nj.gov/drbc/library/documents/silldorff_didymo-update051012.pdf.

Singer, A.C., Smith, D., Jury, W.A., Hathuc, K., Crowley, D.E., “Impact of the plant rhizosphere and augmentation on remediation of polychlorinated biphenyl contaminated soil”, *Environ. Toxicol Chem.*, pp 1998-2004, 2003.

Singh, H.K., Parveen, I., Raghuvanshi, S., Babbar, S.B., “The loci recommended as universal barcodes for plants on the basis of floristic studies may not work with congeneric species as exemplified by DNA barcoding of *Dendrobium* species”, *BMC Res., Notes* 5:42, 2012.

Singh, K., Foley, R., Onate-Sanchez, L., “Transcription factors in plant defense and stress responses”, *Curr. Opin. Plant Biol.*, pp 430–436, 2002.

Sivitz, A.B., Hermand, V., Curie, C., Vert, G., “Arabidopsis bHLH100 and bHLH101 control iron homeostasis via a FIT-independent pathway”, *PLoS One*, 7(9):e44843, 2012.

Skipsey, M., Knight, K., Brazier-Hicks, M., Dixon, D., Steel, P., Edwards, R., “Xenobiotic Responsiveness of *Arabidopsis thaliana* to a Chemical Series Derived from a Herbicide Safener”, *Journal of Biological Chemistry*, pp 32268-32276, 2011.

Somerville, C., Koornneef, M., “A Fortunate Choice: The history of *Arabidopsis* as a model plant”, *Nature Reviews*, pp 883-889, 2002.

Spaulding, S., Elwell, L., “Increase in Nuisance Blooms and Geographic Expansion of the Freshwater Diatom *Didymosphenia geminata*”, *White Paper, January 2007*, United States Environmental Protection Agency, 2007.

Subramanian, S., Schnoor, J.L., Van Aken, B., “Effects of Polychlorinated Biphenyls (PCBs) and Their Hydroxylated Metabolites (OH-PCBs) on *Arabidopsis thaliana*”, *Environ. Sci. Technol.*, pp 7263-7270, 2017.

Swearingen, J., Slattery, B., Reshetiloff, K., Zwicker, S., “*Plant Invaders of Mid-Atlantic Natural Areas*”, 4th ed. National Park Service and U.S. Fish and Wildlife Service, pp 168, 2010

Tanabe, S., “PCB problems in the future: Foresight from current knowledge”, *Environmental Pollution*, 50:5-28, 1988.”

Tehrani, R, Van Aken, B., “Hydroxylated polychlorinated biphenyls in the environment: sources, fate, and toxicities”, *Environmental Science and Pollution Research*, pp 6334-6345, 2014.

Tehrani, R., Lyv, M. M., Kaveh, R., Schnoor, J. L., Aken, B. V., “ Biodegradation of Mono- hydroxylated PCBs by *Burkholderia xenovorans* LB400”, *Biotechnology Letter*, pp 247-252, 2012.

The *Arabidopsis* Genome Initiative, “Analysis of the genome sequence of the flowering plant *Arabidopsis thaliana*”, *Nature*, pp 796-815, 2000.

Tommasini, R., Vogt, E., Fromenteau, M., Hortensteiner, S., Matile, P., Amrhein, N., Martinoia, E., “An ABC-transporter of *Arabidopsis thaliana* has both glutathione-conjugate and chlorophyll catabolite transport activity”, *Plant Journal*, pp 773-780, 1998.

Van Aken, B., Correa, P., Schnoor, J., “Phytoremediation of Polychlorinated Biphenyls: New Trends and Promises”, *Environmental Science & Technology*, pp 2767-2776, 2010.

Van Aken, B., “Transgenic plants for enhanced Phytoremediation of toxic explosives”, *Current Opinion in Biotechnology*, pp 231-236, 2009.

Van De Wiel, C.C.M., Van Der Schoot, J., Van Valkenburg, J.L.C.H., Duistermaat, H., Smulders, M.J.M., “DNA barcoding discriminates the noxious invasive plant species, floating pennywort (*Hydrocotyle ranunculoides* L.f.), from non-invasive relatives”, *Mol. Ecol. Resour.*, pp 1086-1091, 2009.

- Wang, J., Liu, H., Ren, G., “Near-infrared spectroscopy (NIRS) evaluation and regional analysis of Chinese faba bean (*Vicia faba* L.)”, *The Crop Journal* Volume 2, Issue 1, Pages 28-37, 2014
- Wang, X., Teng, Y., Zhang, N., Christie, P., Li, Z., Luo, Y., Wang, J., “Rhizobial symbiosis alleviates polychlorinated biphenyls-induced systematic oxidative stress via brassinosteroids signaling in alfalfa”, *Sci. Total Environ.*, pp 592:68-77, 2017.
- Weber, J.B., Mrozek, E., “Polychlorinated biphenyls: phytotoxicity, absorption and translocation by plants, and inactivation by activated carbon”, *Bull Environ. Contam Toxicol*, pp 412-417, 1979.
- Whitton, B.A., Ellwood, N.T.W., Kawecka, B., “Biology of the freshwater diatom *Didymosphenia*: A review”, *Hydrobiologia*, 630:1-37, 2009.
- Xi, Y., Li, W., “BSMAP: Whole genome bisulfite sequence MAPPING program”, *BMC Bioinformatics*, 10:232-241, 2009.
- Xie, S., Wang, Z., Okano, M., Nogami, M., Li, Y., He, W., Okumura, K., Li, E., “Cloning, expression and chromosome locations of the human DNMT3 gene family”, *Gene*, 236:87-95, 1999.
- Xu J., Yu J., Tesso T., Dowell F., Wang D., “Qualitative and quantitative analysis of lignocellulosic biomass using infrared techniques: A mini-review”, *Applied Energy*, pp 801-809, 2013.
- Yu, P., “Application of advanced synchrotron-based fourier transform infrared microspectroscopy (SR-FTIR) to animal nutrition and feed science: A novel approach”, *Br. J Nutr.*, pp 869–885, 2004.
- Zeeb, B. A., Amphlett, J. S., Rutter, A., Reimer, K. J., “Potential for phytoremediation of polychlorinated biphenyl-(PCB-)contaminated soil”, *Int. J Phytoremediation*, pp 199-221, 2006.

Zhai, G., Lehmler, H. J., Schnoor, J. L., “Identification of hydroxylated metabolites of 3, 3',4,4'-tetrachlorobiphenyl and metabolic pathway in whole poplar plants”, *Chemosphere*, pp 523-528, 2010.

Zhai, G., Lehmler, H. J., Schnoor, J. L., “Sulfate metabolites of 4-Monochlorobiphenyl in Whole Poplar Plants”, *Environmental Science and Technology*, pp 557-562, 2013.

Zhai, G., Lehmler, H. J., Schnoor, J. L., “Hydroxylated Metabolites of 4-Monochlorobiphenyl and Its Metabolic pathway in Whole Poplar Plants”, *Environmental Science and Technology*, pp 3901-3907, 2010.

Zhai, G., Wu, X., Lehmler, H. J., Schnoor, J. L., “Atropisomeric determination of chiral hydroxylated metabolites of polychlorinated biphenyls using HPLC-MS”, *Chemistry Central Journal*, 7:183, 2013

Zhang, X., “Perspective - The epigenetic landscape of plants”, *Science*, 320:489-92, 2008.

Zhang, C., Feng, Y., Liu, Y.W., Chang, H., Li, Z.J., Xue, J.M., “Uptake and translocation of organic pollutants in plants: a review”, *J. Integr. Agric.*, pp 1659–1668, 2017.

Zhang, L., Li, J., Zhao, Y., Li, X., Wen, S., Shen, H., Wu, Y., “Polybrominated diphenyl ethers (PBDEs) and indicator polychlorinated biphenyls (PCBs) in foods from China: levels, dietary intake, and risk assessment”, *J. Agric. Food Chem.*, pp 6544-51, 2013.

Zhu, B., Peng, R. H., Fu, X. Y., Jin, X. F., Zhao, W., Xu, J., Han, H. J., Gao, J. J., Xu, Z. S., Bian, L., Yao, Q. H., “Enhanced transformation of TNT by Arabidopsis plants expressing an old yellow enzyme”, *PLoS One*, 7 (7), e39861. 2012.

Zwiazek, J.J., “Cell wall changes in white spruce (*Picea glauca*) needles subjected to repeated drought stress”, *Physiol. Plant*, pp 513-518, 1991.

APPENDIX
DEVELOPMENT OF A REAL-TIME PCR METHOD FOR THE EARLY
DETECTION OF AQUATIC INVASIVE SPECIES IN PENNSYLVANIA
WATERSHEDS

The sections presented in this chapter have been published in Van Aken B. and Subramanian S. “Development of a Real-time PCR Method for the Early Detection of Aquatic Invasive Species in Pennsylvania Watersheds”

Abstract

The widespread occurrence of aquatic invasive species is a worldwide issue threatening the environment and impacting the intended use of water. Molecular biology methods based on the detection of specific DNA sequences are fast and sensitive and have raised increasing interest for monitoring invasive species. Analyzing environmental DNA in water for the identification of such unique markers is a powerful strategy for detecting low density invasive species in a water body.

A real-time PCR method was developed and optimized using genomic databases and sequence alignment tools for the early detection of target invasive plant species. The designed primers and fluorescent probes were successful in detecting DNA from the target invasive species. The assays were validated by amplification of DNA marker sequences using specific primers or genomic DNA. Near perfect results were observed for the efficiency of the assays. The application of the assay in the field was tested by amplification of DNA from field water samples. The method was robust in detecting the presence of the target invasive species even miles away from the point of contamination. This allows for quick detection of the presence of target species.

Objective

The objective of the proposed research was to develop and optimize an innovative method (based on real-time PCR) for the early detection of three aquatic invasive plants, *Myriophyllum spicatum*, *Trapa natans* and *Hydrilla verticillata*, and the invasive alga, *Didymosphenia geminata* which all constitute a threat for Pennsylvania watersheds.

Experimental Approach

The proposed research involved three specific objectives:

1. To design assays based on real-time PCR for the detection of the target invasive species.
2. To validate the assays and optimize experimental protocols.
3. To test the applicability and robustness of the assays in the field.

Results

Using resources from genomic databases and sequence alignment tools, we designed primers and fluorescent probes specific to the target species, *T. natans*, *M. spicatum*, *H. verticillata*, and *D. geminata*. The primer and probes allowed the detection of DNA signatures from the target invasive species using real-time PCR. The specificity of the primers and probes was successfully tested against a suite of relative plant species.

The quality control and validation of the method provided overall satisfactory results: near-perfect linearity was observed with all *standard curves*, the *dynamic range* of the detection method expanded over at least five orders of magnitude, and the *amplification*

efficiency was within the adequate range, except for one of the assay (*M. spicatum*), which will require additional optimization.

Three field studies provided results consistent with the expectations. When monitoring the three target invasive plant species, *T. natans*, *H. verticillata*, and *M. spicatum*, specific DNA signatures were detected in water samples miles away from the recognized contamination point. The signal intensities were generally several orders of magnitude higher than the signal intensities obtained with negative control samples. When monitoring *D. geminata*, the specific DNA signature was detected in water samples hundred yards downstream a location where the species was historically detected, even though the presence of the invasive alga was not visible at the time of sampling.

Expected Outcome

The innovative aspect of the developed assays relies on the possibility to detect the target species based on the presence of DNA signatures in the water, i.e., without the need to physically observe or collect specimens. The developed method is expected to allow fast screening of a large number of water bodies with limited personal investment, as it does not require time-consuming microscopic identification.

Introduction

Objective

The overall objective of the proposed research was to develop and optimize an effective technology based on real-time PCR for the early detection of selected plant and algal aquatic invasive species (AIS) in Delaware and Susquehanna watersheds. Invasive

species selected for this study include three aquatic plants, *Myriophyllum spicatum*, *Trapa natans*, and *Hydrilla verticillata*, and the alga, *Didymosphenia geminata*.

Background

The widespread occurrence of AIS is a worldwide environmental issue causing disruption to local communities, threatening biodiversity, and impacting the intended uses of water bodies (Van de Wiel et al., 2009). However, univocal discrimination of invasive plant species from related indigenous ones may be challenging, especially in the absence of suitable morphological markers (e.g., flowers or fruits). Similarly, identification of microscopic algae requires microscopic observations in the laboratory, which is challenging at low cell concentrations or in the presence of morphologically similar organisms (Cary et al., 2006). In addition, conventional methods for the detection of AIS are laborious and time-consuming, allowing exotic species to become well established and widespread. Late detection of AIS may therefore impair the timely application of effective eradication plans.

Because of their extreme specificity and sensitivity, molecular biology methods have raised high interest for the early detection of AIS and they are increasingly recognized as valuable decision-making tools (ISAC 2012). All macroscopic aquatic organisms release small amounts of organic material harboring DNA sequences that constitute a fingerprint unique to each species. Analyzing environmental DNA (eDNA) in water for the identification of such unique markers is therefore a powerful strategy for detecting low densities of AIS in a water body (Blanchet, 2012). Specifically, real-time PCR methods using fluorescent probes do not require post-amplification steps and combine the

advantages of speed, accuracy, and sensitivity over other genetic and conventional techniques (Coyne et al., 2005). Real-time PCR methods have been successfully applied for tracing the presence of various animal and algal AIS, including Asian carp, zebra mussel, bullfrog, and toxic dinoflagellates (Coyne et al. 2005, Dejean et al. 2012, ISAC 2012, Singh et al., 2012). To the best of our knowledge, the potential of molecular methods for detecting aquatic invasive *plant* species has not been extensively investigated.

DNA barcoding methods have recently attracted much attention for biodiversity assessment and detection of invasive species (Kress et al., 2005, Lahaye et al., 2008). These methods are based on the identification of species by using short orthologous DNA sequences (DNA *barcodes*), such as the plastid *trnH-psbA* intergenic spacer for vascular plants and the large subunit of RUBISCO (*rbcL*) for algae (Kress et al., 2005, Hamsher et al., 2011). In this application, we propose to use recognized DNA barcodes to design specific primers and probes for the real-time PCR detection, identification, and quantification of selected plant and algal AIS.

Selection of Invasive Species

Hydrilla verticillata (Hydrilla) is a submersed, herbaceous perennial plant which is extremely adaptable and can grow in almost any freshwater environment including marshes, streams, rivers, and tidal zones (Figure 6.1). The plant can exist in only a few inches of water or in water more than 20-foot deep, and can tolerate oligotrophic to eutrophic conditions. Hydrilla is designated as a *federal noxious* weed because of its rapid growth and its impact on the aquatic ecosystem and human activities. In PA, this

species is found in abundance along the Schuylkill and Delaware River and in other scattered sites in the state (CAIP, 2001a, Balciunas et al., 2002, Block and Rhoads, 2011).



Figure A.1 Hydrilla verticillata

(www.sms.si.edu).

Myriophyllum spicatum (Eurasian water-milfoil) is a submersed rooted, herbaceous perennial plant which has become an aquatic weed worldwide and occurs in lakes and rivers throughout PA, particularly in eutrophic waters (Figure 6.2). Eurasian water-milfoil is winter-hardy, with some shoots over-wintering and resuming growth in the spring. It grows quickly and forms dense infestations just below the water surface which negatively affect wildlife and aquatic activities. In consequence, four out of the six *Myriophyllum* species native to PA are listed as endangered, threatened or rare by the PA Natural Heritage Program and they can be easily confused with *M. spicatum* (CAIP, 2001b, Johnson and Blossey, 2002, Block and Rhoads, 2011).



Figure A.2 Myriophyllum spicatum
(clarenbridgegardencentre.ie).

Trapa natans (European water chestnut) is a rooted annual plant which forms floating rosettes that can spread very quickly (Figure A.3). The species is found in scattered lakes, ponds, and river backwaters in eastern PA (Block and Rhoads, 2011). Water chestnut can form dense floating mats which severely impact wildlife and aquatic activities. It produces sharp, barbed fruits that constitute a hazard for water users (Swearingen et al., 2010, Block and Rhoads, 2011).



Figure A.3 Trapa natans

(www.prota4u.org).

All these species have the potential to impact wildlife by forming dense infestations, which limit light penetration, outcompete native plants, alter water chemistry, and/or reduce oxygen levels, with negative effects on aquatic animals. These species also have serious economic and environmental impacts because they interfere with commercial and recreational boating, fishing, swimming, and other aquatic activities. Finally, these AIS have the potential to slow water flow and clog irrigation and flood-control canals.

Didymosphenia geminata is a freshwater alga in the division Bacillariophyta (diatoms). The species has historically been associated with low-nutrient, montane or northern boreal streams in Europe, North America, and Asia (Spaulding and Elwell, 2007, Whitton et al., 2009). Over the past 25 years, *D. geminata* has begun to exhibit invasiveness with more frequent large nuisance blooms in high-nutrient waters outside its original geographical distribution (Flöder and Kilroy, 2009). Since 2007, the species has been detected in the Delaware River, although at low densities. In 2012, numerous occurrences of extensive bloom have been reported throughout the main body of the river (Silldorf 2012). In rivers and streams, *D. geminata* usually attaches to the substrate (i.e., stones or vegetation) by long, branched mucilage (polysaccharide) stalks (Figure 4.4).

Mature colonies form light brown or whitish mat, sometimes up to 20-cm thick. These mat blooms adversely affect fish, plant, and invertebrate species by reducing the habitats, excluding other diatoms, and altering stream ecosystem (Kilroy, 2004, NYIS.INFO, 2011). Infestations also have negative impact on water-associated recreational activities and blooms have been reported to block water intake pipes and canals. The species raises serious economic concerns for fisheries, tourism, irrigation, and hydropower (NYIS.INFO 2011).



Figure A.4 Didymosphenia geminata
(www.lhprism.org).

These AIS pose significant threats to non-infested water bodies in PA because control methods for established populations, such as herbicides and mechanical harvesting, are costly and have not proven successful. A method for *early detection and rapid response* (EDRR) to the dispersion of AIS is therefore critical for defending against the establishment of new populations. Early detection increases the likelihood that localized invasive populations will be found, contained, and eradicated before they become widely

established and rapid response can slow range expansion, and avoid the need for costly long-term control efforts (Invasive.org, 2013).

Relevance to PA Sea Grant Program

This proposal was submitted in response to the PA Sea Grant Program 2014-2016 Request for Applied Research Proposals, Priority Area: "Proposals that improve prevention, early detection, rapid response, or control/management of aquatic invasive species impacting the Erie, Delaware, and Susquehanna watersheds in PA".

Methodology

Overall Approach

The proposed research involved two major phases extending over two years. In the first phase, a molecular method based on real-time PCR was developed and optimized for the detection, identification, and quantification of selected plant and algal AIS. This phase included the Technical Objectives 1 and 2 (see below). In the second phase, the developed method was applied to the detection of AIS in water samples collected in the field (Technical Objective 3).

Technical Objective 1

To design and validate primers and probes for real-time PCR amplification of DNA markers specific to selected aquatic invasive species.

Primer & Probe Design

For the three plant AIS, *M. spicatum*, *T. natans*, and *H. verticillata*, molecular markers specific to the species were designed based on published DNA barcodes. Barcodes were retrieved from the Barcode Of Life Database version 4 (BOLD v4, <http://www.boldsystems.org/index.php/databases>). In brief, three major barcodes were tested for each plant species: ITS2, *matK*, and *rbcL* (CBOL Plant Working Group 2009, Singh et al. 2012). In order to find non-homologous regions in the markers allowing the unvocal determination of the target species, we retrieved from BOLD the barcodes of all species represented in the genera belonging to the target species family and known to exist in PA, according to Block & Rhoads (2011) (Table 6.1). All barcode sequences were pasted in the nucleic acid sequence alignment editor, BioEdit v7.2.5 (<http://www.mbio.ncsu.edu/bioedit/page2.html>). After elimination of redundant sequences – 2 sequences were found redundant if they include no more than 1 mismatch over any 30-bp fragment –, sequences were aligned using the application ClustalW in BioEdit and regions of high variability allowing the design of unique primers/probes were visually identified (e.g., >5 mismatches in any 30-bp sequence). High-variability fragment sequences of the target species were uploaded in the primer design software, PrimerQuest (IDT, <http://www.idtdna.com/primerquest/home/index>) and primers and probes were designed by manually restricting the allowed regions to high-variability areas. This strategy allowed us to design primers and probes with high number of mismatches as compared with homologous sequences in related species susceptible to be found in PA.

Table A.1 List of the target invasive species, *M. spicatum*, *T. natans*, *H. verticillata* and *D. geminata* and a suite of related specimen obtained from different sources.

Invasive Species	<i>Myriophyllum spicatum</i>	<i>Hydrilla verticillata</i>	<i>Trapa natans</i>	<i>Didymosphenia geminata</i>
Family	Haloragaceae	Hydrocharitaceae	Lythraceae	Gomphonemataceae
Subfamily			Trapoideae	
Relatives in PA (Block et al. 2011)	<i>M. aquaticum</i>	<i>Egeria densa</i>	<i>Decodon verticillatus</i>	
	<i>M. farwellii</i>	<i>Elodea canadensis</i>	<i>T. natans</i>	
	<i>M. heterophyllum</i>	<i>E. nuttallii</i>		
	<i>M. humile</i>	<i>E. schweinitzii</i>		
	<i>M. spicatum</i>	<i>Najas flexilis</i>		
	<i>M. tenellum</i>	<i>N. gracillima</i>		
	<i>M. verticillatum</i>	<i>N. guadalupensis</i>		
	<i>Proserpinaca palustris</i>	<i>N. marina</i>		
	<i>P. pectinata</i>	<i>N. minor</i>		
		<i>Vallisneria americana</i>		
Dried Specimens (a)	<i>M. spicatum</i>	<i>H. verticillata</i>	<i>D. verticillatus</i>	
	<i>M. aquaticum</i>	<i>E. densa</i>		
		<i>E. canadensis</i>		
		<i>E. nuttallii</i>		
		<i>N. flexilis</i>		
		<i>N. gracillima</i>		
		<i>N. minor</i>		
		<i>V. americana</i>		
		<i>Zanichellia palustris</i>		
Fresh Specimens (b)	<i>M. spicatum</i>	<i>H. verticillata</i>	<i>T. natans</i>	<i>D. geminata</i> (c)
	<i>M. aquaticum</i>	<i>E. densa</i>		
(a) Archived dried specimens obtained from various herbarium collections				
(b) Fresh specimens collected in the field				
(c) Collected in the field, preserved in formalin				

Molecular methods for the detection of the invasive alga, *D. geminata*, have already been well developed (Cary et al., 2007; Cary et al., 2014; Jaramillo et al., 2015). We therefore chose to use published primer sequences. Based on the reported test and validation results, the 18S rDNA markers published in Cary et al. (2006) were selected.

In addition, 'universal' primers based on 16S rDNA for prokaryotes were designed and used for the normalization of specific biomarker signals and as positive controls.

Primers and fluorescent probes (labeled with 5'-FAMTM and 3'- Iowa Black[®] or 3'-ZENTM black quenchers) were synthesized by Integrated DNA Technology (IDT, <https://www.idtdna.com>).

Invasive & Related Non-Invasive Specimen Collection

A suite of specimens of the three target invasive plant species and related non-invasive species were collected from various sources. Dried achieved specimens were obtained from various local collections and herbariums. A series of fresh specimens were collected in the field in various water bodies in PA: *T. natans* was collected in Bradford reservoir (Bucks County), *H. verticillatum* and *M. spicatum* were collected in Lake Nockamixon (Bucks County). *M. aquaticum* was collected from Armentrout Preserve (Bucks County), *Egeria densa* was collected Robbins Park (Bucks County), and *D. geminata* (preserved in formalin) was obtained from the Delaware River Basin Commission (DRBC), NJ.

DNA was extracted from plant material (dried and fresh) after grounding the specimen under liquid nitrogen using the DNeasy Plant Extraction Kit (Qiagen) following the manufacturer's protocol. DNA was extracted from formalin-preserved *D. geminata* using DNeasy Blood and Tissues Extraction Kit (Qiagen) following the modified manufacturer's protocol for extraction of formalin-treated samples. Extracted DNA was analyzed using a NanoDropTM ND-2000 and conserved at -80°C.

Real-Time PCR Amplification

Real-time (quantitative) PCR amplification was performed on a StepOnePlus™ Real-Time PCR System (Applied Biosystems) using extracted DNA as a template. Real-time PCR was carried out using ABSolute™ Blue SYBR Green ROX mix (Thermo Scientific) when based on intercalating dyes (i.e., SYBR Green) and the PrimeTime® Gene Expression Master Mix (IDT) when based on fluorescent probes. Cycling conditions were adjusted to the different chemistries employed following the manufacturer's instructions.

Specificity of Primers and Probes

The *specificity* (cross-reactivity) of the synthesized primers and probes was assessed by real-time PCR amplification as described previously but using DNA extracted from both the target invasive species and related non-invasive species (see above) as template.

Technical Objective 2:

To develop and validate protocols for real-time PCR amplification of the selected aquatic invasive species.

Sensitivity & Efficiency of Real-Time PCR

For real-time PCR protocol optimization and *sensitivity/efficiency* characterization, DNA marker sequences (e.g., specific barcodes and 16S rDNA positive control marker) were amplified by PCR using specific primers/probes and either extracted genomic DNA or purified PCR products as template. The DNA concentration of the template was

determined using a NanoDrop™ ND-2000 (Cary et al. 2007). PCR results were computed by the StepOnePlus™ Software v2.3 using the Absolute Quantitation method (Applied Biosystems): recorded fluorescence emission signals (ΔR_n) were converted into DNA copy number μL^{-1} by the use of standard curves.

The *sensitivity* of the real-time PCR method was determined by the amplification of log-10 dilutions of target species genomic DNA or purified PCR product obtained using target species DNA as template. The linear trend (CT vs. DNA concentration) was plotted to determine the *dynamic range* and *detection limit* of the assay, expressed as DNA copy number μL^{-1} (Cary et al. 2007). The DNA copy number was calculated based on the estimated genome size and number of copies of the target gene (biomarker) per genome. The dynamic range was determined based by the lowest and highest target DNA concentration that was recorded within the linear portion of the standard curve. The *detection limit* was calculated based on the lowest concentration of DNA positively detected within the *dynamic range*. The *efficiency* of the PCR amplification was calculated from the slope of the linear trend, CT vs. DNA concentration or log copy number μL^{-1} .

Technical Objective 3

To test the applicability and robustness of the method in the field.

Sample Collection

Sampling was conducted in various locations in PA in the vicinity of Philadelphia known to be contaminated with the three target plant species, *T. natans*, *H. verticillata*,

and *M. spicatum*, and one location in Maryland (MD) known to be contaminated with the diatom, *D. geminata*.

Water samples were collected from Little Neshaminy Creek (Bucks County) at increasing distances from the Bradford reservoir (Bucks County), which was visually contaminated by *T. natans*. Samples were collected from eight locations up to approx. 9.2 miles downstream the reservoir. Two sampling campaigns were conducted during the summer 2014. Water samples were then collected during the spring and summer 2016 from different locations in Lake Nockamixon (Bucks County) that was visually contaminated with *H. verticillata* and *M. spicatum*. Samples were collected in the middle of the invasive vegetation, from a pier located approx. 180 yards from the plants, at the Lake inlet (without visible contamination), and at the lake outlet located at approx. three miles from the plants (without visible contamination). In addition, fresh plant specimens of *T. natans*, *H. verticillata*, and *M. spicatum*, were collected from these two locations. Finally, water samples were collected from the Big Gunpowder Falls (Baltimore County, MD) near the estimated location of a *D. geminata* contamination site. Three water samples were collected up to 270 yards downstream the reported contamination site. In addition, biofilm material was scraped from stones and rocks at the reported contamination location to collect *D. geminata* biomass, as the alga was not visually detected at the time of sampling.

Real-Time (quantitative) PCR

When arrived in the laboratory, approx. one liter of water was filtered in on 0.45- μ m filter membrane and the total DNA was extracted from the filters using the MoBio

PowerSoil DNA Extraction Kit. DNA was extracted from plant specimen as previously described and from the river stone material (*D. geminata*) using the MoBio PowerSoil DNA Extraction Kit. Extracted DNA was analyzed using a NanoDrop™ ND-2000 and conserved at -80°C. Real-time PCR amplification was performed on a StepOnePlus™ Real-Time PCR System (Applied Biosystems) as previously described. PCR results were computed by the StepOnePlus™ Software v2.3 using the Absolute Quantitation method (Applied Biosystems): recorded fluorescence emission signals (ΔR_n) were converted into Relative Amplification levels. Results obtained with SYBR Green chemistry were expressed as both Relative Amplification levels and prokaryotic 16S rDNA-normalized Relative Amplification levels.

Results & Discussion

Technical Objective 1

To design and validate primers and probes for real-time PCR amplification of DNA markers specific to selected aquatic invasive species.

The search for barcodes in BOLD v4 for the three plant target species, *M. spicatum*, *T. natans*, and *H. verticillata*, and relative species returned many entries. From them, we selected the barcodes, ITS2, *matK*, and *rbcL*, in species known to be found in PA. After elimination of redundant sequences, sequences were aligned and compared manually with the target barcode sequences. The design of primers and probes was based on the number of mismatches between the target barcode sequence and the relatives' barcode sequences in suitable primer/probe regions.

For *T. natans*, ITS2 was the most variable barcode, which allowed designing primer and probe sets with a high number of mismatches with all relative species (Table 6.2). Due to the high number of mismatches in the primer and probe sequences, it was expected that the assay would be selective based only on the primer sequence – i.e., using SYBR Green chemistry. Several primer pairs were designed in an attempt to improve the amplification efficiency.

Table A.2 List of primer and probe sequence specific to the three target plant species, *M. spicatum*, *T. natans*, and *H. verticillata*, and the diatom, *D. geminata*.

Target Species	Sequence
<i>Trapa natans</i>	
Trapa-ITS2-F-127	GCACTTGCTCTCCTCGTAAC
Trapa-ITS2-R-256	TACTAGAGACAGGCATGATACCC
Trapa-ITS2-130-F	CTTGCTCTCCTCGTAACGCA
Trapa-ITS2-251-R	AGAGACAGGCATGATACCCC
Trapa-ITS2-67-F	ATTGCCAACAATCCTGGCCG
Trapa-ITS2-223-R	CACATGGTGGATGTGCCCC
Trapa-ITS2-F-50	GACAGACCAGCGAACTCATT
Trapa-ITS2-P-225	FAM-CTTGCCCGGGGTATCATGCCTGTCTCTAGT-BHQ
Trapa-ITS2-R-441	TGTGGGCGGAATGTTGAG
<i>Hydrilla verticillata</i>	
Hydr-matK-F-278	ACTTTATGGAGCGAACCCATTT
Hydr-matK-P-387	FAM-TATTAGATCTGAGGAAAATGGTATTCTTG-BHQ
Hydr-matK-R-677	CCATGACAGCAATAACTGGAACTA
<i>Myriophyllum spicatum</i>	
Myrio-matK-F-57	CTTCAAGCCCTTCGCTACC
Myrio-matK-P-327	FAM-ATAAACCTTTTTATAGGAGTCTTTGCTA-BHQ
Myrio-matK-R-437	TCAGAAGAGGTGTGCCTTTG
<i>Didymosphenia geminata</i>	
Didymo-18S-F-602	GTTGGATTTGTGATGGAATTTGAA
Didymo-18S-R-753	AATACATTCATCGA GTAAGTC
Universal Prokaryotes	
16S-341-F	CCTACGGGRSGCAGCAG
16S-532-R	TACCGCGGCKGCTGRCAC

Testing the specificity of the primers only (SYBR Green) and primer/probe sets (fluorescent probe – FAM-BHQ) against *T. natans* and all relative species that we collected showed that both assays were selective for the target species.

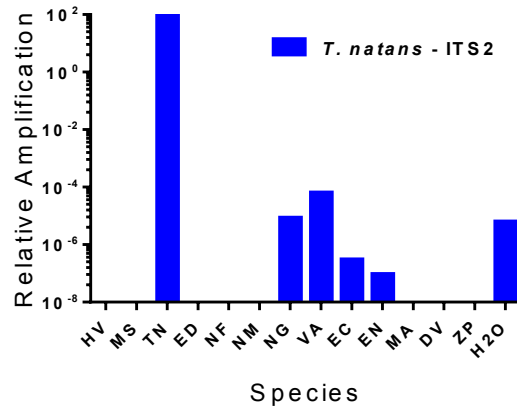


Figure A.5 Relative real-time PCR amplification signals of *T. natans*

biomarker (ITS2 – SYBR Green) obtained with DNA from the three target species and relative species from PA. HV: *H. verticillata*, MS: *M. spicatum*, TN: *T. natans*, ED: *E. densa*, NF: *N. flexilis*, NM: *N. minor*, NG: *N. gracillima*, VA: *V. americana*, EC: *E. canadensis*, EN: *E. nuttallii*, MA: *M. aquaticum*, DV: *D. verticillatus*, ZP: *Z. pallustris*, H2O: Non-template control

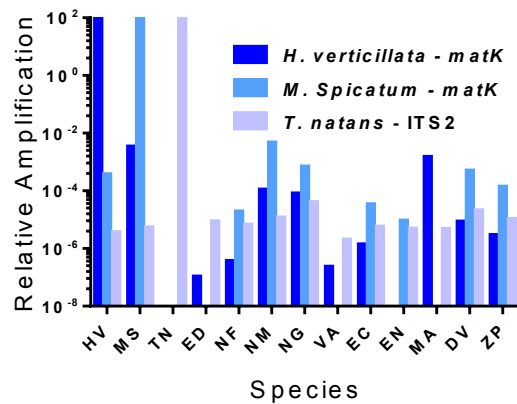


Figure A.6 Relative real-time PCR amplification signals of *H. verticillata*

fluorescent biomarker (matK – FAM-BHQ), *M. spicatum* fluorescent biomarker (matK – FAM-BHQ), and *T. natans* fluorescent biomarker (ITS2 – FAM-BHQ), obtained

with DNA from the three target species and relative species from PA. HV: *H. verticillata*, MS: *M. spicatum*, TN: *T. natans*, ED: *E. densa*, NF: *N. flexilis*, NM: *N. minor*, NG: *N. gracillima*, VA: *V. americana*, EC: *E. canadensis*, EN: *E. nuttallii*, MA: *M. aquaticum*, DV: *D. verticillatus*, ZP: *Z. pallustris*, H2O: Non-template control.

For *H. verticillata*, *matK* was the most variable barcode, which allowed designing primer and probe sets with a reasonable number of mismatches with all relative species (Table 6.2). However, only probe sequences could be designed with a number of mismatches high enough (4 – 5) with all relative species. It was therefore expected that the assay would require fluorescent probe chemistry (FAM-BHQ) to be selective enough. Indeed, testing the specificity of the primers only (SYBR Green) and the primer/probe set (FAM-BHQ) against *H. verticillata* and all relative species that we collected showed that only the fluorescent assay was selective for the target species

For *M. spicatum*, *matK* was the most variable barcode, which allowed designing primer and probe set with a reasonable number of mismatches with all relative species (Table 6.2). However, only probe sequences could be designed with a number of mismatches high enough (4 – 5) with all relative species. It was therefore expected that the assay would require fluorescent probe chemistry (FAM-BHQ) to be selective enough. Indeed, testing the specificity of the primers only (SYBR Green) and the primer/probe set (FAM-BHQ) against *M. spicatum* and all relative species that we collected showed that only the fluorescent assay was selective for the target species.

For the alga, *D. geminata*, the primer sequences were obtained from published reports and articles (Table 6.2). The primers were validated by in silico comparison with corresponding 18S rDNA sequences of closely-related diatom species and validated by

testing on several locations where *D. geminata* was known to be present (Cary et al. 2006, Cary 2014). The assay for *D. geminata* detection was based on 18S rDNA primers only – SYBR Green chemistry –, which was motivated by the fact that the assay based on primer specificity has been shown satisfactory (Cary et al. 2006, Jaramillo et al. 2015) and on financial considerations.

Technical Objective 2

To develop and validate protocols for real-time PCR amplification of the selected aquatic invasive species.

Serial 10x dilutions of either genomic DNA extracted from target specimens or purified PCR products were prepared to draw standard curves and derive essential real-time PCR specifications, including the dynamic range, *detection limit*, and *amplification efficiency*. This analyses were conducted for the promising assays based on the results of the prior Technical Objective, i.e., SYBR Green assays for *T. natans*, *D. geminata*, and prokaryotes, and fluorescent FAM-BHQ assays for *M. spicatum* and *H. verticillata*.

For all assays characterized, a near-perfect linearity was observed within a large portion of the standard curve – CT values vs. \log_{10} (DNA concentration). Based on specificity tests, primer sets worked well for *T. natans*, *D. geminata*, and prokaryotes, but not for *M. spicatum* and *H. verticillata*. All three primer/probe sets for *T. natans*, *M. spicatum* and *H. verticillata* worked well.

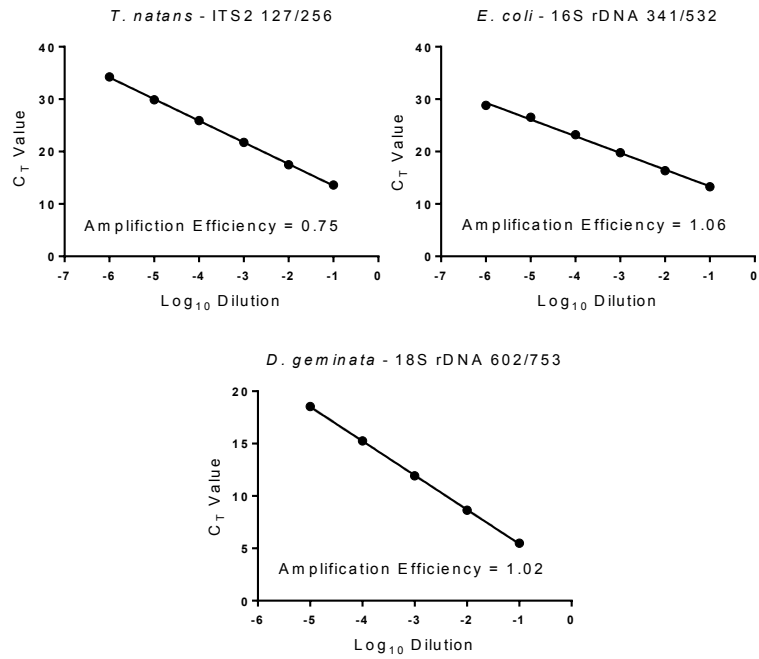


Figure A.7 Standard curves of SYBR Green assays for *T. natans*, *D. geminata*, and prokaryotes (using *E. Coli* DNA).

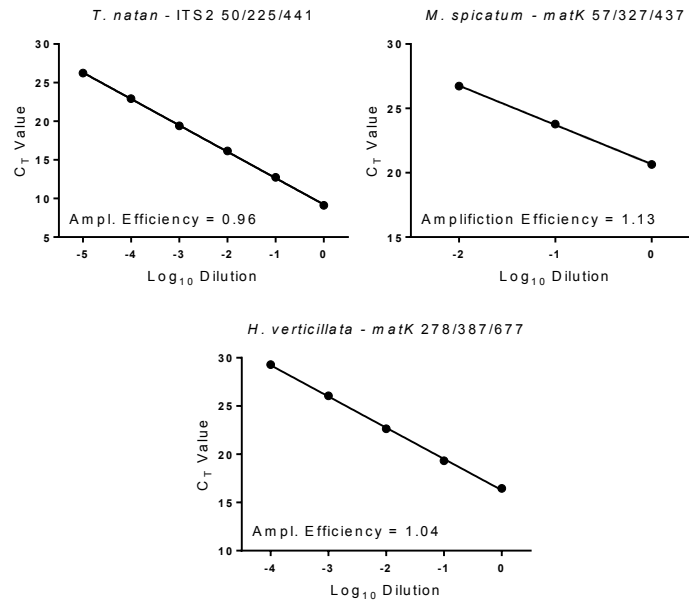


Figure A.8 Standard curves of fluorescent assays for *T. natans*, *M. spicatum*, and *H. verticillata*.

The calculated amplification efficiency was reasonably good ranging from 96 to 113%, except for *T. natans* ITS2 – SYBR Green, which was only 75%. Two other primer sets for *T. natans* ITS2 – SYBR Green were tested in an attempt to improve the amplification efficiency (Table 6.2), but without significant success (77% with primer set ITS2 130/251 and 66% with primer set ITS2 67/223). Although the opinion about this question is divided in the literature, one considers often that as long as the standard curve is linear, it can be used for the calculation of the gene or cell copy number, regardless of the actual amplification efficiency. The low efficiency observed with *T. natans* ITS2 - SYBR Green may reflect secondary structures in DNA amplification. Several primer pairs were tested which did not improve the amplification efficiency, indicating the potential presence of plant-specific inhibitors. The dynamic range of the assays was also generally good and spanned five or six order of magnitude, except for *M. spicatum* *matK*

– FAM-BHQ, which was likely the result of the use of a low DNA concentration as template.

The detection limit of the assays was determined based on the lower concentration of standard DNA falling within the linear range of the assay. The genome copy number μL^{-1} was calculated based on the estimated mass of the genomic DNA and the measured DNA concentration in the non-diluted standard – i.e., without taking in to account the gene copy number per genome. The high detection limit of the *M. spicatum* matK – FAM-BHQ therefore reflects the narrow dynamic range of this assay, as shown by the limited linear portion of the standard curve.

Table A.3 Assay characterization for the six biomarkers for T. natans, H. verticillata, M. spicatum, D. geminata, and prokaryotes: the standard curve characteristics (number of points, R2, equation), the estimated detection limit of the assay, and the amplification efficiency are presented

Species	Biomarker	Chemistry	Std. Curve			Sensitivity (copy #/ μL)	Ampl. Efficiency (%)
			# of Points	R2	Equation		
<i>T. natans</i>	ITS2	SYBR Green	6	1.000	$\text{CT} = -4.13 \cdot \log(\text{copy\#}) + 40.38$	32	74.6
<i>T. natans</i>	ITS2	FAM-BHQ	6	1.000	$\text{CT} = -3.42 \cdot \log(\text{copy\#}) + 30.45$	16	96.1
<i>H. verticillata</i>	matK	FAM-BHQ	5	0.999	$\text{CT} = -3.24 \cdot \log(\text{copy\#}) + 32.06$	7	103.5
<i>M. spicatum</i>	matK	FAM-BHQ	3	1.000	$\text{CT} = -3.05 \cdot \log(\text{copy\#}) + 37.6$	3,483	112.7
<i>D. geminata</i>	18S rDNA	SYBR Green	5	1.000	$\text{CT} = -3.27 \cdot \log(\text{copy\#}) + 25.5$	136	102.2
Prokaryote	16S rDNA	SYBR Green	6	0.997	$\text{CT} = -3.19 \cdot \log(\text{copy\#}) + 34.78$	52	105.8

Technical Objective 3

To test the applicability and robustness of the method in the field.

For the *T. natans* field study, water samples were collected from Little Neshaminy Creek (Bucks County) at increasing distances from the Bradford reservoir, which was contaminated by *T. natans* shows the amplification level recorded in the water from the reservoir itself to the furthest location in the Little Neshaminy Creek about 9.5 miles downstream the reservoir. Results obtained with ITS2 – SYBR Green and ITS2 – FAM-

BHQ chemistries were rather consistent, although it seems that low signals were detected at higher level with the fluorescent biomarker (ITS2 – FAM-BHQ). Positive signals were detected in all water samples at significantly higher level than in the non-template controls, except for the Almshouse Road sample detected using the FAM-BHQ chemistry.

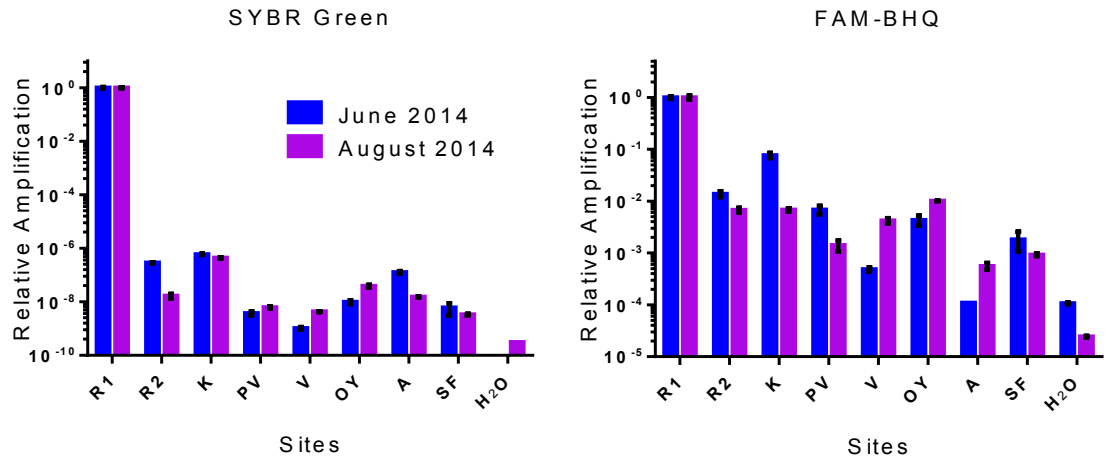


Figure A.9 Amplification levels of *T. natans* biomarkers

(ITS2 – SYBR Green and FAM-BHQ) recorded in water samples collected from Little Neshaminy Creek (Bucks County) at increasing distances from Bradford reservoir: Bradford reservoir (water surrounding *T. natans* vegetation, 0.0 mile): R1, Bradford reservoir (outfall, 0.0 mile): R2, Kansas Rd (0.8 mile): K, Paul Valley Rd (1.8 mile): PV, Valley Rd (2.7 miles): V, Old York Rd (4.8 miles): OY, Almshouse Rd (7.1 miles): A, Sacketts Ford Rd (9.5 miles): SF.

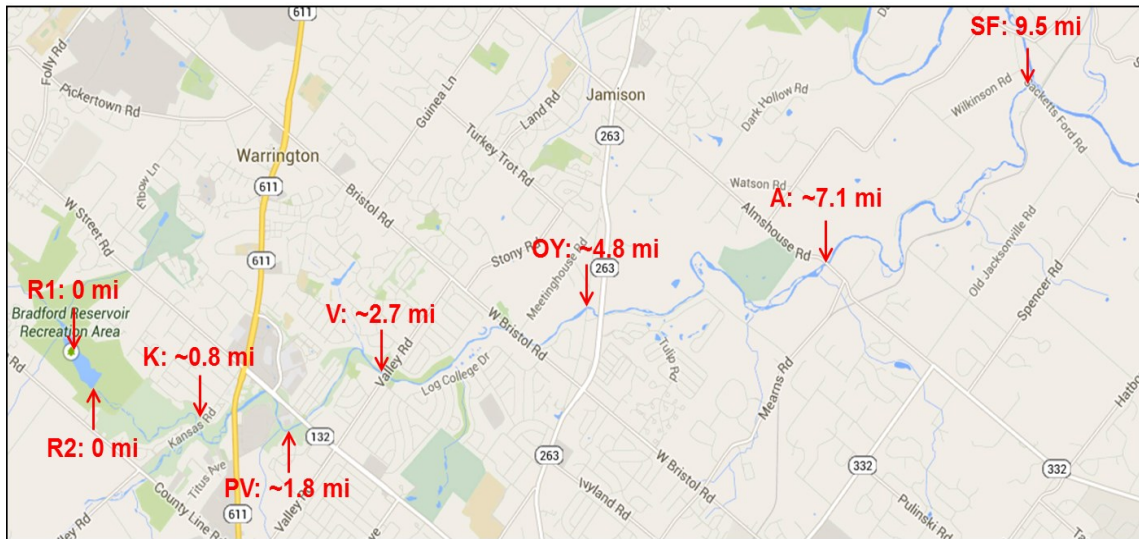


Figure A.10 Map of sampling points along Little Neshaminy Creek

(Bucks County) downstream the *T. natans*-contaminated Bradford reservoir.

For the *H. verticillata* and *M. spicatum* field study, samples were collected from different locations in Lake Nockamixon (Bucks County), which was visually contaminated with the two target species. Shows a high positive detection of both markers (*matK* – FAM-BHQ) in the water directly surrounding the respective plant vegetation. A lower signal was observed for the *H. verticillata* marker in the water surrounding *M. spicatum* vegetation and vice versa. Also a lower but positive signal was observed for both markers in the water sample collected from a pier at approx. 180 yards from the vegetation and from the lake outlet at about three miles from the vegetation. Only a faint signal was detected at the lake inlet for the *H. verticillata* biomarker, suggesting the presence of the species at some locations upstream the lake. Strong and specific signals were obtained with DNA extracted directly for the specimens collected from the lake.

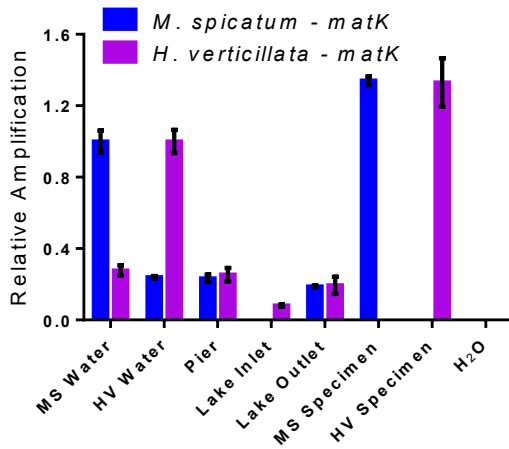


Figure A.11 Amplification levels of *H. verticillata* and *M. spicatum* biomarkers (*matK* – *FAM-BHQ*) recorded in water samples and fresh plant specimens collected from Lake Nockamixon (Bucks County).

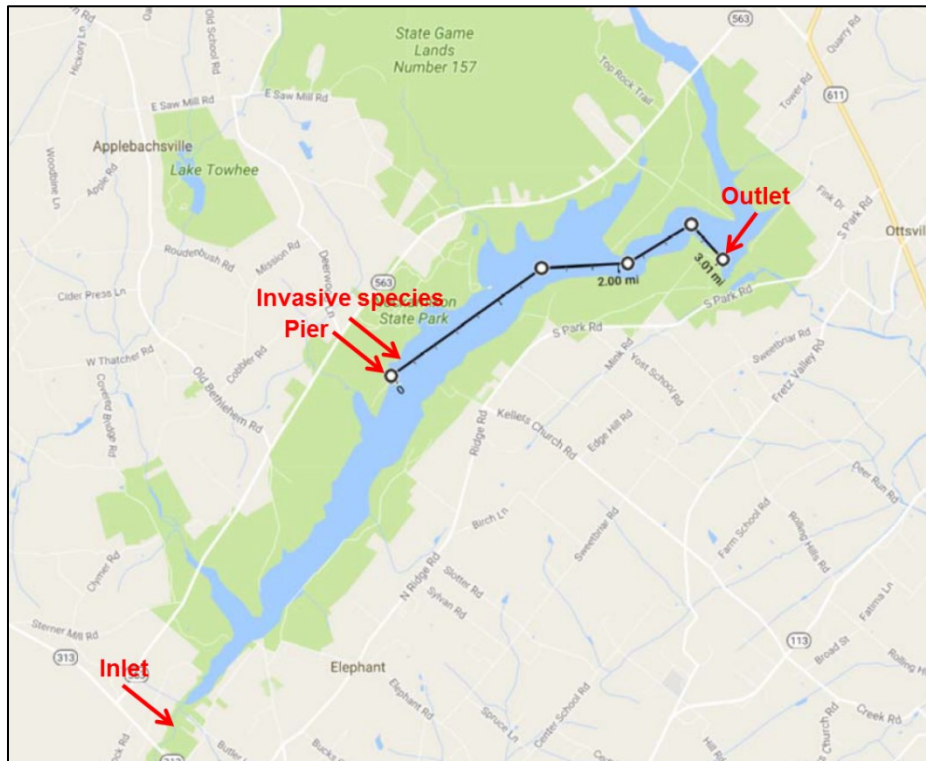


Figure A.12 Map of sampling points on Lake Nockamixon (Bucks County) contaminated with *H. verticillata* and *M. spicatum*.

For *D. geminata* field study, samples were collected from different locations in the Big Gunpowder Falls (Baltimore County, MD) at a location that has a history of contamination by *D. geminata*. Although the alga was not positively observed, samples were collected from several stones and rocks immersed in the river as well as from the water at increasing distance (up to 270 yards) from the reported prior contamination shows a positive detection of the biomarker in the material collected from river stones as well as from the downstream water samples. No signals were detected from the negative controls (water samples from Little Neshaminy Creek and Lake Nockamixon) without history of contamination by the invasive alga. Interestingly, the *D. geminata* signal (18S rDNA – SYBR Green) normalized by the 'universal prokaryotic' signal (16S rDNA – SYBR Green) in the water samples downstream the contamination point was significantly higher than the non-normalized signal, suggesting a positive correlation between the abundance of *D. geminata* and bacteria.

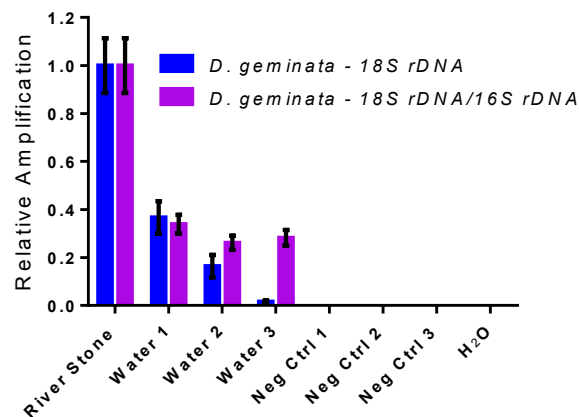


Figure A.13 Amplification levels of *D. geminata* biomarker

(18S rDNA – SYBR Green) recorded in water samples and stones collected from Big Gunpowder Falls (Baltimore County, MD). Relative amplification signals of *D. geminata*

biomarker (18S rDNA) and *D. geminata* biomarker normalized by the 'universal prokaryotic' biomarker (18S rDNA/16S rDNA) are shown.

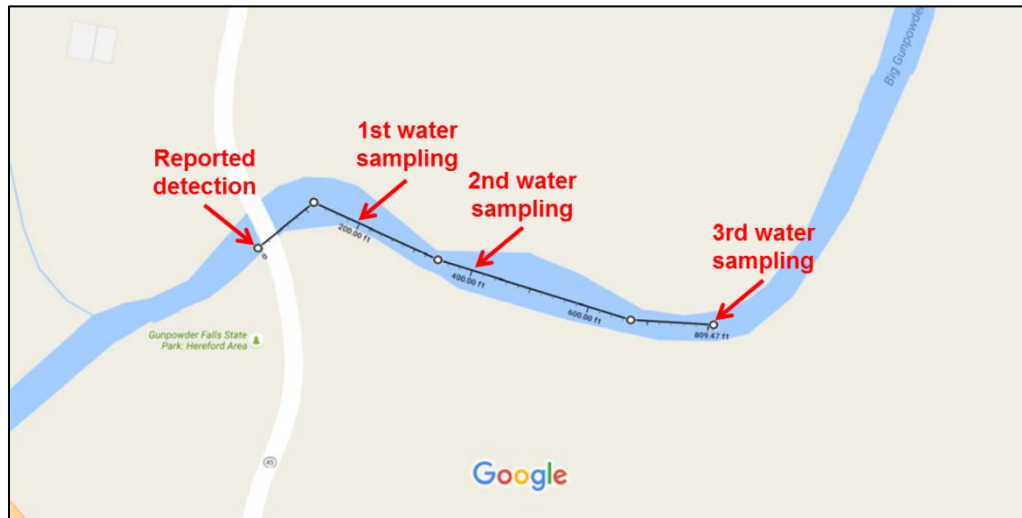


Figure A.14 Map of sampling points along the Big Gunpowder Falls (Baltimore County, MD) downstream the reported *D. geminata*-contaminated point.

Conclusions

The overarching goal of this study was to demonstrate that small amounts DNA released in the water by living organisms could be detected by real-time PCR and used as biomarkers for the specific and sensitive detection of AIS. Results from this research have showed that combination of primers and probes allows the detection of DNA signatures for all target species, *M. spicatum*, *T. natans*, *H. verticillata*, and *D. geminata*, miles away from the contamination point, providing a very sensitive method for their early detection.

We designed five primer sets to be used in SYBR Green assays for the detection of the three plant species, the diatom, and the 'universal prokaryotic' marker. SYBR Green is a fluorescent DNA binding dye which allows monitoring DNA synthesis during the

course of the PCR. The specificity of SYBR Green-based PCR is based on the primers only. We have also designed three primer/fluorescent probe sets for the detection of the three plants species. The 'probe'-based real-time PCR uses a fluorescent-labeled probe specific to the target sequence. The specificity of probe-based PCR is based on both the primers and fluorescent probes, resulting in increased selectivity. Based on specificity tests using both the target AIS and a range of relative species, the designed primer sets (SYBR Green chemistry) provided satisfactory results for the detection of *T. natans*, *D. geminata*, and prokaryotic DNA. All three primer/probe sets (FAM-BHQ) provided satisfactory results for the detection of *T. natans*, *M. spicatum*, and *H. verticillata*.

The quality control and validation of the assays provided overall satisfactory results. Near-perfect linearity was observed with all standard curves ($r^2 > 0.99$). The dynamic range of the assays spanned five or six orders of magnitude, except for *M. spicatum matK* – FAM-BHQ. The amplification efficiency was within the 95 – 110% range, except for *T. natans* ITS2 – SYBR Green. For *T. natans*, the assay based on fluorescent probe, ITS2 – FAM-BHQ, provided good results and can be used. The calculated detection limit ranged from 7 to 136 copies μL^{-1} , except again for *M. spicatum matK* – FAM-BHQ, which is a consequence of the narrow dynamic range recorded with this marker. Additional quality control of the *M. spicatum matK* – FAM-BHQ marker is warranted.

The three field studies showed results consistent with the expectations. With the three target invasive plant species, *T. natans*, *H. verticillata*, and *M. spicatum*, we observed signals in the water samples that were roughly inversely proportional to the distance from the actual location of the invasive specimen. In each case, the signal was detected miles downstream the contamination point, even though one cannot rule out the presence of the

species at other locations closer to the water sampling points. For each species – except for the *T. natans* fluorescent biomarker, ITS2 – FAM-BHQ, at one sampling point 7 miles downstream the initial contamination –, the positive signals were several orders of magnitude higher than the signals from non-template controls or other negative control samples. For *D. geminata*, we also observed positive signals in the water samples hundred yards downstream a historically contaminated location, even though the presence of the invasive alga was not visible at the time of sampling.

For the four target species – even though some additional quality control should be performed for one of the biomarkers –, we have developed bioassays which are readily applicable for monitoring the species through the analysis of water samples. The innovative aspect of the developed assays relies on the possibility to detect the presence of the target species based on the presence of DNA signatures in the water, without the need to physically observe or collect specimens.

Future Research

Additional validation studies are recommended, especially to confirm further the specificity of the developed biomarkers. This will require obtaining additional 'relative species', extracting their DNA, and testing further the specificity of the designed biomarkers. In addition, it would be advisable to perform sequencing of the PCR amplification products from the target specimens and from water samples and compare the sequences with DNA databases. The developed methodology can be easily be applicable to other aquatic invasive species, including plants, algae, and animals.